สมบัติการต้านเชื้อแบคทีเรียของพอลิเอทิลีนและยางซิลิโคนที่ดัดแปรผิวด้วยพลาสมาที่กำเนิดจากเครื่องพลาสมาโฟกัส

นายวีรวัฒน์ ศรีประไพ

วิทยานิพนธ์นี้เป็นส่วนหนึ่งของการศึกษาตามหลักสูตรปริญญาวิทยาศาสตรมหาบัณฑิต
สาขาวิชาวิทยาศาสตร์พอลิเมอร์ประยุกต์และเทคโนโลยีสิ่งทอ ภาควิชาวัสดุศาสตร์
คณะวิทยาศาสตร์ จุฬาลงกรณ์มหาวิทยาลัย
ปีการศึกษา 2552
ลิขสิทธิ์ของจุฬาลงกรณ์มหาวิทยาลัย

ANTIBACTERIAL PROPERTIES OF POLYETHYLENE AND SILICONE RUBBER SURFACE-MODIFIED BY PLASMA GENERATED FROM PLASMA FOCUS DEVICE

Mr. Werawat Sriprapai

A Thesis Submitted in Partial Fulfillment of the Requirements

for the Degree of Master of Science Program in Applied Polymer Science and Textile Technology

Department of Materials Science

Faculty of Science

Chulalongkorn University

Academic Year 2009

Copyright of Chulalongkorn University

Thesis Title	ANTIBACTERIAL PROPERTIES OF POLYETHYLENE AND SILICONE RUBBER SURFACE-MODIFIED BY PLASMA GENERATED FROM PLASMA FOCUS DEVICE
By	Mr.Werawat Sriprapai
Field of Study	Applied Polymer Science and Textile Technology
Thesis Advisor Associate	Professor Vimolvan Pimpan, Ph.D.
Thesis Co-Advisor	Assistant Professor Rattachat Mongkolnavin, Ph.D.

Accepted by the Faculty of Science, Chulalongkorn University in Partial Fulfillment of the Requirements for the Master's Degree

…….. Dean of the Faculty of Science
(Professor Supot Hannongbua, Dr.rer.nat.)

THESIS COMMITTEE

…….. Chairman
(Assistant Professor Sirithan Jiemsirilers, Ph.D.)

…….. Thesis Advisor
(Associate Professor Vimolvan Pimpan, Ph.D.)

…….. Thesis Co-Advisor
(Assistant Professor Rattachat Mongkolnavin, Ph.D.)

…….. Examiner
(Assistant Professor Usa Sangwatanaroj, Ph.D.)

…….. External Examiner
(Associate Professor Paiparn Santisuk)

วีรวัฒน์ ศรีประไพ : สมบัติการต้านเชื้อแบคทีเรียของพอลิเอทิลีนและยางซิลิโคนที่ดัดแปรผิวด้วยพลาสมาที่กำเนิดจากเครื่องพลาสมาโฟกัส. (ANTIBACTERIAL PROPERTIES OF POLYETHYLENE AND SILICONE RUBBER SURFACE-MODIFIED BY PLASMA GENERATED FROM PLASMA FOCUS DEVICE) อ. ที่ปรึกษาวิทยานิพนธ์หลัก: รองศาสตราจารย์ ดร.วิมลวรรณ พิมพ์พันธุ์, อ. ที่ปรึกษาวิทยานิพนธ์ร่วม: ผู้ช่วยศาสตราจารย์ ดร.รัฐชาติ มงคลนาวิน, 120 หน้า.

การดัดแปรผิวพอลิเอทิลีนและยางซิลิโคนสามารถทำได้โดยใช้พลาสมาที่กำเนิดจากเครื่องพลาสมาโฟกัส ซึ่งทำงานในภาวะที่ใช้ชนิดของแก๊สแตกต่างกัน ได้แก่ ไนโตรเจน ออกซิเจน และอาร์กอน รวมทั้งมีการเปลี่ยนจำนวนครั้งในการยิงพลาสมาเป็น 3 5 7 และ 10 ครั้ง จากการศึกษาพบว่า ปัจจัยที่มีผลต่อลักษณะเฉพาะและสมบัติการต้านเชื้อแบคทีเรียของตัวอย่างที่ผ่านการดัดแปร คือ ปริมาณทองแดงที่หาจากเทคนิคอะตอมมิกแอบซอร์ปชันสเปกโทรสโกปี การเกิดหมู่ฟังก์ชันที่ชอบน้ำซึ่งยืนยันด้วยเทคนิคฟูเรียร์ทรานสฟอร์มสเปกโทรสโกปี และความขรุขระของผิวซึ่งวิเคราะห์ด้วยเทคนิคอะตอมมิกฟอร์ซไมโครสโกปี ในกรณีของพอลิเอทิลีน พบว่า เมื่อใช้พลาสมาไนโตรเจน 3 ครั้ง หรือพลาสมาออกซิเจน 5 ครั้ง ได้ตัวอย่างที่มีประสิทธิภาพในการต้านเชื้อ *S. aureus* สูงสุด ซึ่งเป็นผลจากการที่ตัวอย่างทั้งสองมีความขรุขระของผิวต่ำ ส่วนกรณีของยางซิลิโคน พบว่า ประสิทธิภาพในการต้านเชื้อ *S. aureus* มีค่าสูงสุด เมื่อใช้พลาสมาไนโตรเจน 3 ครั้ง เนื่องจากการเกิดหมู่ที่ชอบน้ำขึ้นบนผิวและมีความขรุขระของผิวต่ำ ผลของการดัดแปรทั้งสองพอลิเมอร์นี้แสดงให้เห็นว่า การฝังไอออนทองแดงสามารถปรับปรุงประสิทธิภาพในการต้านเชื้อ *S. aureus* แต่วิธีการนี้ไม่สามารถปรับปรุงสมบัติการต้านเชื้อแบคทีเรีย *E. coli* ของพอลิเอทิลีนและยางซิลิโคนได้

ภาควิชา วัสดุศาสตร์ ลายมือชื่อนิสิต.....

สาขาวิชา วิทยาศาสตร์พอลิเมอร์ประยุกต์

และเทคโนโลยีสิ่งทอ ลายมือชื่ออ.ที่ปรึกษาวิทยานิพนธ์หลัก.....

ปีการศึกษา 2552 ลายมือชื่ออ.ที่ปรึกษาวิทยานิพนธ์ร่วม.....

5172461023 : MAJOR APPLIED POLYMER SCIENCE AND TEXTILE TECHNOLOGY
KEYWORDS : ANTIBACTERIA / PLASMA FOCUS / POLYETHYLENE / SILICONE RUBBER / SURFACE MODIFICATION

WERAWAT SRIPRAPAI: ANTIBACTERIAL PROPERTIES OF POLYETHYLENE AND SILICONE RUBBER SURFACE-MODIFIED BY PLASMA GENERATED FROM PLASMA FOCUS DEVICE. THESIS ADVISOR: ASSOC.PROF.VIMOLVAN PIMPAN, Ph.D. THESIS CO-ADVISOR: ASST.PROF.RATTACHAT MONGKOLNAVIN, Ph.D., 120 pp.

Surface modifications of polyethylene and silicone rubber were done using plasma generated from a plasma focus device operated with different types of gas including nitrogen, oxygen and argon. The number of plasma shots were also varied from 3, 5, 7 to 10 shots. It was found that the factors affecting the characteristics and antibacterial property of plasma-modified samples were copper content determined from atomic absorption spectroscopy, the formation of hydrophilic functional groups confirmed by FTIR spectroscopy and the surface roughness analyzed by atomic force microscopy. The results revealed that in the case of polyethylene, using 3 shots of nitrogen plasma or 5 shots of oxygen plasma resulted in highest antibacterial efficiency against *S. aureus* due to low surface roughness of the samples. For silicone rubber, highest antibacterial efficiency against *S. aureus* was obtained when 3 shots of nitrogen plasma were used. This was a result of the formation of hydrophilic functional groups and low surface roughness of the sample. Both cases indicated that copper ion implantation improved antibacterial efficiency against *S. aureus*. However, this method did not improve antibacterial property against *E. coli* of polyethylene and silicone rubber.

Department: Materials Science Student's Signature……

Field of Study: Applied Polymer Science and Textile Technology Advisor's Signature……...

Academic Year: 2009 Co-Advisor's Signature…..……

ACKNOWLEDGEMENTS

I would like to acknowledge and extend my heartfelt gratitude to the following persons who have made the completion of this thesis.

First of all, I would like to express my deep gratitude to my thesis advisor, Associate Professor Dr.Vimolvan Pimpan, and thesis co-advisor Assistant Professor Dr.Rattachat Mongkolnavin for their kindly reviewing this manuscript. Although many problems had occurred during the completion of my thesis, with their great suggestion and excellent guidance, this thesis is accomplished properly.

I also would like to extend my respectfully gratitude to Assistant Professor Dr.Sirithan Jiemsirilers, Associate Professor Paiparn Santisuk, and Assistant Professor Dr.Usa Sangwatanaroj for their kindly participation as thesis committee and for their valuable comments, suggestions and time to read this thesis.

I also sincerely appreciate to teachers and staffs at Department of Materials Science for the knowledge, suggestion and give the great experience during studied. I pleasure thanks to Asian African Association for Plasma Training (AAATP) for supporting UNU/ICTP Plasma Focus Device. I also appreciative to Dr. Dusit Ngamrungroj and staffs at Plasma Technology and Nuclear Fusion Research Unit for their suggestion for operating the plasma focus device. Thanks go towards staffs at Scientific and Technological Research Equipment Center (STREC) for their assistance in AFM and AAs. Many thanks also go to Mr.Thanit Singhaboonpong for antibacterial testing.

Special thanks for Miss. Aroonsri Ngamaroonchote, Miss Thanawan Ritthichai, Miss Anyaporn Boonmahitthisud, Miss Sasimon Koonarangsri, all my friends and everyone whose names are not mentioned here for their friendship, love, support, motivation, inspiration and help me in anytime when I have problems. These are much valuable and meant a lot to me.

Finally, and the most of all, I would like to express my appreciation to my family for their unconditionally love, moral support and understanding. My family impresses in my mind always and forever.

CONTENTS

Page

ABSTRACT (THAI) iv

ABSTRACT (ENGLISH) v

ACKNOWLEDGEMENTS vi

CONTENTS vii

LIST OF TABLES x

LIST OF FIGURES xi

CHAPTER I INTRODUCTION 1

CHAPTER II THEORY AND LITERATURE REVIEW 2

2.1 Antibacterial Property 2

2.2 Polyethylene 6

2.3 Polysiloxane 9

2.4 Copper 11

2.5 Plasma Modification 12

2.5.1 Plasma Theory 12

2.5.2 Classification of Plasma 15

2.5.3 Polymer Modification by Plasma 16

2.5.3.1 Ion Implantation 16

2.5.3.2 Plasma Etching 18

2.5.3.3 Radical Formation 19

2.5.3.4 Functionalization on Polymer Surface 20

CHAPTER III EXPERIMENTAL 23

3.1 Materials and Chemicals 24

3.2 Instruments 24

Page

3.3 Plasma Treatment Procedure 24
3.3.1 Preparation of Polyethylene Samples 24
3.3.2 Preparation of Silicone Rubber Samples 25
3.3.3 Plasma Treatment Process 25
3.4 Characterization and Testing 27
3.4.1 Determination of Copper Content 27
3.4.2 Analysis of Topography 28
3.4.3 Functional Group Analysis 29
3.4.4 Wettability Characterization 30
3.4.5 Antibacterial Test 31

CHAPTER IV RESULTS AND DISCUSSION 33
4.1 Characteristics and Properties of Polyethylene 33
4.1.1. Copper Content 33
4.1.2. Surface Roughness 38
4.1.3. Surface Chemical Structure 41
4.1.4. Wettability 46
4.1.5. Antibacterial Property 48
4.2 Characteristics and Properties of Silicone 49
4.2.1. Copper Content 49
4.2.2. Surface Roughness 52
4.2.3. Surface Chemical Structure 54
4.2.4. Wettability 59
4.2.5. Antibacterial Property 61

CHAPTER V CONCLUSIONS AND RECOMMENDATIONS 63
5.1 Conclusions 63
5.2 Recommendations 64

Page

REFERENCES 65

APPENDICES 69

Appendix A 70

Appendix B 82

BIOGRAPHY 120

LIST OF TABLES

Table		Page
4.1	Topography, RMS and Ra of PE samples treated by nitrogen plasma placed at position 1	40
4.2	Topography, RMS and Ra of PE samples treated by oxygen plasma placed at position 1	40
4.3	Topography, RMS and Ra of PE samples treated by argon plasma placed at position 1	41
4.4	%Reduction of *S. aureus* of plasma-treated PE samples placed at position 1	48
4.5	%Reduction of *E. coli* of plasma-treated PE samples placed at position 1	49
4.6	Topography, RMS and Ra of silicone rubber samples treated by nitrogen plasma at position 1	53
4.7	Topography, RMS and Ra of silicone rubber samples treated by oxygen plasma at position 1	53
4.7	Topography, RMS and Ra of silicone rubber samples treated by argon plasma at position 1	53
4.9	%Reduction of *S. aureus* of plasma-treated silicone rubber samples placed at position 1	61
4.10	%Reduction of *E. coli* of plasma-treated silicone rubber samples placed at position 1	62

LIST OF FIGURES

Figure		Page
2.1	An electron micrograph of *Staphylococcus aureus*	3
2.2	SEM photograph of *Escherichia coli*	3
2.3	The biofilm life cycle	4
2.4	SEM photograph of a staphylococcal biofilm on the surface	5
2.5	Chemical structure of polyethylene	6
2.6	Branched structures of (a) LDPE, (b) HDPE and (c) LLDPE	7
2.7	Chemical structure of poly(dimethylsiloxane)	9
2.8	Ring-opening polymerization of octamethylcyclotetrasiloxane	10
2.9	Reddish copper rod	11
2.10	States of a matter: (a) solid, (b) liquid, (c) gas and (d) plasma	12
2.11	Types of electron-molecule interactions	14
2.12	Types of plasma based on electron temperature and plasma density	15
3.1	The experimental scope of this research	23
3.2	Placement positions of polyethylene samples	25
3.3	UNU/ICTP plasma focus device	26
3.4	Diagrams showing four phases of plasma focus formation	27
3.5	Treated samples in 0.1% aqueous nitric acid solution	28
3.6	AAS model SpectrAA-300 atomic absorption spectrometer	28
3.7	Nanoscope IV, Scanning Probe Microscope, Atomic Force Microscope	29
3.8	Nicolet6700 Fourier-Transformed Infrared Spectrophotometer	29
3.9	CAM-PLUS Tentec contact angle meter	30
3.10	Contact angle of water droplet when (a) $\theta < 90^{\circ}$, and (b) $\theta > 90^{\circ}$	30
3.11	Antibacterial testing	32
4.1	The placement positions of the polymer samples in the plasma chamber	33

Figure		Page
4.2	Copper content of PE sample treated by nitrogen plasma	34
4.3	Copper content of PE samples treated by oxygen plasma	34
4.4	Copper content of PE samples treated by argon plasma	35
4.5	Appearances of untreated PE and PE samples treated with 10 shots of (a) nitrogen plasma, (b) argon plasma and (c) oxygen plasma	37
4.6	Appearances of untreated PE and PE samples treated without copper using 10 shots of (a) nitrogen plasma, (b) argon plasma and (c) oxygen plasma	38
4.7	Topography of untreated PE sample	39
4.8	ATR-FTIR spectra of untreated PE and PE samples treated by nitrogen plasma placed at position 1	42
4.9	ATR-FTIR spectra of untreated PE and PE samples treated by 5 shots of nitrogen plasma	43
4.10	ATR-FTIR spectra of untreated PE and PE samples treated by 5 shots of oxygen plasma	44
4.11	ATR-FTIR spectra of untreated PE and PE samples treated by 5 shots of argon plasma	45
4.12	Water contact angle of PE samples treated by nitrogen plasma	46
4.13	Water contact angle of PE samples treated by oxygen plasma	47
4.14	Water contact angle of PE samples treated by argon plasma	47
4.15	Copper content of silicone rubber samples treated by nitrogen plasma	50
4.16	Copper content of silicone rubber samples treated by oxygen plasma	50
4.17	Copper content of silicone rubber samples treated by argon plasma	50
4.18	Appearances of (a) untreated silicone rubber and silicone rubber samples treated with 10 shots of (b) nitrogen plasma, (c) oxygen plasma and (d) argon plasma	51
4.19	Topography of untreated silicone rubber	52

Figure Page

4.20 ATR-FTIR spectra of untreated silicone rubber and silicone rubber samples treated by nitrogen plasma placed at position 1 55
4.21 ATR-FTIR spectra of untreated silicone rubber and silicone rubber samples treated by 5 shots of nitrogen plasma 56
4.22 ATR-FTIR spectra of untreated silicone rubber and silicone rubber samples treated by 5 shots of oxygen plasma 57
4.23 ATR-FTIR spectra of untreated silicone rubber and silicone rubber samples treated by 5 shots of argon plasma 58
4.24 Water contact angle of silicone rubber samples treated by nitrogen plasma 59
4.25 Water contact angle of silicone rubber samples treated by oxygen plasma 60
4.26 Water contact angle of silicone rubber samples treated by argon plasma 60

CHAPTER I

INTRODUCTION

Polyethylene and silicone rubber have become important materials for using in medical devices. Polyethylene is used for many applications including biomedical materials due to its good chemical resistance, ease to process and low cost. In case of silicone rubber, it is very inert to organic compound and has good environmental resistance. For this reason, both materials can be used as catheter. However, these polymers especially polyethylene exhibit hydrophobic characteristic; therefore, bacteria causing an infection in human such as *Staphylococcus aureus* (*S. aureus*) and *Escherichia coli* (*E.coli*) can easily form the biofilm on its surface [1,2]. Consequently, it is necessary to modify these polymers in order to improve their antibacterial properties.

Plasma treatment has been increasingly applied for surface modification of many polymers since its process is more environmental friendly than conventional chemical treatment. Furthermore, it can modify the surface without changing the bulk properties of the polymers. In plasma process, many reactions and interactions such as functionalization, ion implantation and etching can occur depending on several parameters including the operating condition, the type of gas and the type of substrate. Therefore, by controlling these parameters, the characteristics and the properties of plasma-treated polymers can be achieved as desired.

In this research, copper which is a well known element that has antibacterial property [3] is implanted on the surfaces of polyethylene and silicone rubber using UNU/ICTP plasma focus device. Different types of gas and numbers of plasma shots are employed in order to find the optimum condition for the treatment. Several techniques including atomic absorption spectroscopy, atomic force microscopy, water contact angle measurement and Fourier-transform infrared spectroscopy are used for characterizations of the copper ion implantation, the surface topography and the functionalization. Antibacterial properties against *S. aureus* and *E.coli* are also stu

CHAPTER II

THEORY AND LITERATURE REVIEW

2.1 Antibacterial Property

Antibacterial compounds are the substances that interfere with the growth and reproduction of bacteria. They are classified into two groups according to their speed of action and residue production. The first group acts rapidly to destroy bacteria through the inhibition of cell wall synthesis of the bacteria. This group includes the substances such as alcohols, chlorine, peroxides, and aldehydes. The second group consists mostly of newer compounds that leave long-acting residues on the surface to be disinfected and thus have a prolonged action (referred to as *residue-producing*) via inhibition of the protein synthesis of the bacterial. Common examples of this group are triclosan, triclocarban, and benzalkonium chloride [4, 5].

However, the heavy metals such as silver (Ag), zinc (Zn), and copper (Cu) exhibit similarly antibacterial property. In the case of copper, it has a toxic effect on most microorganisms. Even though, the exact antibacterial mechanism of copper for killing bacterial is still being studied. Several theories exist and suggest that the antibacterial mechanism of copper occur through the inhibition of bacterial cell wall; for examples, copper causes the leakages of potassium or glutamate through the outer membrane of bacteria, substitution of essential ions, disturb osmotic balance, and blocking of functional groups of proteins, and causes the oxidative stress by generating hydroperoxide free radicals via membrane bound copper [6]. Moreover, copper has the ability to kill *Staphylococcus aureus* and *Escherichia coli* which are commonly bacteria that cause the infection in human body.

Staphylococcus aureus (*S. aureus*) is a genus of gram-positive coccus, which appears as grape-like as shown in Figure 2.1. The word of gram-positive is defined as the type of bacteria which are strained into dark blue or violet by Gram strain technique. *S. aureuse* has been and continues to be, a major cause of human disease because staphylococci are parasites on the body surfaces of warm blooded animals. Indeed, it is

one of the most feared pathogens because of their ability to cause irrestible sepsis and death [7,8].

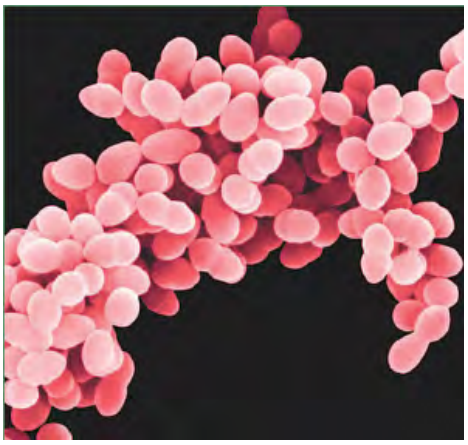

Figure 2.1 An electron micrograph of *Staphylococcus aureus* [8].

The other type of bacteria is gram-negative which cannot retain the crystal violet and appears in red or pink color classified by Gram strain technique [9]. Figure 2.2 illustrates *Escherichia Coli (E. coli)* which is a gram-negative rod-shaped bacterium. *E. coli* is usually found in the lower intestines of warm blooded animals including humans. Once expelled, it lives in penury and hazardous water, sediment, and soil. *E. coli* is a minor constituent of the human gut [10, 11].

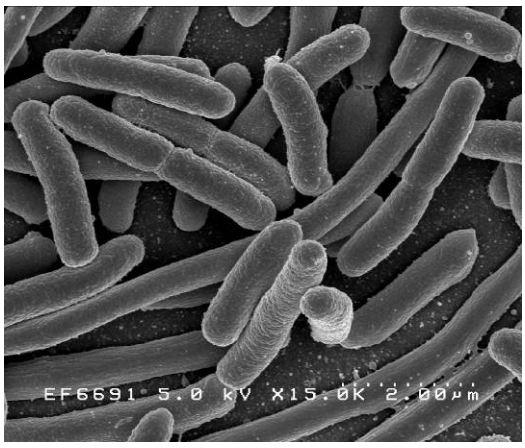

Figure 2.2 SEM photograph of *Escherichia coli* [12].

Both of *S. aureus* and *E.coli* are single-cell microorganisms which reproduce via binary fission to form the colony. Bacterial colony is defined as a visible cluster of microorganisms growing on the surface or within a solid medium, theoretically cultured from a single cell [13]. The colonies of single bacterium are clearly different from each other. In the case of bacteria which do not completely separate, the direct method for counting bacteria cannot be used due to the result is below the number of individual cells. The technique called colony forming unit is utilized for this situation. This technique measures viable cells in which a colony represents an aggregate of cells derived from a single progenitor cell [14]. The result is given as CFU/mL (colony-forming units per milliliter) or CFU/g (colony-forming units per gram).

Figure 2.3 shows the biofilm life cycle. At first, the bacteria attach themselves by physicochemical interactions with the surface of a material, electrostatic attraction and physical forces. Some of these cells permanently adhere to the surface with their extracellular polymeric substances (EPS) [15]. Afterwards, the biofilm is a growth through colonization and combination of colonies. Finally, the biofilm can propagate via detachment of bacteria. These bacteria go to attach other surface and result in the biofilm spreading on the surface as shown in Figure 2.4.

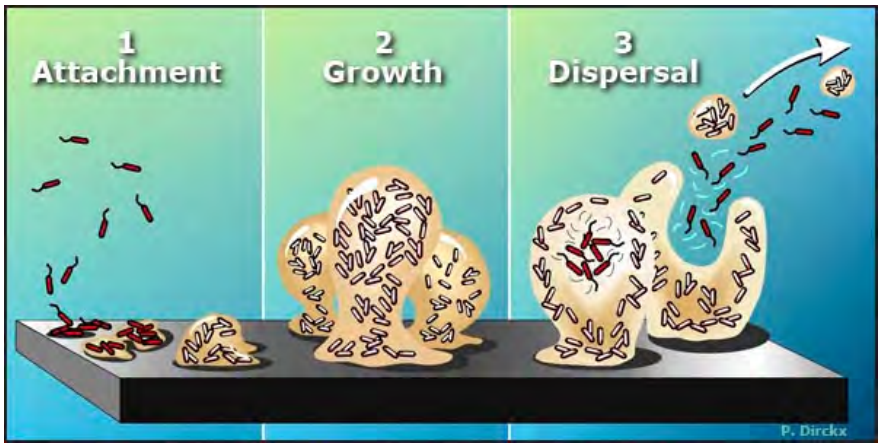

Figure 2.3 The biofilm life cycle [16]

In 1998, Y. H. An , et al. [2] reported that bacteria adhesion was a very complicated process affected by many factors such as the characteristics of the bacteria itself, the material surface and the environmental parameters. For a given

material surface, different bacterial species and strains adhere differently; this could explain physicochemically because physicochemical characteristics of bacteria are different between species and strains. The material surface is one factor that influences bacteria adhesion that is affected by surface charge energy, hydrophobicity and surface roughness or physical configuration. The effect of the surface roughness shows that rough surface has a greater surface area and the depression in the roughened surfaces provided more favorable sites for colonization. Depending on the hydrophobicity of both bacteria and the surface of the material, the bacteria adhere differently to the materials with different hydrophobicities. Hydrophilic materials are more resistant to bacterial adhesion than hydrophobic materials.

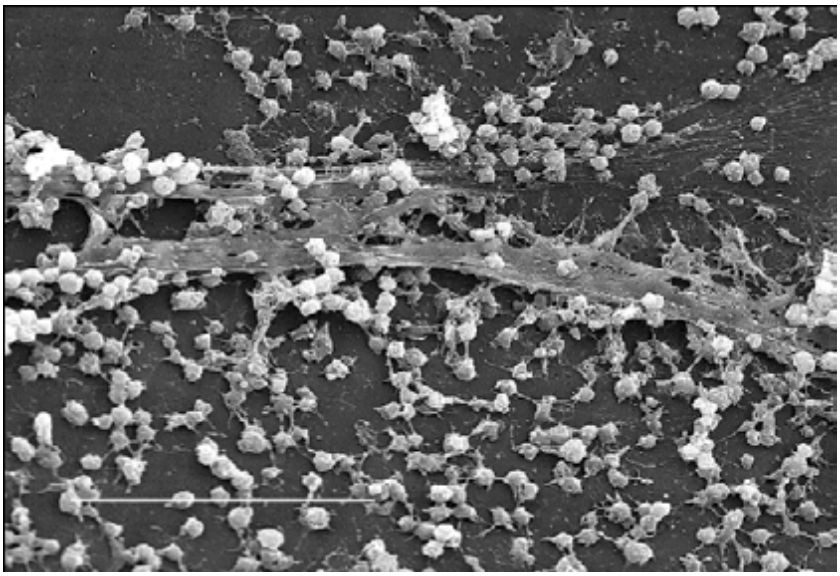

Figure 2.4 SEM photograph of a staphylococcal biofilm on the surface [14].

Biofilm are found on the surface of the materials such as metals, ceramics, composite materials, organic materials, or polymers.

2.2 Polyethylene

Polyethylene (PE) was discovered in 1933 by Reginald Gibson and Eric Fawcett at the British industrial giant, Imperial Chemical Industries (ICI) [17]. PE is a thermoplastic polymer derived from the polymerization of ethylene monomer (CH_2=CH_2). The main chain of PE has only carbon and hydrogen atoms (-CH_2-CH_2-). Their carbon atoms are in regular tetrahedral geometry. Accordingly, the structure of PE is usually a zig-zag plane, as illustrated in Figure 2.5.

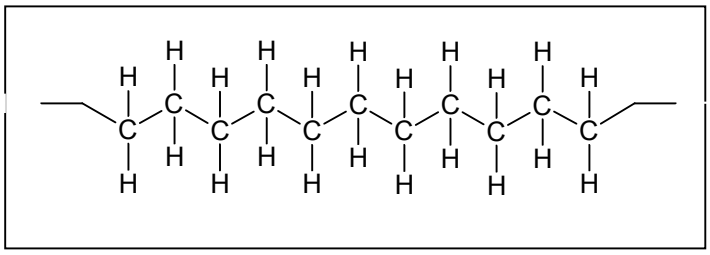

Figure 2.5 Chemical structure of polyethylene

PE can be synthesized via 3 main polymerization reactions. The first reaction is free radical chain polymerization which is used for synthesizing highly branched low density polyethylene (LDPE). The process is done using high pressures, between 1000 to 3000 atmospheres and temperatures of 150-300 ºC. An initiator is used for starting the polymerization by attacking double bond of the monomer to provide active species from which a reaction proceeds quickly by a domino effect [18]. The second reaction is coordination polymerization by Ziegler-Natta catalyst. This reaction may be called Ziegler-Natta polymerization, and named after its inventors. It is used to make high density polyethylene (HDPE) and linear low density polyethylene (LLDPE). Branched structures of LDPE, HDPE, and LLDPE are shown in Figure 2.6 (a), Figure 2.6 (b) and Figure 2.6 (c), respectively. In this method, the temperature of 70-150 ºC and the pressure less than 10 atms are employed.

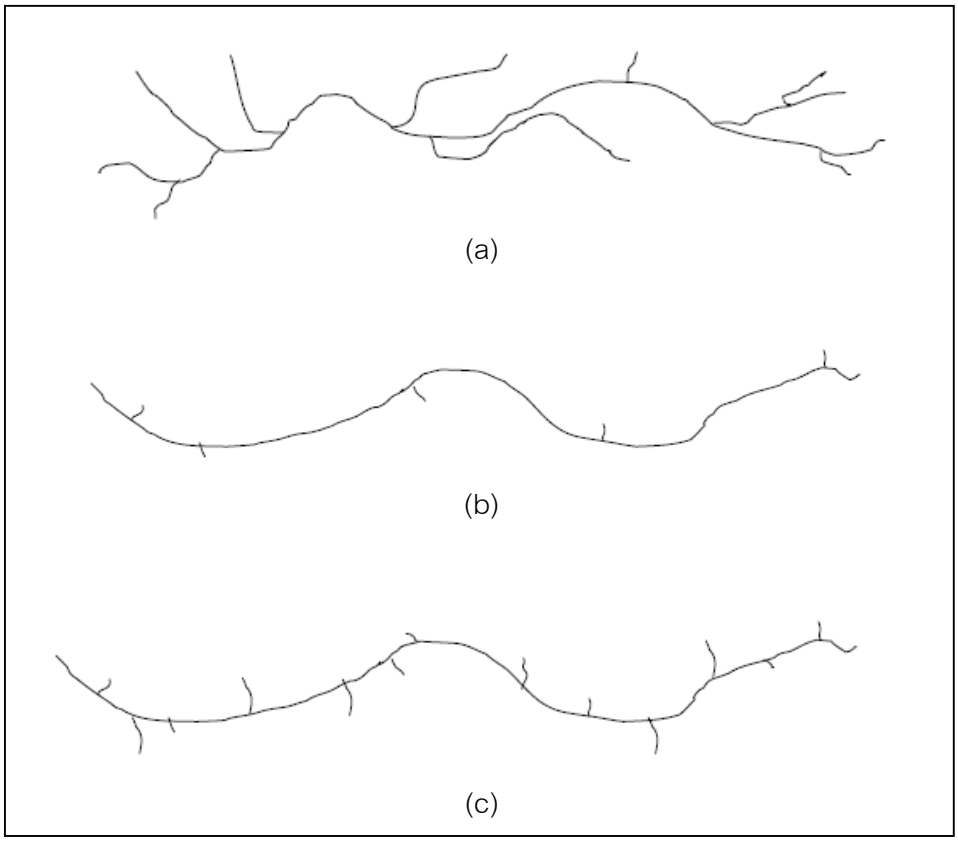

Figure 2.6 Branched structures of (a) LDPE, (b) HDPE and (c) LLDPE

The other reaction is metallocene catalytic polymerization. Metallocenes are sandwich-type organometallic molecules in which two unsaturated rings are coordinated to a metal. The polymerization of ethylene by a metallocene initiator has had a major impact on polyolefin production since it has more advantages than Ziegler-Natta systems by developing grades with even lower density and higher molecular weight [19].

PE is utilized in many applications depending on its structure. Since PE is a semi-crystalline polymer, its properties depend on the crystallinity. Highly crystalline PE has high viscosity and good mechanical properties but it is opaque. On the other hand, low crystalline PE is transparent or translucent but it has lower in mechanical properties than highly crystalline PE.

Chemical structure of HDPE contains primarily of unbranched molecules exhibiting nearly linear structure. Consequently, HDPE is highly crystalline that has good

mechanical properties thus it is also used in geo-membrane, water pipe, snow board etc. On the other hand, LDPE has short side chains due to the backbiting reaction occurring during the polymerization process. The hindered structures prevent the polymer molecules from packing closely which results in low-crystalline region. LDPE is widely used for manufacturing various containers, plastic bags, plastic wraps. In addition, there are more specific types of PE; for examples, ultra high molecular weight polyethylene (UHMWPE) which has extremely long chain. This results in a very tough material which can use a biomaterial or synthesizing the microfiber for advance textile application. Very low density polyethylene (VLDPE) is considerably linear polymer with high levels of short-chain branches synthesizing by copolymerization with short-chain alpha-olefins. VLDPE are used for hose and tubing, ice and frozen food bags.

Although, there are different kinds of PE, they share the same quality which is highly inert to chemical solvent and good biocompatible; therefore, PE is also used for medical devices or biomaterials. But it has a problem concerning its hydrophobic property. Because it is suitable for bacteria biofilm formation from *S. aureus*, it is necessary to improve the antibacterial property.

W. Zhang, et al. [20] modified antibacterial property of polyethylene through plasma immersion ion implanter equipped with a copper catholic arc plasma source, in 2006. The arc was ignited using pulse duration of 300 microseconds, repetition rate of 20 Hz, and arc current of 1 A. The antibacterial performance against *S. aureus* (ATCC6538) and *E. coli* (ATCC10536) were determined by plate-counting. XPS results showed that copper was implanted on PE surface. The surface roughness was increased as confirmed by AFM. Moreover, PE showed the increases in hydrophilic property and in antibacterial property against *E. coli* and *S. aureus* 96.2% and 86.1%, respectively. The improvement of antibacterial properties by plasma ion immersion implantation (PIII) of copper and silver ions were studied by W. Zhang, et al. in 2008 [3]. Their results showed that copper PIII and silver PIII enhanced the antibacterial properties of PE.

2.3 Polysiloxane

Polysiloxane is an inorganic polymer with a repeating unit of silicon (Si) and oxygen (O) atoms. This structure differs from other polymers in which it contains silicon atoms in main chain unlike other polymers that have carbon backbone.

Silicon-oxygen bond has one of the highest torsional obilities in any polymer backbone. Hence, provided side groups are small enough to allow that flexibility to be retained. Si-O-Si bond angle can vary over a wide range from 120^{o} to at least 140^{o} in response to an external force, and this undoubtedly reduces any intramolecular restrictions to bond torsion that might otherwise exist [19].

Siloxane bond is apparently more stable to thermooxidative attack than is the aliphatic carbon-oxygen bond. However, in solution, Si-O bond is quite sensitive to a variety of reagents, including acids and bases.

Poly(dimethylsiloxane) or PDMS is amajor commercial inorganic elastomer, known widely as silicone rubber [21]. It has lowest glass transition temperature compared to other rubbers and also serves as a high-temperature elastomer [22]. The chemical structure of PDMS composes of dimethyl groups on the silicon atoms as illustrated in Figure 2.7.

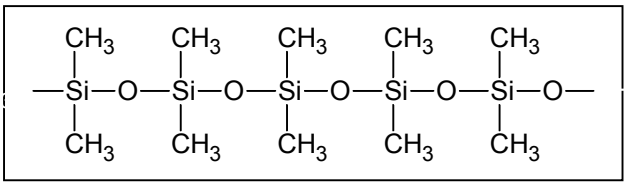

Figure 2.7 Chemical structure of poly(dimethylsiloxane)

High molecular weight polysiloxane is obtained by ring-opening polymerization of cyclic oligomers such as $(R_2Si\text{-}O)_4$ [19, 21]. The principle cyclic oligomer employed for ring-opening polymerization is octamethylcyclotetrasiloxane, which is obtained by the hydrolysis of diethyldichlorosilane. This hydrolysis yields a mixture of small rings and short chains. When heated above 100 degree Celsius with a trace of acid or base, it polymerizes following an ionic ring opening process as shown in Figure 2.8.

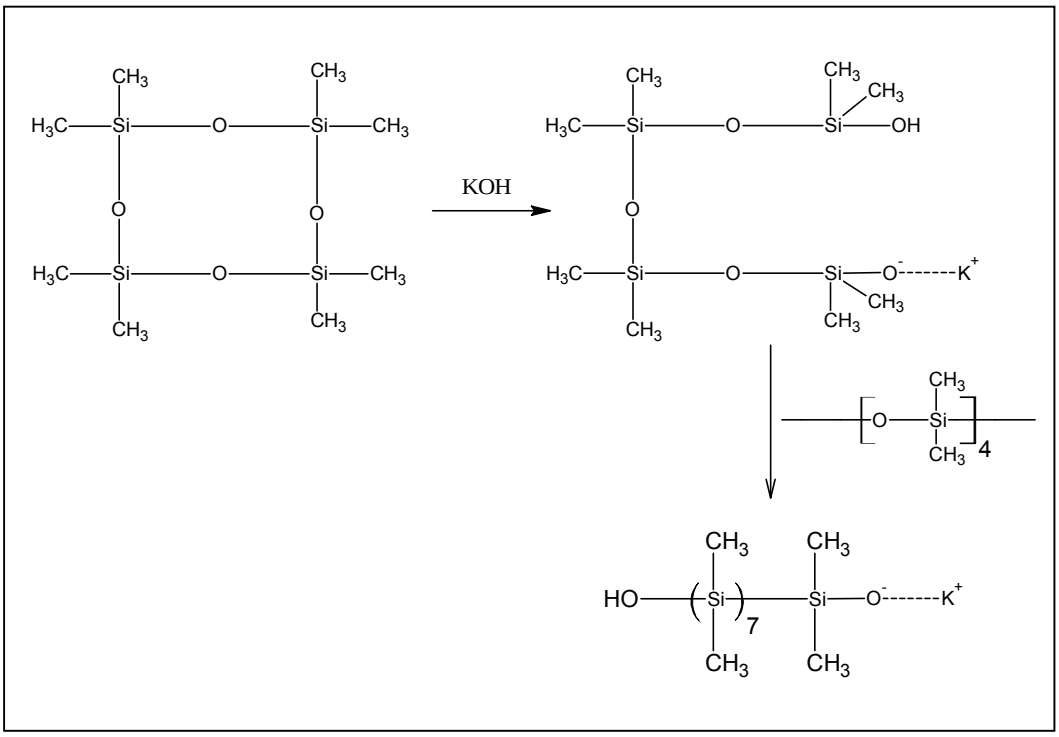

Figure 2.8 Ring-opening polymerization of octamethylcyclotetrasiloxane

Silicone rubber is made from the silicone gum (uncured rubber) by cross-linking the chains via free-radical type process. Cross-linking can also take place via hydrolysis reactions or by the addition of Si-H bonds to vinyl side groups. Silicone stop cock grease contains lower-molecular-weight dimethylsiloxane polymers or oligomer plus silica as filler. Moreover, silicone is widely used for medical device or biomedical materials because it is very inert material [19].

Silicone rubber is used for Complications of Peritoneal Dialysis (CAPD). The CAPD is one method of kidney dialysis which using catheter in the process. This catheter must be avoiding from bacteria. Thus many researches are studying modified antibacterial properties to their surface which are using chemical modification or physical modification. For example, R. Bayston, et al. [23] modified catheter using chemical method. Rifampicin, tricosan and trimethoprim were dissolved in chloroform to give concentration (w/v) of 0.2%, 1% and 1%, respectively. Silicone discs (6 mm diameter 1 mm thick) or tubing were immersed in the solution at room temperature for 1 hour, during which they swelled to approximately twice the original volume. They were then removed, briefly rinsed in ethanol and air-dried. They were then packaged and sterilized by autoclaving at 121 ^{o}C for 15 min. After that, treated sample were tested

antibacterial property against *S.epdermis*, *S.aureus* (meticillin-susceptible, MSSA), *S. aureus* (Meticillin-resistant, MRSA) and *E. coli*. In conclusion, treated sample's exhibited antibacterial efficiency about 99%.

2.4 Copper

Copper is reddish and has a bright metallic luster as shown in Figure 2.9. Copper is a transition metal with electronic configuration [Ar] $3d^{10}$ $4s^{1}$. It forms the compounds with oxidation numbers of +1 and +2: copper (I) [Ar] $3d^{10}$ and copper (II) [Ar] $3d^{9}$, respectively. In the copper (I), where the full set of filled 3d orbitals is present, the compounds are often white in color and do not have the typical properties of a transition metal compound. However, in the copper (II), it shows the typical transition metal properties. The higher charge on the copper ion gives stronger bonding, compensating for the extra energy required to remove an electron from the 3d orbital in addition to one form the 4s orbital [24].

Figure 2.9 Reddish copper rod [25]

Copper has negative electrode potentials for both Cu/Cu^{2+} and Cu/Cu^{+} systems and relatively low reactivity. When exposed to oxygen in the presence of carbon dioxide, copper is oxidized very slowly to form a green film of basic copper (II) carbonate, $CuCO_3.Cu(OH)_2$. Moreover, copper reacts with acid only in oxidizing conditions. It is not affected by hydrochloric acid. It reacts with moderately diluted and concentrated nitric acid to form copper (II) nitrate, and it is oxidized much more rapidly by concentrated

nitric acid. In addition, the most stable oxidation number of copper is +2 and most copper compounds contain Cu^{2+} ion [25].

Copper is malleable, ductile, and a good conductor of heat and electricity. Moreover, it is utilized in medical device due to its antibacterial property. Bacteria do not grow on copper because it is biostatic. Copper doorknobs are used by hospitals in order to reduce the transfer of disease, and Legionnaires' disease is suppressed by copper tubing in air-conditioning systems.

2.5 Plasma Modification

2.5.1 Plasma Theory

Plasma is an ionized gas state, may be defined as the fourth state of a matter. This state is a result of increasing energy to the matter and this transforms the matter from solid into liquid, then into gas, and finally into plasma state. The atoms are brokendown into electron, neutron and ions [26]. Figure 2.10 shows the states of a matter.

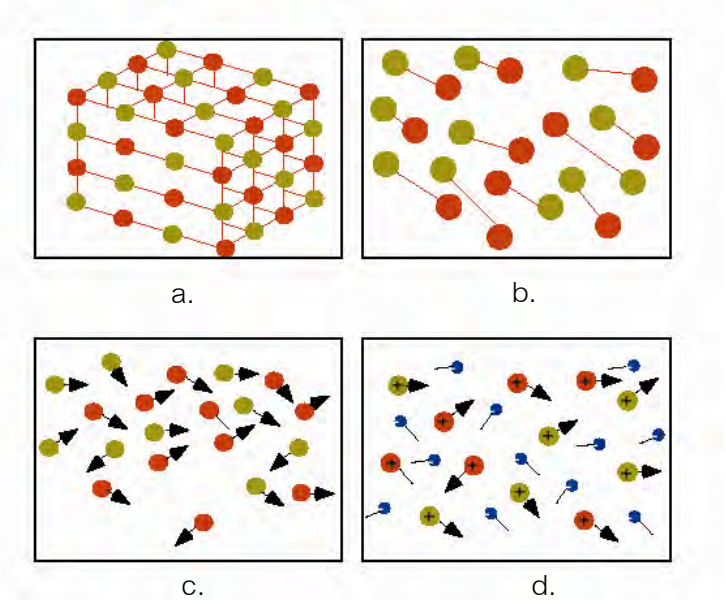

Figure 2.10 States of a matter: (a) solid, (b) liquid, (c) gas and (d) plasma

Plasma is a collection of electrons, ions, and neutral atoms in which the net Coulomb force between the charged particles dominates the behavior of the group. Resulting from ionization of neutral gas, plasma contains equal numbers of positive and negative charges in the system. In this situation, plasma is generally quasi-neutral which describes as charge neutrality of a plasma overall when the oppositely charged are strongly coupled, and tend to electrically neutralize one another on macroscopic length scales. Three important factors used to define a plasma are Debye length (λ_D), plasma frequency (ω_{pe}) and plasma parameter (Λ). Debye length is the distance in plasma over the static electric fields of their initial length. Plasma frequency is the rate at which electrons collectively oscillate back and forth when disturbed from their equilibrium positions. Plasma parameter is the number of charged particles in a sphere having one Debye length in radius [27].

The first elementary of plasma process is an ionized gas which means conversion of neutral atoms or molecules into electrons and positive ions. The ionization process is a result of the collision between the electrons with atoms or molecules. The collision is divided into two types: elastic and inelastic. The elastic collision means that the internal energy of electron does not change. Therefore, total kinetic energy is conserved. On the other hand, inelastic process results in geometric scattering and redistribution of kinetic energy [28]. The ionization of plasma is caused by inelastic collision which results in energy transfer from the kinetic energy of colliding partners into internal energy.

Figure 2.11 shows the important types of electron-molecule interactions. When the energetic electrons collide with neutral atoms, it transfers the energy through inelastic collision. The chemical effects of particles in plasma occur;

1. Scattering : $e^- + A \rightarrow A + e^-$
2. Excitation : $e^- + A \rightarrow A^* + e^-$
3. Ionization : $e^- + A \rightarrow A^+ + 2\,e^-$
4. Recombination : $e^- + A^+ \rightarrow A + (hv)$

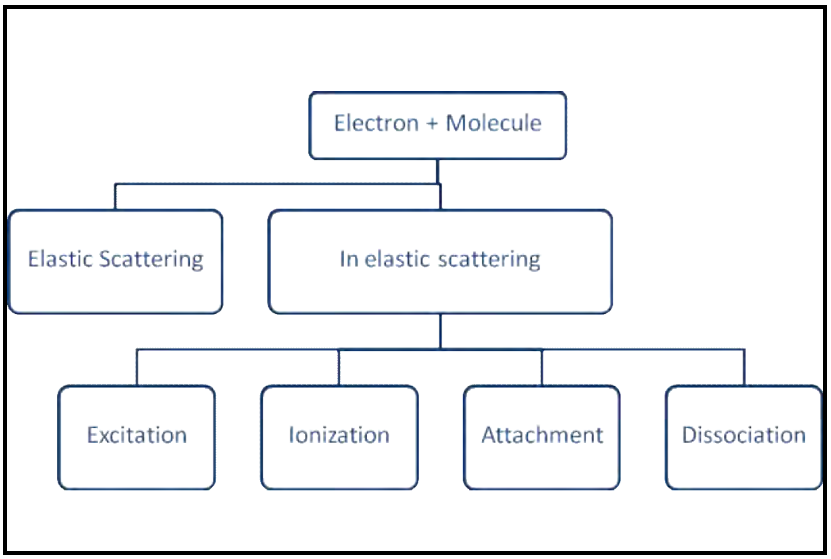

Figure 2.11 Types of electron-molecule interactions

The impact of energetic electrons with neutral atoms or molecules leads to exited state. Moreover, energetic electrons can ionize a neutral molecule and generate the positive ion. Afterwards, electrons and ions may recombine resulting in neutral atom and causing irradiation, for examples, photon, X-rays etc.

Plasma is usually found in the universe such as the solar corona, solar wind, and nebula. However, plasma can occur in Earth's atmosphere. The best known natural plasma phenomena in Earth's atmosphere is lighting and the most beautiful plasma phenomena is aurora borealis. Plasma also occurs from man-made device with a wide range of pressure, electron temperature, and electron density [29]. Figure 2.12 shows the types of plasma categorized in terms of electron temperature and plasma density as shown in. Electron temperature is expressed in electron volts (eV) where 1 eV is equal to approximately 11,600 K. Manmade plasma ranges from slightly above room temperature to the temperatures comparable to the interior of stars.

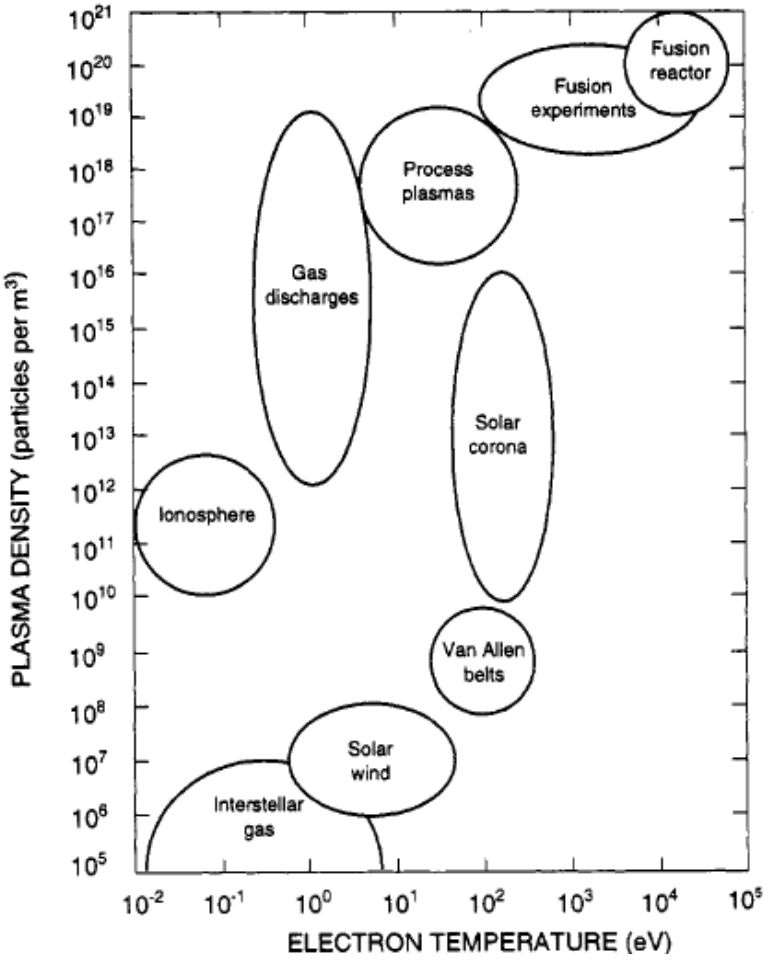

Figure 2.12 Types of plasma based on electron temperature and plasma density [29]

2.5.2 Classification of Plasma

Plasma may be classified into two types: cold plasma and hot plasma. Cold plasma is partially ionized gas which is usually used in industry due to the ease to generate the plasma at low pressures or at low power levels. The disadvantage of cold plasma is that its generating process uses longer time which can cause the degradation of a material. For examples, in 2007, T. Kobayashi, et al [30] showed that plasma generated heat on the material surface. In this research, silicone catheters were treated with argon plasma generated from pulsed radio frequency (13.56 MHz, 500 W) for 30 minutes. During the process, the temperature of the sample surface was not measured

but the temperature behind the sample was below 95^{o}C as measured by a sticker-type temperature indicator.

Hot plasma is defined as fully ionized gas. In this system, the electron temperature is equally with the temperature of heavy particles at nearly 1 eV (T_e=T_h=11000K). Hot plasma generated in pulse utilized for surface modification of several materials has been reported [31]. Because plasma exposure is easier to control and shorter time (microsecond) is used; thus, most polymeric materials having low heat resistance can be modified by this system with less degradation when compared to conventional continuous plasma generating process. From this point of view, pulsed-plasma treatment is selected for surface modifition of polyethylene and silicone rubber in this work.

2.5.3 Polymer Modification by Plasma

The different properties of plasma-treated polymers are depended on the treatment conditions such as the type of gas, the power, the pressure, and the exposure time. Different plasma species exhibit different reactions and/or interactions with the polymer surface.

The modification process starts when plasma is exposed to the polymer surface. The electron, ions, and neutral species in plasma collide with the molecules on the surface leading to several reactions and interactions. While some layers of the treated surface are removed by the process called etching, new functional groups can be formed via the reactions such as oxidation. Moreover, radical species can be obtained by chain scission which can later combine to form crosslinks or initiate grafting reaction. The presence of a metal can cause an ion implantation on the polymer surface.

2.5.3.1 Ion Implantation

Ion implantation is a surface modification process in which energetic ion beam is injected into the near-surface region of a substrate [32]. This process can be done on many types of substrate including metals, ceramics, and polymers [33].

Plasma ion immersion implantation or PIII is one process used for ion implantation. In this process, a substrate is immersed in a high density plasma (10^{10}-10^{11}/cm^3) produced by efficient ionization sources such as microwave source operating at 21.45 GHz. The substrate is negatively biased by a direct or by a pulsed voltage. These two operation modes are called dc PIII and pulsed PIII, respectively. When an abrupt voltage is applied to the substrate, the electrons near the surface are repelled, leaving behind a uniform density sheath of positive ions. These ions are accelerated toward the negatively biased substrate. The ion movement lowers the ion density and the sheath-plasma boundary expands. Other positive ions are extracted until a steady state condition is reached and the current becomes space-charge limited as in a diode [34]. The main use of PIII in microelectronics has been the formation of shallow junctions with depths < 100 nm and with the preservation of ultrathin (<10 nm) gate dielectrics. These applications are of interest in ultra-large-scale integrated circuit fabrication [34].

In 2006, T.L. Schiller, et al studied PIII of poly(tetrafluoroethylene) (PTFE) [35]. It was used with a filtered cathodic arc to implant copper and carbon ions onto the surface of PTFE. PTFE substrates for copper implantation were placed perpendicular to the plasma beam, while those for carbon implantation were oriented parallel to the drift velocity of the beam to minimise the deposition of low energy ions. Electrodes in the form of a backing plate and a mask with holes were used to apply the pulsed bias from the PIII supply. The structures of PTFE induced by both copper and carbon implantations were determined by X-ray photoelectron spectroscopy (XPS). Raman spectroscopy of the carbon implanted samples showed the presence of an amorphous carbon peak, which remained even after cleaning the surface for removing loosely bound carbon. This indicated both carbon implantation and carbon deposition on the surface. In the case of copper, this method resulted in well-adhered films. The implanted PTFE was examined for changes in wear resistance. Both copper and carbon modified surfaces showed the improvement of wear resistance.

In 2008, W. Zhang and P. K. Chu [3] investigated and compared the effects of Cu and Ag PIII on polyethylene (PE). The growth and behavior of different cell lines on the modified surfaces were determined. It was found that although Ag elemental depth profiles were similar to those of Cu, there was a larger amount of Ag on the surface

compared to Cu possibly due to the different charge states in the plasma. Photoluminescence was found to be enhanced after Cu and Ag PIII based on Raman studies. Antibacterial tests against *E. coli* showed that both Ag PIII and Cu PIII improved antibacterial property. However, Ag PIII resulted in better antibacterial properties than Cu PIII in spite of using similar parameters. Based on cell assays, all PE samples exhibited excellent biocompatibility for bone cells. However, Chinese hamster ovary (CHO) cells showed a non-uniform distribution on their surfaces after incubating for 2 days. Therefore, the surface of PE after Cu and Ag PIII exhibited little adhesion and biocompatibility for CHO cells.

The characteristics of copper oxide films deposited by plasma based ion implantation and deposition using a copper antenna as radio frequency sputtering ion source were studied by X. Ma, et al [36], in 2006. A gas mixture of $Ar+O_2$ was used as working gas. During the process, copper was sputtered from the rf antenna reacted with oxygen and deposited on a silicon substrate. The composition and the chemical state of the deposited films were analyzed by XPS. X-ray diffraction (XRD) was used to determine the composition of the films. XPS results suggested that there were CU_2O and CuO on the treated silicon substrate. The composition of the deposited film as a result of plasma treatment was Cu_2O, while CuO occurred due to the oxidation of Cu_2O with the oxygen in ambient air during the sample storage. An appropriate applied voltage of 2 kV under the present conditions caused the electrical resistance. It was also seen that the maximum light absorbance of the deposited films moved to lower wavelength with increasing applied voltage.

2.5.3.2 Plasma Etching

Plasma etching or ablation is a removal of the weak bond layer from the surface by the plasma [37, 38]. Amorphous polymer is removed many times more rapidly than either its crystalline counterpart or inorganic materials. The gas type can determine whether the treatment can induce higher or lower degree of etching. Reactive gases such as oxygen and tetrafluoromethane, can have much greater etching effect than non-reactive gases [39] Plasma etching strongly affects the surface roughness of a

material either by increasing or decreasing this characteristic depending on the gas type and the type of substrate as previously mentioned. Furthermore, it can cause a weight loss and a reduction of the molecular weight. However, etched fragments may re-deposited on the substrate by interaction with the active particles on the substrate surface leading to undesirable results on etching processing. The etching and re-deposition can repeatedly occur many times during the process.

Plasma etching has many applications especially in semiconductor and optoelectronic processings, such as photoresist removal, thin film etching, and polymer etching. In optoelectronic manufacturing, plasma etching has been employed to produce stripped fibers through the controlled removal of the urethane acrylate buffer coating [40].

V. Sˇvorcı´k et al. [41] studied the ablation and etching of high density polyethylene (HDPE) exposed to argon plasma for 240 s at 8.3 W power. It was found that under the experimental conditions ca. 30 nm thick layer was ablated, the surface topography analyzed by atomic force microscopy (AFM) changed dramatically and surface roughness increased. The cleavage of macromolecular chains was proved by the presence of surface free radicals. Oxygen containing groups known to enhance the surface solubility were detected. Under present laboratory conditions ca. 20 nm thick surface layer was dissolved during 24 h. After water dissolution of the surface, the roughness increased.

2.5.3.3 Radical Formation

Radicals are atoms, molecules, or ions with unpaired electrons. Radical formation in plasma chemistry is resulted of the collision between active species and molecules on substrate surface or UV-radiation via breaking of covalent bonds. The formation of radical sites occurs via ionization or excitation of the polymers through electrostatic interaction between fast moving electrons and the orbital electrons in the polymers. The consequent ionization leads to molecular fragmentation and the formation of a free radical. In the same way, excitation results in dissociation of the excited polymers, also the formation of free radicals [26].

$$e^- + AB \xrightarrow{\text{radiation}} AB^+ + e\text{-} \text{ (Ionization)}$$

$$e^- + AB \xrightarrow{\text{radiation}} A^+ + B + e^-$$

$$AB \xrightarrow{\text{radiation}} AB^* \text{ (Excitation)}$$

$$AB^* \longrightarrow A\cdot + B\cdot \text{ (Dissociation)}$$

Radical formation can induce the grafting, cross-linking or radical polymerization. Moreover, in plasma assisted chemical vapor deposition (PCVD) [26], the radicals do not chemically react with the substrate. Instead, the radicals combine to form stable chemicals.

H. Yasuda et al. [42] pointed out an important aspect of radical formation by interactions between polymeric materials and plasma. A glass rod was coated with polyethylene films, and the polyethylene-coated glass rod was exposed to nitrogen plasma at an RF power (13.56 MHz frequency) of 75 or 100 W at a pressure of 0.12 torr. The spin concentration generated in the glass rod was measured by electron spin resonance (ESR) spectroscopy. On the ESR spectra, some spins were observed, indicating that the radicals were generated by the plasma exposure. The spin scarely decayed 20 hr after completing the plasma exposure, even if the glass rod was stored in air. The spin concentration (arbitrary unit) in the polyethylene-coated glass rod was 5.2 and 4.9 after the air exposure time of 0.25 and 20 hr, respectively. This lower decay time meaned that radicals were caged and stable in the polyethylene chains without transfer reactions of the radicals.

2.5.3.4 Functionalization on Polymer Surface

Surface functionalization introduces the chemical functional groups on the surface region for capable of interaction with adhesive or other materials deposited on the polymer.

Nitrogen plasma and nitrogen containing plasma are widely used for functionalization of amino, amine, imine, and imide groups. The presence of these

groups can improve the hydrophilicity of the polymer surface. N. Inagaki, et al. [43] used NO, NO_2, O_2 or N_2 for generating plasma by radio frequency. The contact angles of water, glycerol, formamide, diiodomethane and tricresyl phosphate were used for measuring the wettability of the treated samples. The results showed that treated samples exhibited distinguished hydrophilic characteristic with dramatically decay.

Surface modification by oxygen plasma is designed to create the polar groups such as carboxyl, hydroxyl, ether, etc. through activated oxygen species. The total surface oxygen concentration can be controlled by varying the processing parameters including the exposure time and the plasma density.

On the other hand, fluorine plasma and fluorine-containing plasma are utilized for decreasing the surface energy of the polymer resulting in an increase in its hydrophobicity. For example, Y. Khairallah, et al. [44] studied the surface fluorination of polyethylene films by different glow discharge. Carbontetrafluoride was feeded into the plasma reactor. Parallel-plate radio-frequency (RF) reactors operating at 13.56 MHz were used for this experiment. The wettability of the treated surface decreased due to the formation of the fluorinated groups on the surface as confirmed by XPS.

Moreover, the functionalization can utilize for improving specific properties including antibacterial property or biocompatibility of medical devices. In 2004, R.L. Williams, et al. [45] studied the effect of low-power plasma treatment of silicone rubber on the interfacial aspect of blood compatibility. The treatment was operated using radio frequency of 13.6 MHz in 1 minutes. Four different gases which were O_2, N_2, Ar and NH_3 were varied. Aging property in phosphate buffer saline or air for up 1 month of the treated samples were investigated. The resultes showed that all treatments increased the wettability. Thromboplastin was used for indicating the influence of surface modification on the blood compatibility. It was demonstrated that O_2 and Ar plasma treatments reduced the performance of the silicone but N_2 and NH_3 treatments had significantly beneficial effect on the activation of the coagulation cascade.

In 2005, P. Jumpa, [46] et al used the plasma focus device for enhancing mechanical properties of polypropylene and polyester/cotton composites. Polypropylene (PP) nonwoven was surface-modified using a small 3 kJ plasma focus device operated with nitrogen or oxygen gases at a pressure of 1.5 mbar and 4 plasma

shots. Water contact angle analysis revealed an increase in hydrophilicity of the surface of plasma-modified PP nonwoven due to the formation of hydrophilic groups on fabric surface confirmed by ATR-FTIR spectroscopy. The lamination of PP and polyester/cotton (PET/C) nonwovens at weight ratio of 80:20 was carried out by compression molding at 190°C for 12 minutes to obtain PP-PET/C composite material. It was found that impact strength of all surface-modified composites greatly increased when compared to those of unmodified composite and PP plastic while their tensile and flexural properties were comparable. It was also found that the type of gas and the treatment position of PP nonwoven in the chamber affected the mechanical properties of the composites. Overall results indicated that the composite prepared from PP nonwoven surface-modified by oxygen plasma had the best mechanical properties, when PP nonwoven was placed directly on top of the focusing position.

Since the above research suggests the application of a plasma focus device on a polymer having low heat resistance such as PP, it is selected to be used in this research for surface modification of polyethylene and silicone rubber. It is expected that besides functionalization and etching, copper ion implantation should possibly occur as was reported by P. Kamsing, et al [47], in 2000. Due to the toxicity of copper toward the bacteria as previously mentioned, the presence of copper should improve the antibacterial property of these polymers which is the aim of this research.

CHAPTER III
EXPERIMENTAL

In this chapter, polyethylene and silicone rubber were treated by high temperature-pulsed plasma generated from UNU/ICTP plasma focus device in order to improve their antibacterial property. All plasma-treated polyethylene and silicone rubber were characterized and their characteristics and properties were compared to those of the untreated ones. The scope of this research is shown in Figure 3.1.

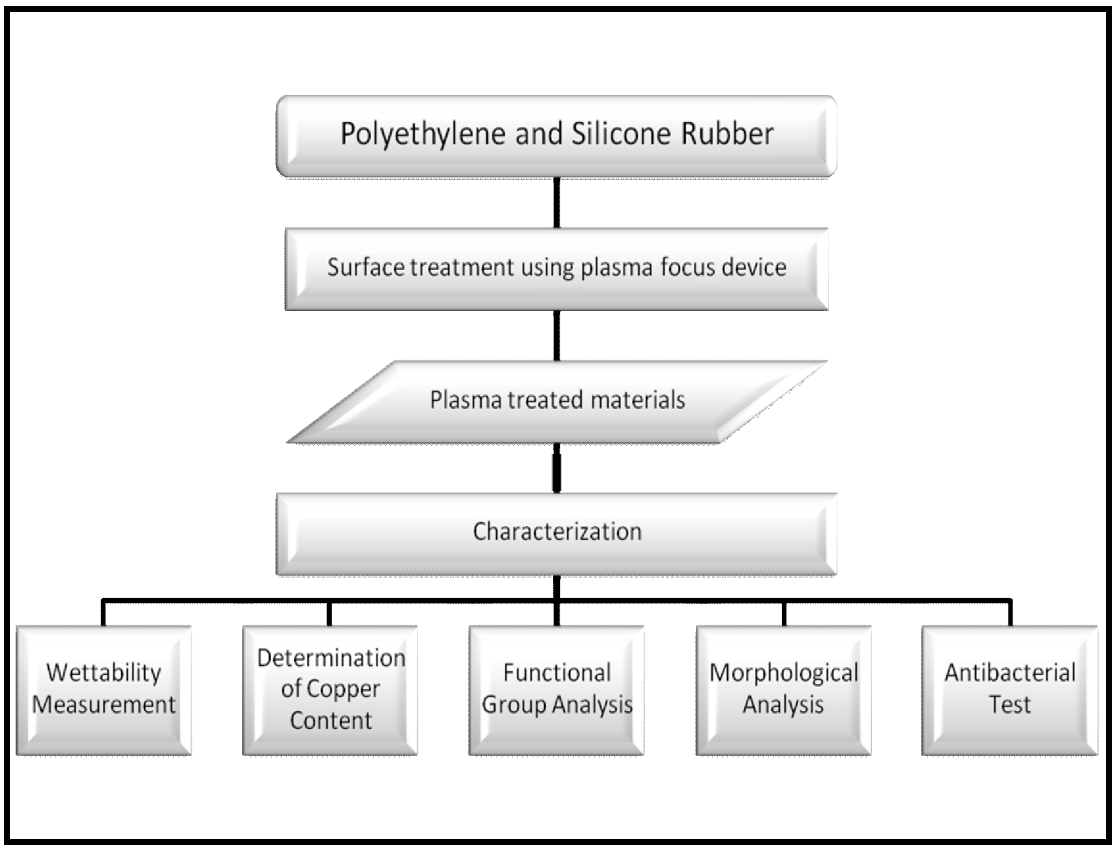

Figure 3.1 The experimental scope of this research

3.1 Materials and Chemicals

3.1.1 Low density polyethylene in the form of sheet was purchased from Daiso sankyo (Thailand).

3.1.2 Silicone rubber in the form of tube was purchased from Charoenchai rubber.

3.1.3 65% w/v Nitric acid was purchased from APS Ajax Finechem.

3.1.4 Oxygen gas having a purity of 99.5% was purchased from Thai Industrial Gases public Co., Ltd.

3.1.5 Nitrogen gas having a purity of 99.9% was purchased from Thai Industrial Gases public Co., Ltd.

3.1.6 Argon gas having a purity of 99.9% was purchased from Thai Industrial Gases public Co., Ltd.

3.2 Instruments

3.2.1 Plasma focus device: United Nation University/International Center for Theoretical Physics (UNU/ICTP)

3.2.2 Atomic absorption spectrometer: AAS model SpectrAA-300

3.2.3 Atomic force microscope: Nanoscope IV, Scanning Probe

3.2.4 Fourier Transformed Infrared Spectrophotometer: Nicolet6700

3.2.5 Contact angle meter: CAM-PLUS Tentec

3.3 Plasma Treatment Procedure

3.3.1 Preparation of Polyethylene Samples

Polyethylene sheet was cut into the squared samples having the dimension of 4 cm x 4 cm (width x length). Afterward, the samples were adhered on the chamber cover of UNU/ICTP plasma focus device at 3 different positions using double-sided foam tape.

Positions 1 and 3 were the sides of the cover and the middle of the cover was position 2 as shown in Figure 3.2.

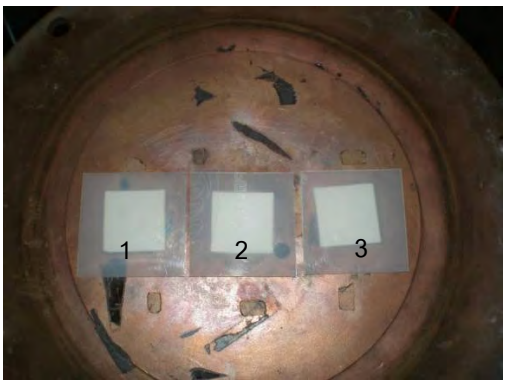

Figure 3.2 Placement positions of polyethylene samples

3.3.2 Preparation of Silicone Rubber Samples

Silicone tube was cut into the squared samples having a dimension of 4 cm x 4 cm (width x length). The samples were inserted into the wooden frame and then adhered on the chamber cover of UNU/ICTP plasma focus device to overcome the non-stick property of silicone rubber. The placement positions were the same as employed for polyethylene samples.

3.3.3 Plasma Treatment Process

After closing the chamber cover, the remaining gas in the chamber was removed from UNU/ICTP plasma focus device by vacuum pump before starting the process. In general, this device generates the plasma having a short life but high temperature and high density through a pulsed coaxial accelerator using pulsed DC current with high voltage. The plasma focus tube composes of one tube of the copper anode surrounded by six rods of the copper cathode as shown in Figure 3.3. When the plasma focus is generated, the copper ions, x-rays, and other radiations are emitted from the copper anode by ion bombardment. These copper ions can implant on the

surface of a material while x-rays and other radiations may react or interact with the material.

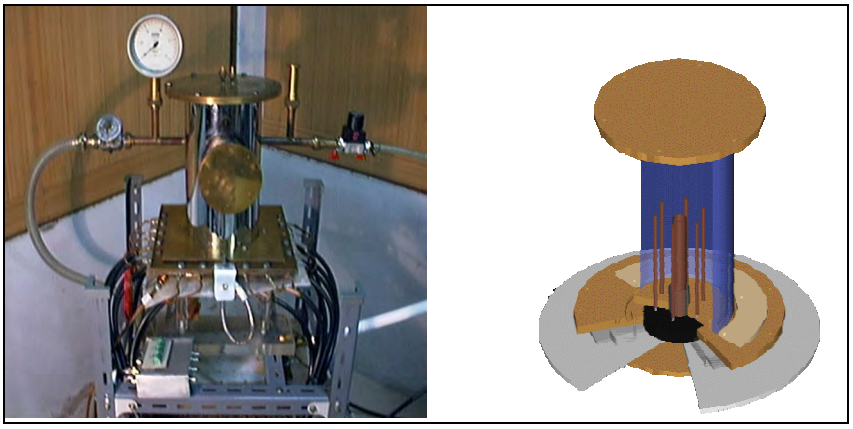

Figure 3.3 UNU/ICTP plasma focus device

The plasma generating process begins after charging the energy to the capacitor bank. When the optimum voltage is adjusted, the trigger is used for discharging the current from the capacitor bank to plasma focus tube. The first step is breakdown phase starting from the base of the anode as shown in Figure 3.4a. The symmetrical plasma sheath is formed along the electrode axis and lifts off from the glass insulator.

When the plasma sheath completely lift-off from the glass insulator at the base of the anode, the current flows radially outward from the inner anode to the outer cathodes. After a thicker plasma sheath is built, it moves up along the Z-direction from the base of the top of the anode. This phase is called the "axial acceleration phase" as shown in Figure 3.4b. The axial acceleration phase is very important because the structure of the dense plasma or pinched plasma at the end of the process is determined from this phase. The dense plasma is formed based on 2 factors. They are the regularity of the current sheet and the structure of the plasma sheath which must be balance and suitable for generating the plasma focus [48].

The third phase is the radial phase. The plasma sheath moves in radial direction. Then, the plasma sheath collapses radially as shown in Figure 3.4c. At the end of the radial phase, a dense plasma column is formed on the axis of the focus tube just off the face of the anode. During this dense plasma phase, soft X-rays and other types of

radiations can be emitted from the plasma. This final phase is the focusing phase as shown in Figure 3.4d [31].

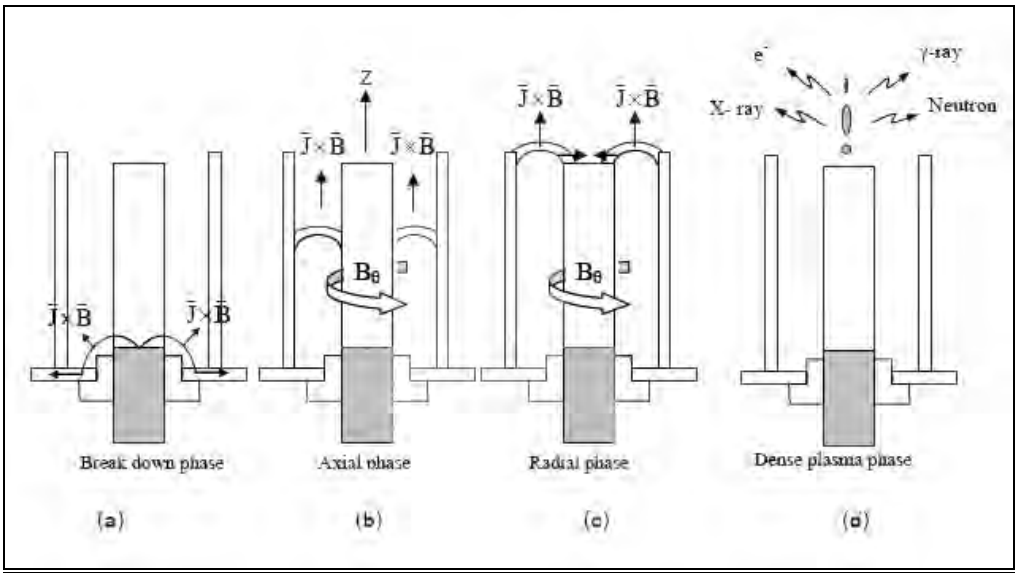

Figure 3.4 Diagrams showing four phases of plasma focus formation [31]

In this research, the plasma focus device was operated at a pressure of 1.5 mbar and a discharge voltage of 12.5 kV. The types of gas were changed from nitrogen, oxygen and argon while the numbers of plasma shot were varied from 3, 5, 7 to 10 shots. After the process completed, the samples were removed from the chamber and characterized.

3.4 Characterization and Testing

3.4.1 Determination of Copper Content

Plasma-treated samples were cut into the small pieces and put in the beaker containing 0.1% aqueous nitric acid solution (as shown in Figure 3.5) at room temperature for 24 hours in order to dissolve the copper from the sample. Afterwards, the atomic absorption spectrometer (AAS model SpectrAA-300) as shown in Figure 3.6 was used to detect the amount of the copper in the solution.

Figure 3.5 Treated samples in 0.1% aqueous nitric acid solution

Figure 3.6 AAS model SpectrAA-300 atomic absorption spectrometer.

3.4.2 Analysis of Topography

Atomic force microscope (AFM) was used to investigate the surface roughness of untreated and plasma-treated samples. The absolute surface roughness (Ra) and the root mean square roughness (RMS) of samples were obtained. Average absolute deviation of the roughness irregularities from the mean line over one sampling length is Ra while the root mean square roughness of the profile height deviations from the mean line, recorded within the evaluation length is RMS. High numbers of RMS and Ra imply high surface roughness.

Each sample with a dimension of 1 cm x 1 cm (width x length) was scanned by Nanoscope IV scanning probe microscope as shown in Figure 3.7 using a tapping-mode at a scan rate of 1.197 Hz. The scanning area was 5 μm x 5 μm.

Figure 3.7 Nanoscope IV, Scanning Probe Microscope, Atomic Force Microscope

3.4.3 Functional Group Analysis

Functional groups on the surface of untreated and plasma-treated samples which were characterized by Nicolet6700 Fourier-Transformed Infrared Spectrophotometer as shown in Figure 3.8 using a frequency range of 600-4000 cm^{-1}, 32 consecutive scans and 4 cm^{-1} resolution. PE sheet and silicone tube were cut into the samples having a dimension of 4 cm x 4 cm.

Figure 3.8 Nicolet6700 Fourier-Transformed Infrared Spectrophotometer

3.4.4 Wettability Characterization

CAM-PLUS Tentec contact angle meter as shown in Figure 3.9 was used to determine the water contact angle of each sample at room temperature according to ASTM D5725-99.

Figure 3.9 CAM-PLUS Tentec contact angle meter

10 ml of distilled water were dropped on the surface of each sample. Water contact angle as shown in Figure 3.10 was measured. For each sample, water contact angles from 3 postions were determined and the average value was reported.

θ = contact angle

Figure 3.10 Contact angle of water droplet when (a) $\theta < 90^{\circ}$, and (b) $\theta > 90^{\circ}$

3.4.5 Antibacterial Test

Figure 3.11 shows the schematic diagram for antibacterial testing. Antibacterial properties against *S. aureus and E. coli* were investigated using the same method. Before testing, untreated and plasma-treated samples were sterilized by UV radiation at the wavelength of 260-270 nm. Afterwards, each sample was immersed in 50 ml of bacterial solution composing of 500 μl with 10^5 CFU/ml of bacteria and nutrient broth, NB. The bacteria were incubated at 37 ^{o}C for 24 hours. Then 1 ml of this solution was diluted with 9 ml of 0.85% NaCl solution for 6 times. To investigate the living bacteria, 0.1 ml of the diluted solution was cultured in nutrient agar for 24 hours at 37 ^{o}C. Thereafter, bacteria colonies were counted and the antibacterial efficiency was calculated by the following equation:

$$\%R = \frac{A-B}{A} x100$$

When R = %reduction of bacterial colonies.

A = the number of bacteria recovered from the inoculated untreated specimen incubated over the desired contact period (control specimen)

B = the number of bacteria recovered from the inoculated treated specimen incubated over the desired contact period. (test specimen)

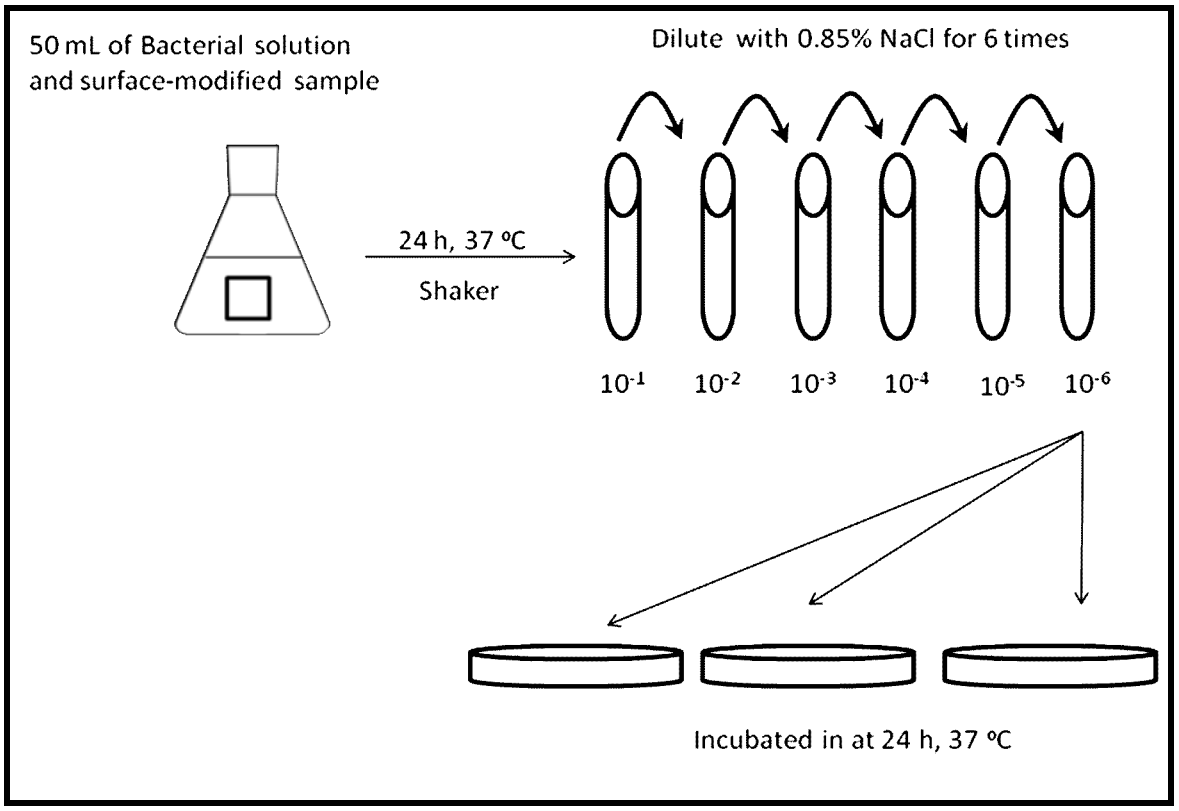

Figure 3.11 Antibacterial testing

CHAPTER IV

RESULTS AND DISCUSSION

This work emphasized on the characteristics and properties of polyethylene and silicone rubber after treatment by high temperature-pulsed plasma generated from a plasma focus device. The number of plasma shots and the type of gas were varied while other discharge parameters were kept constant in each experiment. In addition, the effect of the placement positions of the polymer samples in the plasma chamber as shown in Figure 4.1 was also investigated.

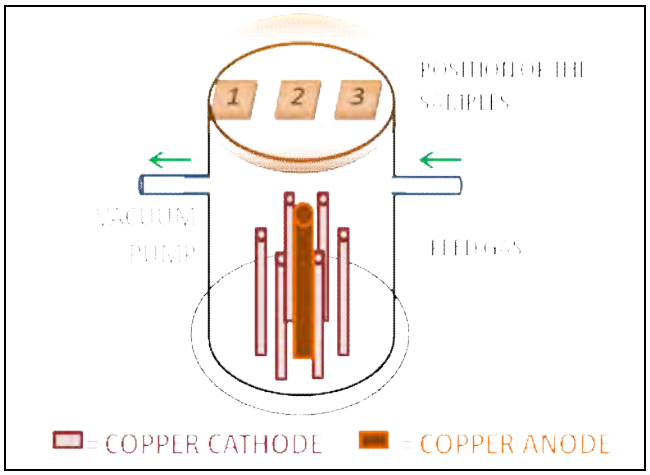

Figure 4.1 The placement positions of the polymer samples in the plasma chamber

4.1 Characteristics and Properties of Polyethylene

4.1.1. Copper Content

From Figure 4.2, it is clearly seen that nitrogen plasma-treated PE samples placed at positions 1 and 3 have higher copper contents than that placed at position 2. This was due to the plasma generating process of UNU/ICTP plasma focus device as previously described in 3.3.3. Since the plasma sheath collapses radially to form a dense plasma on the axis of the focus tube just off the face of the anode, at the focusing

phase, this dense plasma mainly expose at position 2 while the copper ions and other types of radiations can spread out from the focusing position. Therefore, it is possible for copper ion implantation to occur at positions 1 and 3 more than at position 2 resulting in higher copper contents of the samples placed at these positions. Furthermore, this figure also shows that the copper contents of nitrogen plasma-treated PE samples increase with increasing the number of plasma shots. This indicates that higher number of plasma exposure results in higher copper ion implantation on PE surface.

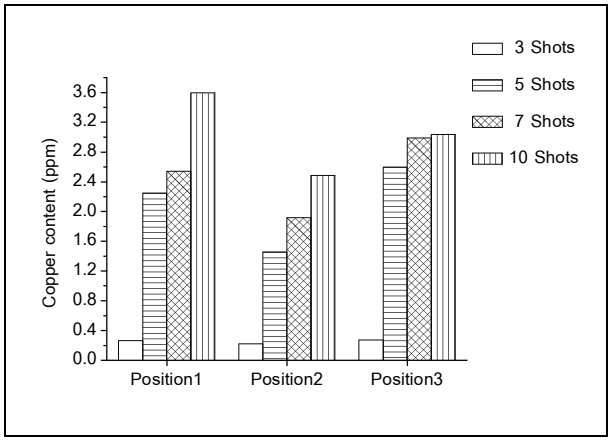

Figure 4.2 Copper content of PE samples treated by nitrogen plasma

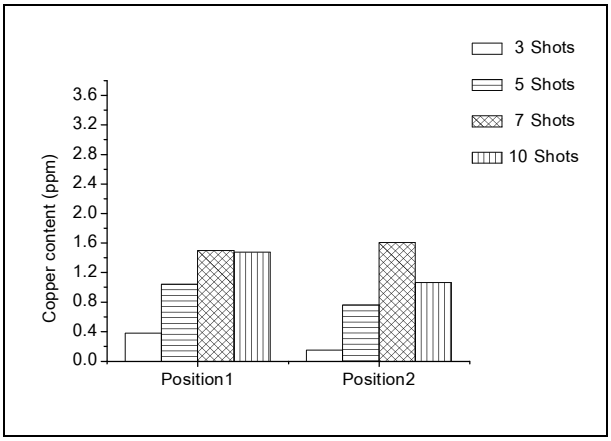

Figure 4.3 Copper content of PE samples treated by oxygen plasma

Due to the symmetry of the plasma exposure at positions 1 and 3, the copper contents of oxygen plasma-treated PE samples placed at positions 1 and 2 are illustrated in Figure 4.3. It can be seen from this figure that the samples placed at postion 1 exhibit the same trend as was observed for those treated with nitrogen plasma but with lower copper content. This may be because oxygen plasma is more reactive than nitrogen plasma; as a result, etching is easier to occur in oxygen plasma treatment than in nitrogen plasma treatment. Consequently, a removal of the copper which already implanted on PE surface can occur in the former case more than in the latter case resulting in lower copper content. This effect is clearly seen at position 2 because at this position, the energy exposed on the sample is higher than at position 1. Therefore, a decrease in copper content at higher number of plasma shots such as 10 shots is observed due to an increase in plasma etching with increasing the number of plasma shots.

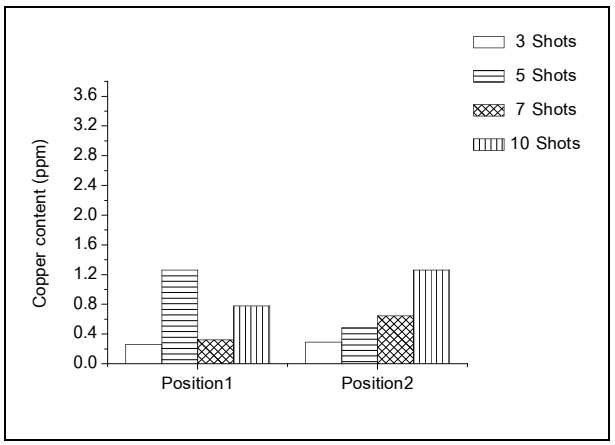

Figure 4.4 Copper content of PE samples treated by argon plasma

On the other hand, Figure 4.4 reveals that argon plasma-treated samples have lowest copper contents when compared to those treated with nitrogen plasma and oxygen plasma. Because of its less reactivity, copper ion implantation is more difficult to be induced by argon plasma at lower number of plasma shots. Therefore, higher number of plasma shots is needed in order to achieve higher copper content as was observed at position 2 where lower density of copper ions was emitted from the anode. However, at position 1 where higher density of copper ions present, the highest copper

content was achieved when 5 shots of argon plasma was used. As the number of plasma shots was increased to 7 shots, plasma etching became dominant than the implantation. In order to overcome this effect, higher number of plasma shots such as 10 shots is needed.

Figure 4.5 also supports the results obtained by atomic absorption as previously shown in Figures 4.2-4.4. It is clearly seen Figure 4.5 (a) that nitrogen plasma-treated PE samples placed at positions 1 and 3 have red-brown stain of copper metal on their surface but at position 2, the surface of treated PE sample is slightly yellow due to the degradation of the polymer surface as was reported by J. Srisawat [44]. Figure 4.5 (b) reveals that PE samples treated by argon plasma placed at positions 1 and 3 exhibit slightly dark-green color of copper (II) oxide all over the surface area whereas the sample placed at position 2 has some stain only around its edge. In the case of oxygen plasma treatment, the samples exhibit slightly red-brown color of copper metal as shown in Figure 4.5 (c). In order to confirm the above observation, PE samples were treated without copper by covering the top of copper anode with ceramic plate. All samples as shown in Figure 4.6 do not show any color indicating the presence of copper atom or ion.

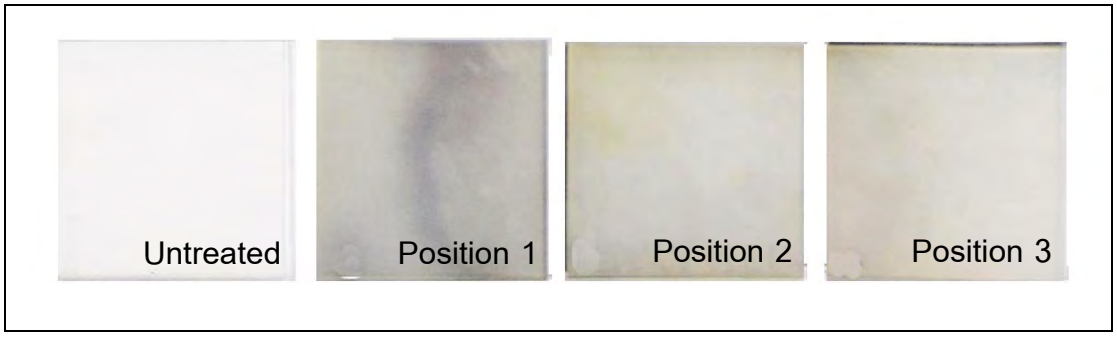

(a)

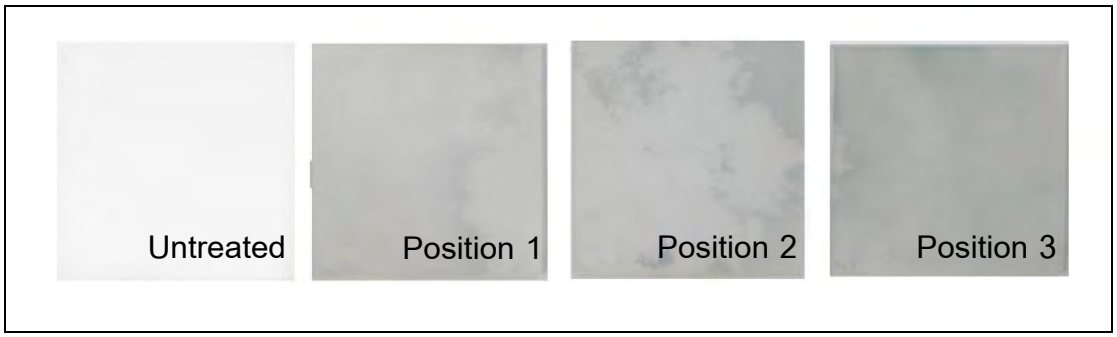

(b)

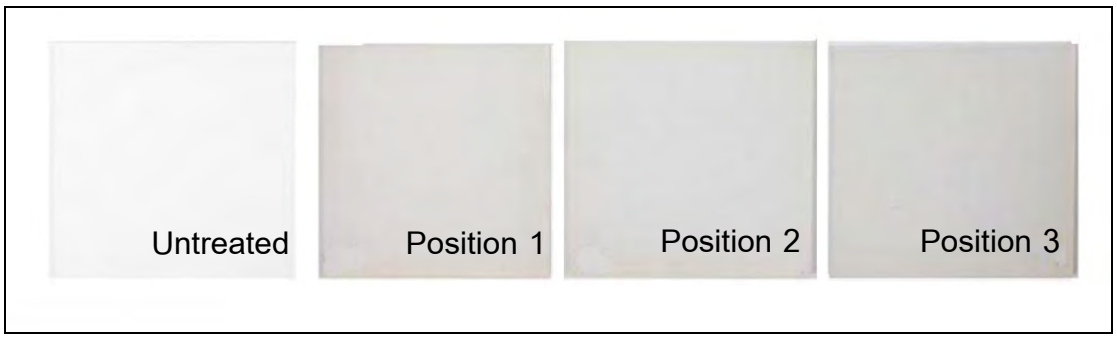

(c)

Figure 4.5 Appearances of untreated PE and PE samples treated with 10 shots of (a) nitrogen plasma, (b) argon plasma and (c) oxygen plasma

(a)

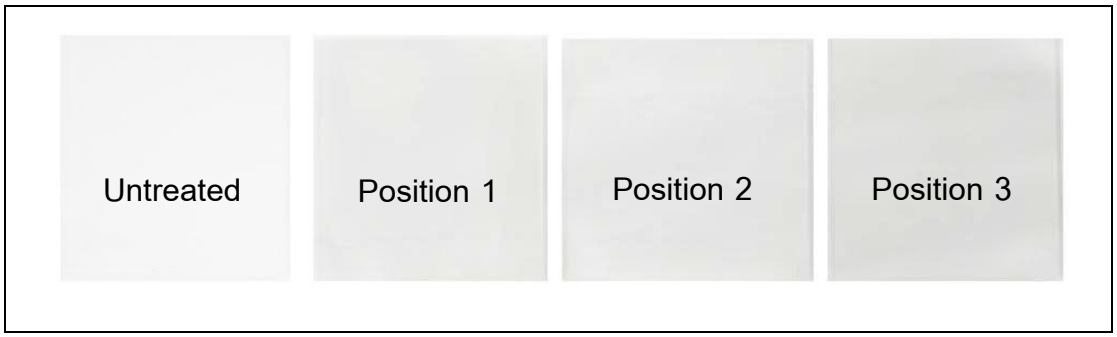

(b)

(c)

Figure 4.6 Appearances of untreated PE and PE samples treated without copper using 10 shots of (a) nitrogen plasma, (b) argon plasma and (c) oxygen plasma

4.1.2. Surface Roughness

AFM was used to analyze the surface roughness of plasma-treated PE samples at position 1. The root mean square roughness (RMS) and the absolute surface roughness (Ra) of untreated and treated PE samples are illustrated in Table 4.1-4.3. The topography of untreated PE sample is shown in Figure 4.7. Its RMS and Ra are 11.475 nm and 9.469 nm, respectively.

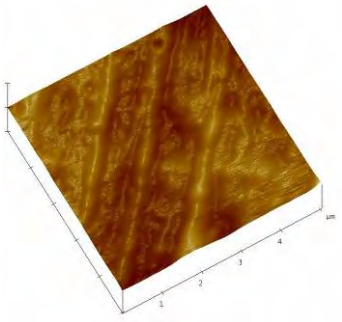

Figure 4.7 Topography of untreated PE sample

In this work, two factors which are copper ion implantaion and plasma etching affect the surface roughness of plasma-treated PE samples. While the implantation creates the uneven or even layers of copper or copper oxide on the treated surface depending on the distribution of the plasma and other radiations, the etching removes few layers of the substrate and also the implanted atoms or ions. Table 4.1 clearly shows the effect of the implantation. From Figure 4.2, small amounts of copper atom were implanted on PE surface treated by nitrogen plasma at 3 shots and the copper contents suddenly increases with increasing the number of plasma shots from 5 to 10 shots. Consequently, PE surface treated by nitrogen plasma at 3 shots is slightly rougher than the untreated one while the surface roughness of other samples is high and becomes rougher with increasing the number of plasma shots. However, the removal of the implanted copper by etching also shows in this table. At 7 shots, this effect slightly dominates the implantation effect; therefore, the surface roughness of PE sample treated by nitrogen plasma at 7shots is lower than that of the sample treated at 5 shots.

On the other hand, Table 4.2 clearly shows the etching effect of oxygen plasma. As previously mentioned, oxygen plasma is more reactive than nitrogen plasma; consequently, the etching effect strongly dominated during the treatment causing the surface of the treated samples to be smoother with increasing the number of plasma shots. Since at 3 shots, lowest amount of copper was implanted but etching already occurred, the surface roughness of this sample is lower than the untreated one.

Table 4.1 Topography, RMS and Ra of PE samples treated by nitrogen plasma placed at position 1

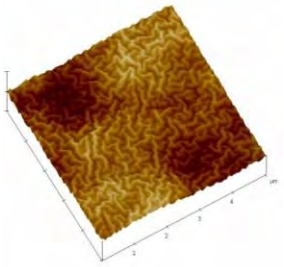	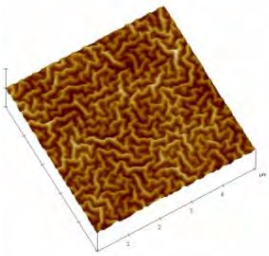	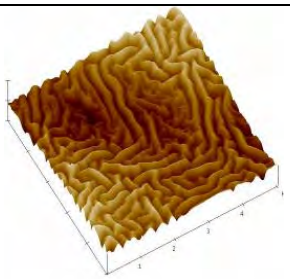	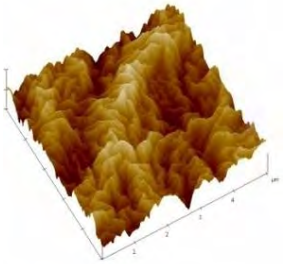
3 shots	5 shots	7 shots	10 shots
RMS =14.705 nm	RMS = 41.328 nm	RMS = 30.722 nm	RMS = 58.906 nm
Ra = 12.423 nm	Ra = 33.633 nm	Ra = 25.120 nm	Ra = 48.757 nm

Table 4.2 Topography, RMS and Ra of PE samples treated by oxygen plasma placed at position 1

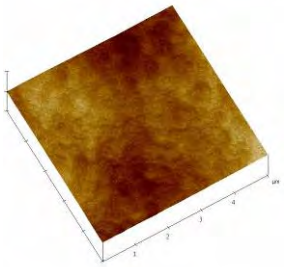	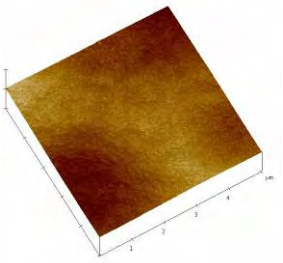	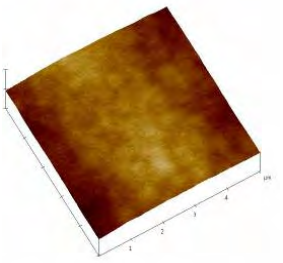	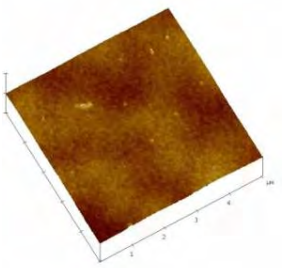
3 shots	5 shots	7 shots	10 shots
RMS =8.693 nm	RMS = 11.16 nm	RMS = 9.827 nm	RMS = 4.08 nm
Ra = 7.193 nm	Ra = 9.33 nm	Ra = 8.337 nm	Ra = 3.173 nm

In case of argon plasma treatment, the effect of the implantation is different from nitrogen plasma treatment because in this case, the layers of copper (II) oxide were formed as shown in Figure 4.5 (b) while some stains of copper metal were formed in the other case as shown in Figure 4.5 (a). Since these layers cover almost all the area of the surface, this makes the surfaces of argon plasma-treated PE samples to be smoother than those of nitrogen plasma-treated PE samples as shown in Table 4.3. In addition, the etching effect in this treatment is also different from the other treatments due to the much larger size of argon compared to oxygen and nitrogen. Therefore, it can etch the

surface much deeper and wider than the others. As a result, the surface roughness increases with increasing the number of plasma shots.

Table 4.3 Topography, RMS and Ra of PE samples treated by argon plasma placed at position 1

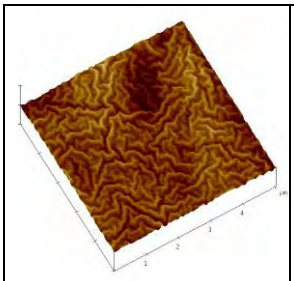	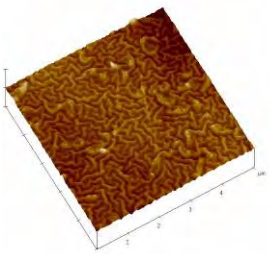	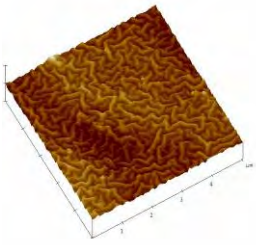	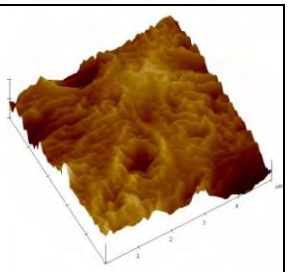
3 shots	5 shots	7 shots	10 shots
RMS =19.147 nm	RMS = 16.067 nm	RMS = 23.357 nm	RMS = 48.083 nm
Ra = 15.484 nm	Ra = 12.717 nm	Ra = 18.795 nm	Ra = 35.689 nm

4.1.3. Surface Chemical Structure

Surface chemical structures of PE samples were characterized by ATR/FT-IR for evaluating the formation of any new functional groups, or the alteration of existing groups on PE surface after plasma treatment.

Figure 4.8 shows the increasing intensities of the peaks corresponding to N-H stretching at 3,200-3,600 cm^{-1}, –NH bending at 1615 cm^{-1} and C=N bond at 1715 cm^{-1} as the number of plasma shots increases. These results indicate the formation of hydrophilic functional groups on PE surface after nitrogen plasma treatment. In addition, Figure 4.9 also confirms that plasma etching dominates at position 2 over functionalization since the spectrum at this postion is similar to that of the untreated one.

Because etching effect strongly occurred in oxygen plasma treatment as shown in Table 4.2, the functional groups already formed on the surface can be possibly removed. Therefore, no change in all spectra is observed as shown in Figure 4.10.

Figure 4.11 indicates the formation of hydrophobic functional groups at postions 1 and 3 after argon plasma treatment due to an increase in the intensities at 966 cm^{-1} of =C-H bending and at 1043 cm^{-1} of $–CH_3$ while the etching is still dominant at position 2.

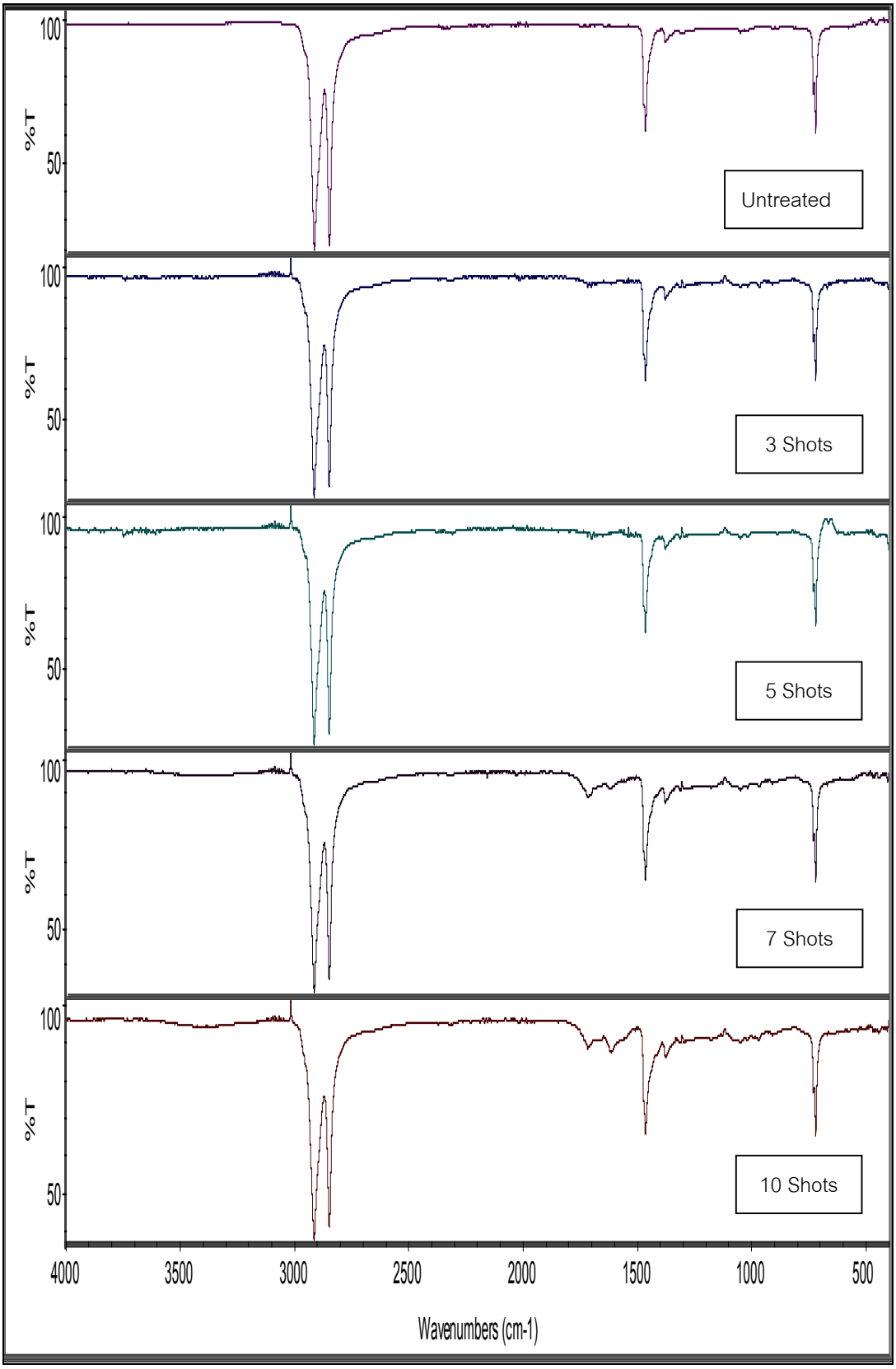

Figure 4.8 ATR-FTIR spectra of untreated PE and PE samples treated by nitrogen plasma placed at position 1

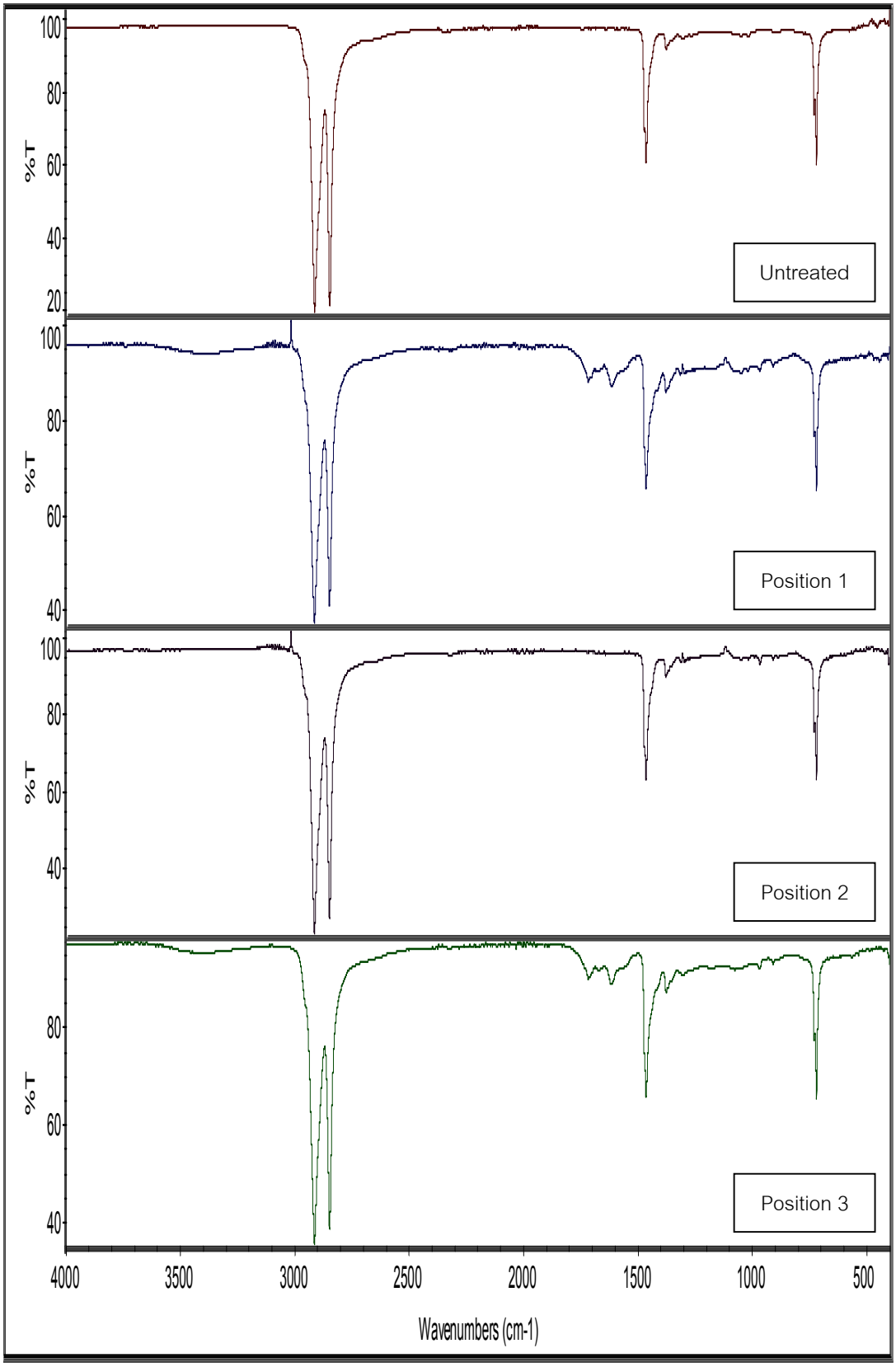

Figure 4.9 ATR-FTIR spectra of untreated PE and PE samples treated by 5 shots of nitrogen plasma

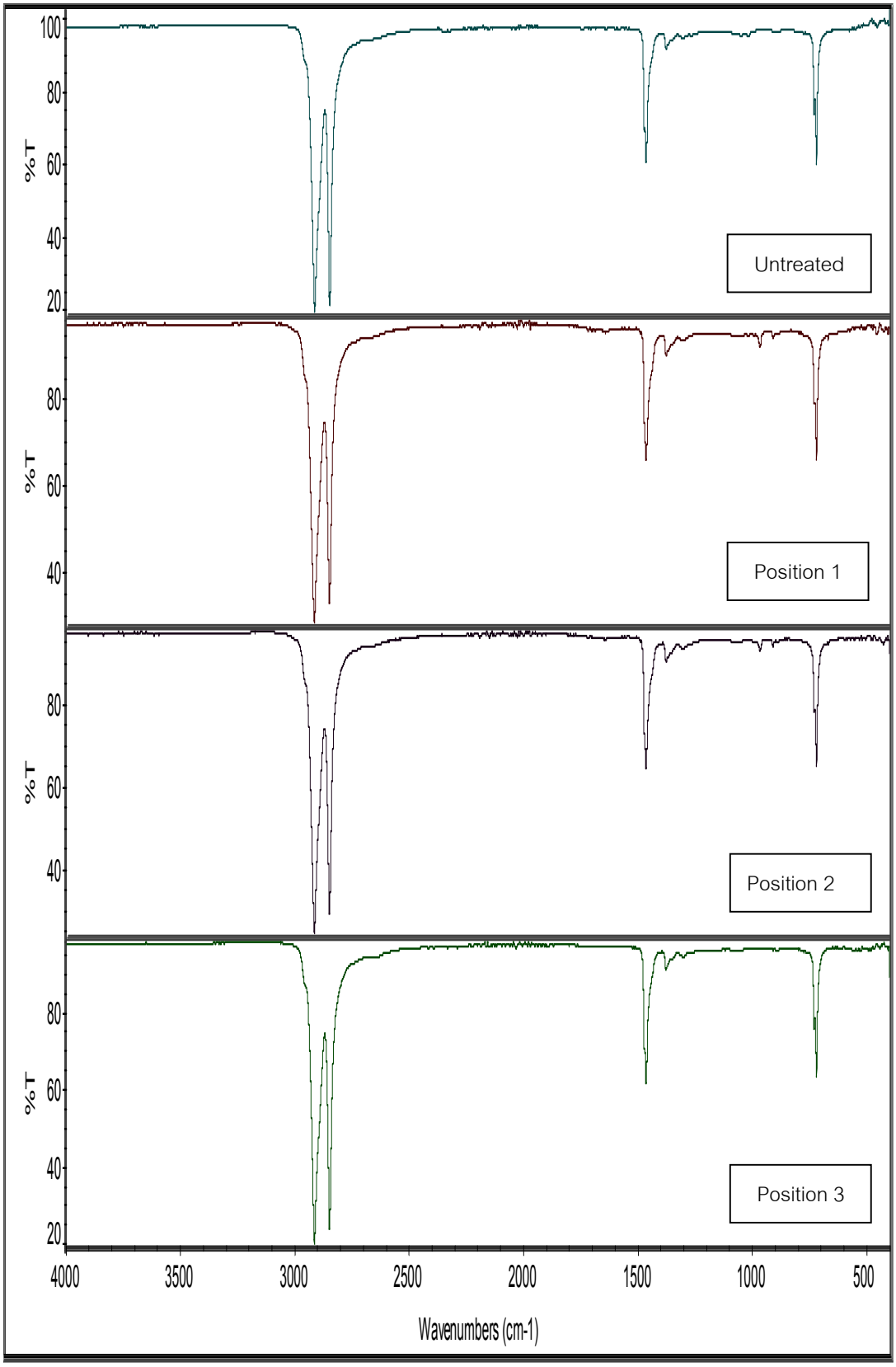

Figure 4.10 ATR-FTIR spectra of untreated PE and PE samples treated by 5 shots of oxygen plasma

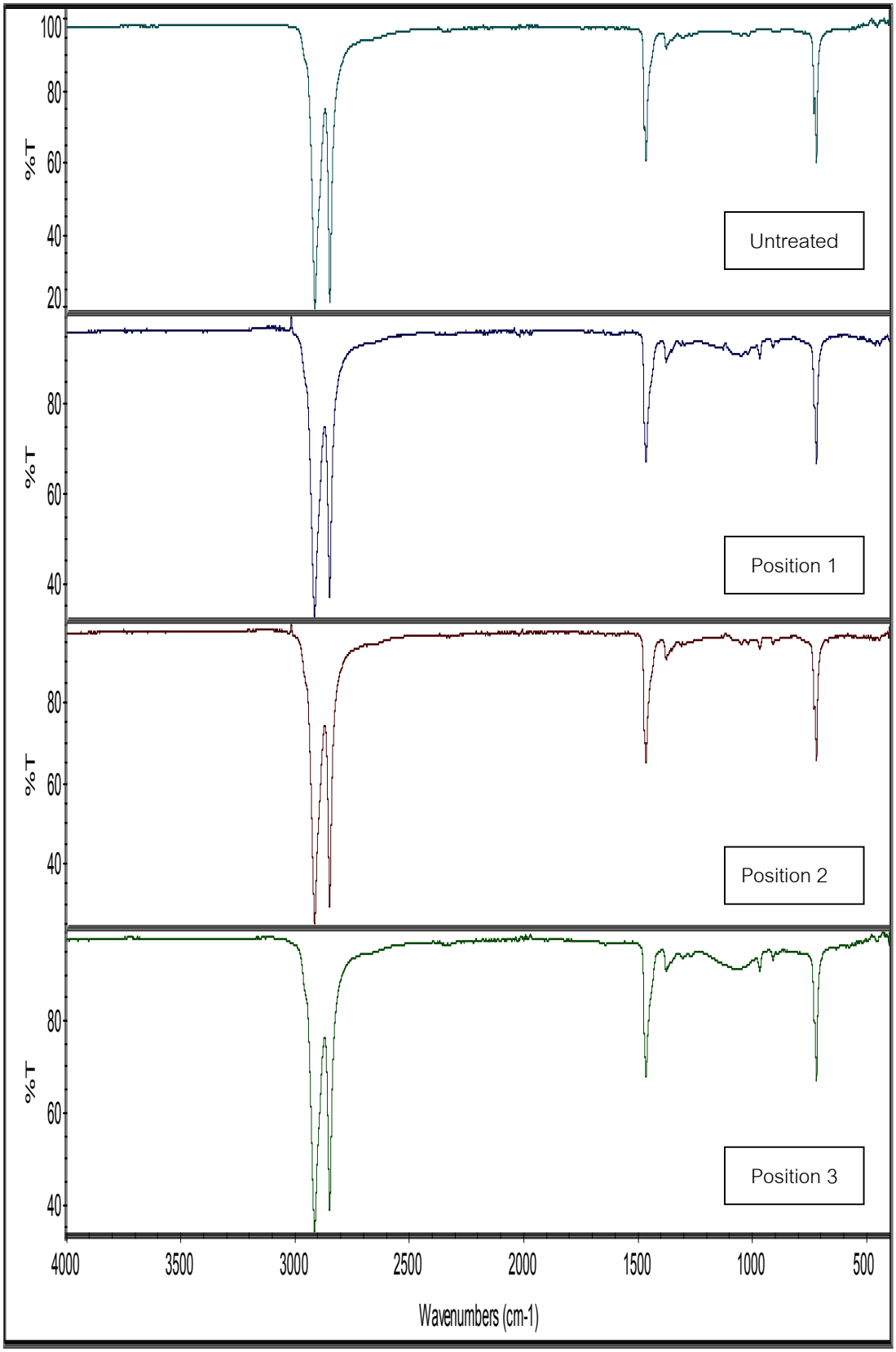

Figure 4.11 ATR-FTIR spectra of untreated PE and PE samples treated by 5 shots of argon plasma

4.1.4. Wettability

Since Figure 4.8 revealed the formation of hydrophilic functional groups and Figure 4.2 indicated the copper implantation in nitrogen plasma treatment, it is expected that the water contact angles of PE samples obtained from this method are lower than that of untreated PE sample (80^{o}) as shown in Figures 4.12 indicating an increase in hydrophilic characteristic.

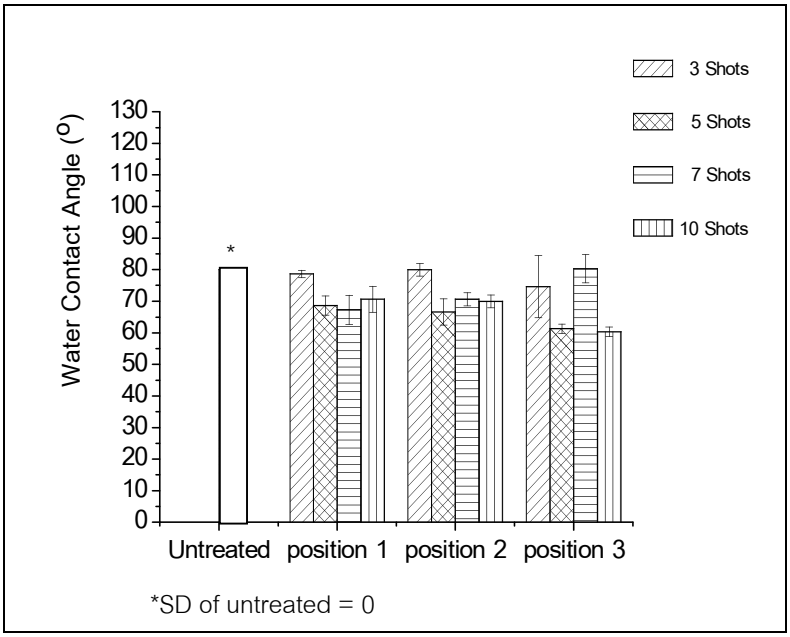

Figure 4.12 Water contact angle of PE samples treated by nitrogen plasma

Because no hydrophilic functional groups were formed but only small amounts of copper were implanted during oxygen plasma treatment, the water contact angles of most oxygen plasma-treated PE samples are comparable or slightly lower than that of the untreated one as shown in Figure 4.13 except for those treated with 3 shots. At this condition, the surface of the treated sample is smoother than the untreated one. This combining with the copper implanted and hydrophilic functional groups which can possibly formed can aid the adhesion between the surface and the water resulting in lower water contant angle.

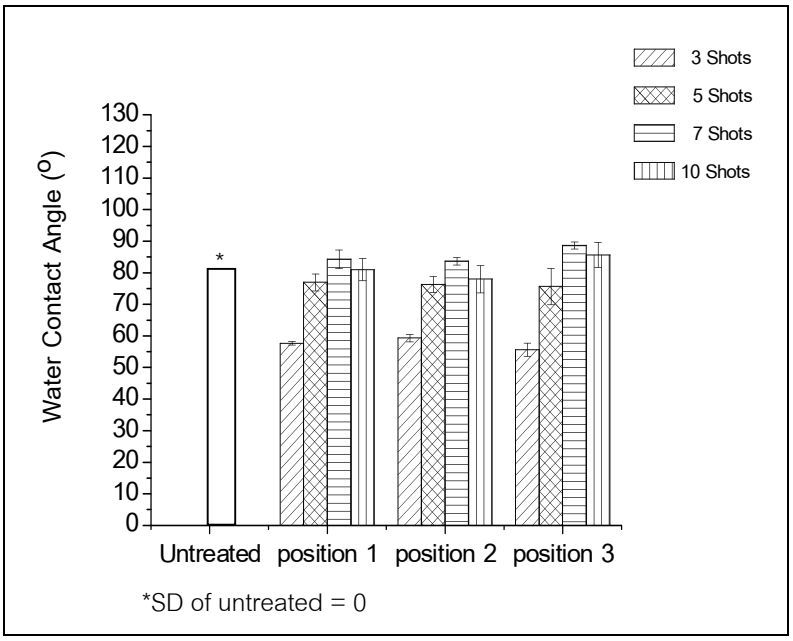

Figure 4.13 Water contact angle of PE samples treated by oxygen plasma

As shown in Figure 4.14, all PE treated with argon plasma exhibit slightly higher water contact angles than the untreated sample. This is due to an increase in the amounts of hydrophobic functional groups as revealed in Figure 4.11.

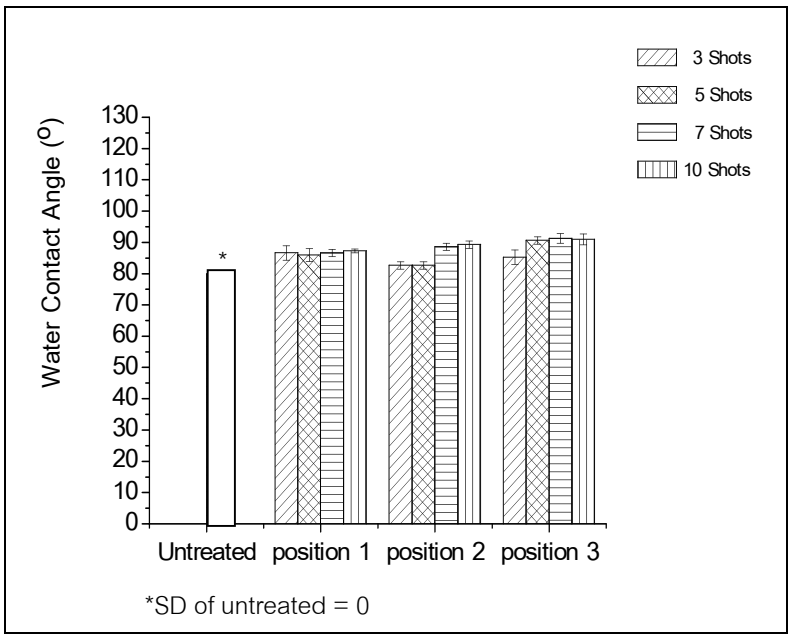

Figure 4.14 Water contact angle of PE samples treated by argon plasma

4.1.5. Antibacterial Property

Since the characteristics of treated PE samples placed at position 1 are comparable to those of treated PE samples placed at position 3 and better than those of treated PE samples placed at position 2, these samples were selected for antibacterial tests.

Nitrogen-plasma PE samples were selected for studying the effect of the number of plasma shots since these samples have higher copper contents than other samples treated by different types of plasma. Table 4.4 shows that %reduction of *S. aureus* of PE was improved by copper ion implantation. However, the main factor affecting this improvement was the surface roughness since at 3 shots, lowest copper content was observed but this condition yielded the sample with highest %reduction. The results obtained when the effect of the gas type also exhibited the similar trend. Even though PE sample treated by 5 shots of nitrogen plasma has higher copper content than oxygen plasma-treated sample as shown in Figures 4.2 and 4.3, the latter also shows highest %reduction of *S. aureus* since it has lower surface roughness which is more difficult for the bacteria to form the biofilm. In case of argon plasma-treated PE sample, because of low copper content and increasing hydrophobicity of its surface, the bacteria can still adhere and grow on its surface; therefore, less %reduction of *S. aureus* is observed as shown in Figure 4.4.

Table 4.4 %Reduction of *S. aureus* of plasma-treated PE samples placed at position 1

Type of plasma	Shots	The number of bacteria CFU/mL	% reduction
Untreated	-	8.3×10^7	0
Nitrogen plasma	3	3.6×10^7	56.62
Nitrogen plasma	5	6.8×10^7	16.27
Nitrogen plasma	7	6.6×10^7	20.48
Nitrogen plasma	10	6.4×10^7	22.89
Oxygen plasma	5	3.6×10^7	56.62
Argon plasma	5	6.9×10^7	16.86

Table 4.5 %Reduction of *E. coli* of plasma-treated PE samples placed at position 1

Type of plasma	Shots	The number of bacteria CFU/mL	% reduction
Untreated	-	4.1×10^8	0
Nitrogen plasma	3	4.4×10^8	0
Nitrogen plasma	5	3.8×10^8	5.66
Nitrogen plasma	7	4.7×10^8	0
Nitrogen plasma	10	4.7×10^8	0
Oxygen plasma	5	4.1×10^8	0
Argon plasma	5	3.5×10^8	13.33

However, the results from Table 4.5 indicate that *E. coli* has higher resistance to copper than *S. aureuse*. This suggests that antibacterial efficiency also depends on the types of the bacteria and the metal used.

4.2 Characteristic and Properties of Silicone Rubber

4.2.1. Copper Content

Since positions 1 and 3 exhibit the same characteristics as was reported for PE, the results for silicone rubber are presented only of the samples placed at positions 1 and 2.

Due to an inert characteristic of silicone rubber, it is clearly seen from Figure 4.15 that copper content of nitrogen plasma-treated silicone rubber was lower than that of PE as shown in Figure 4.2. The number of plasma shots at 5 shots is the optimum condition where copper ion implantation may be highest and the etching may be lowest. But at 7 shots, plasma etching became dominant than the implantation. Therefore, higher number of plasma shots such as 10 shots is needed in order to increase the implantation even though it can also increase the etching effect. However, it is clearly seen that the effect of placement position is similar to that of PE.

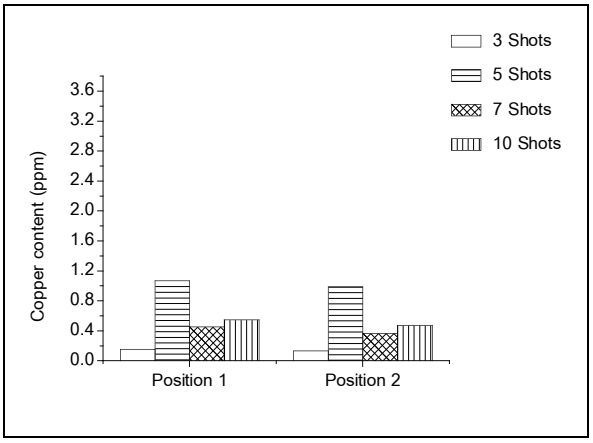

Figure 4.15 Copper content of silicone rubber samples treated by nitrogen plasma

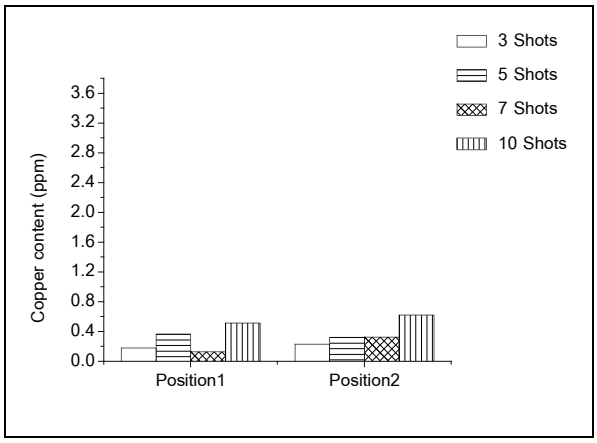

Figure 4.16 Copper content of silicone rubber samples treated by oxygen plasma

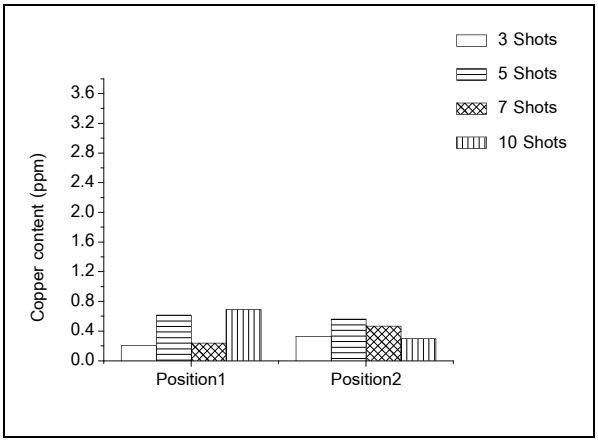

Figure 4.17 Copper content of silicone rubber samples treated by argon plasma

On the other hand, due to etching effects of highly reactive oxygen plasma and large-sized argon plasma, the copper contents of oxygen plasma-treated and argon plasma-treated silicone samples are lower than those of nitrogen plasma-treated silicone samples as shown in Figures 4.16 and 4.17. However, slightly higher amounts for the latter case were observed due to less etching effect.

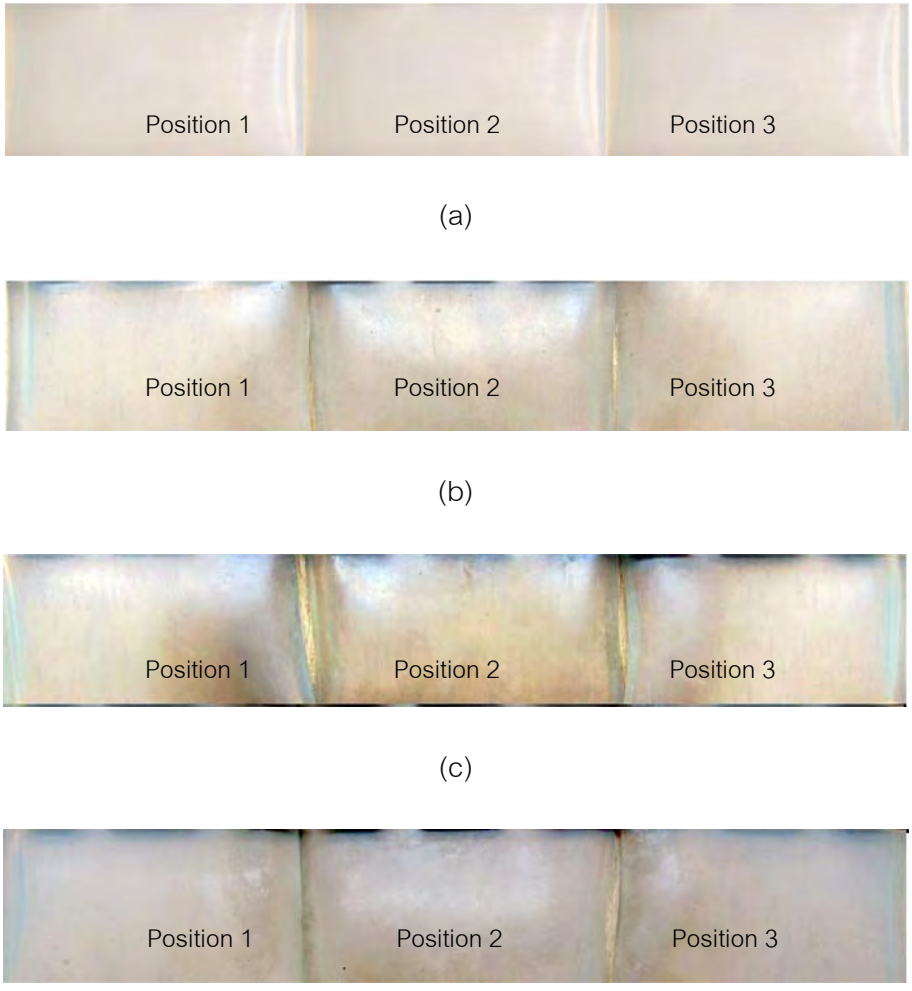

Figure 4.18 Appearances of (a) untreated silicone rubber and silicone rubber samples treated with 10 shots of (b) nitrogen plasma, (c) oxygen plasma and (d) argon plasma

These results also suggest higher degradation of the samples treated by oxygen plasma and argon plasma compared to those treated by nitrogen plasma which can be confirmed by Figure 4.18. Not only this figure shows the sign of burning on the surface of oxygen plasma-treated sample but also indicates that the degradation at postion 2

are higher than at positions 1 and 3 as was observed in plasma treatment of PE. In addition, due to loosely structure of the rubberlike material as silicone rubber compared to more densed structure of the plastic as PE, etching is easier to occur in the former than the latter. Therefore, higher degradation is observed for plasma-treated silicone rubber.

4.2.2. Surface Roughness

The morphology of untreated silicone rubber was shown in Figure 4.19. The RMS and Ra of untreated silicone rubber are 46.822 nm and 35.899 nm, respectively.

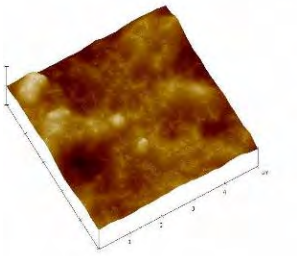

Figure 4.19 Topography of untreated silicone rubber

Due to softer texture and more loosely structure of silicone rubber, all plasma can etch its surface deeper when compared to PE. Etching effect occurred in plasma treatment of silicone rubber was different from that occurred in plasma treatment of PE. In this case as seen from Tables 4.6 – 4.7, as the number of the plasma shots increases, the surface roughness increases. However, there is another factor which plays an important role in affect the surface roughness of plasma-treated silicone rubber. This factor is copper ion implantation. It is clearly seen from Figure 4.8 in argon plasma treatment that at 5 shots which copper ion implantation may be highest and the etching may be lowest, the surface roughness is highest. But at 7 shots, the etching became dominant and low copper implanted; thus less surface roughness was observed. At 10 shots, the implantation dominated again causing the surface to be rougher.

Table 4.6 Topography, RMS and Ra of silicone rubber samples treated by nitrogen plasma at position 1

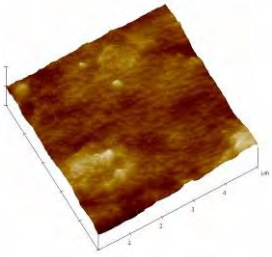	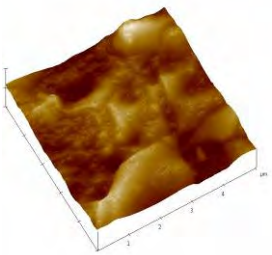	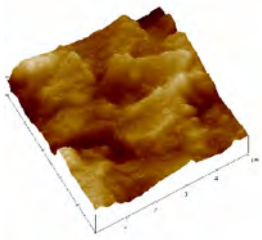	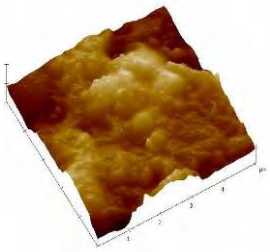
3 shots	5 shots	7 shots	10 shots
RMS = 40.81 nm	RMS = 61.446 nm	RMS = 93.703	RMS = 108.24 nm
Ra = 31.119 nm	Ra = 49.563 nm	Ra = 73.260	Ra = 87.825 nm

Table 4.7 Topography, RMS and Ra of silicone rubber samples treated by oxygen plasma at position 1

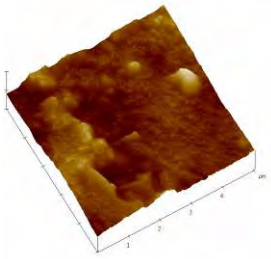	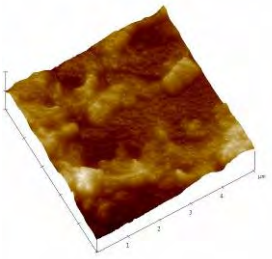	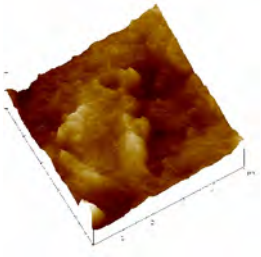	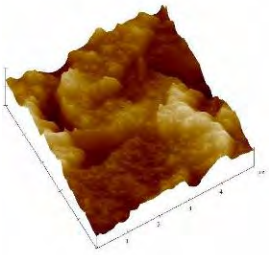
3 shots	5 shots	7 shots	10 shots
RMS =52.661 nm	RMS = 62.251 nm	RMS = 101.87 nm	RMS = 133.65 nm
Ra = 39.458 nm	Ra = 50.11 nm	Ra = 81.795 nm	Ra = 108.62 nm

Table 4.8 Topography, RMS and Ra of silicone rubber samples treated by argon plasma at position 1

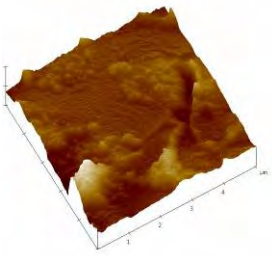	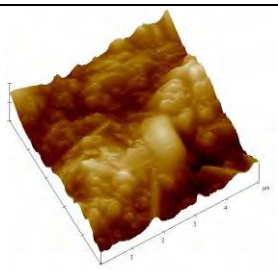	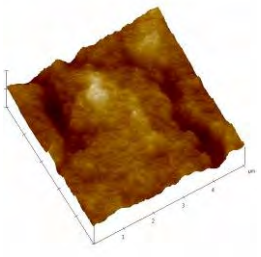	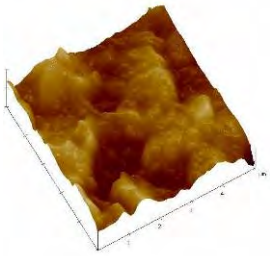
3 shots	5 shots	7 shots	10 shots
RMS =84.323 nm	RMS = 134.41 nm	RMS = 93.076 nm	RMS = 112.72 nm
Ra = 58.365	Ra = 110.23	Ra = 69.096 nm	Ra = 93.182

4.2.3. Surface Chemical Structure

ATR-FTIR spectra of nitrogen plasma-treated silicone rubbers in Figure 4.20 show the peak at 3200-3600 cm^{-1} corresponding to N-H stretching and of the peak at around 1700 cm^{-1} indicating C=N bond. The intensities of these peaks increase with increasing the number of plasma shots. Figure 4.21 reveals the effect of the placement positions is the same as was reported in plasma treatment of PE.

In case of oxygen plasma-treated and argon plasma-treated samples, no new peaks significantly appear as shown in Figures 4.22 and 4.23. This may possibly due to an inert surface of silicone rubber; therefore, it is difficult for the reactions between plasma species and the silicone rubber. These results suggest that in this case nitrogen plasma is more reactive for functionalization toward silicone rubber than oxygen plasma and argon plasma.

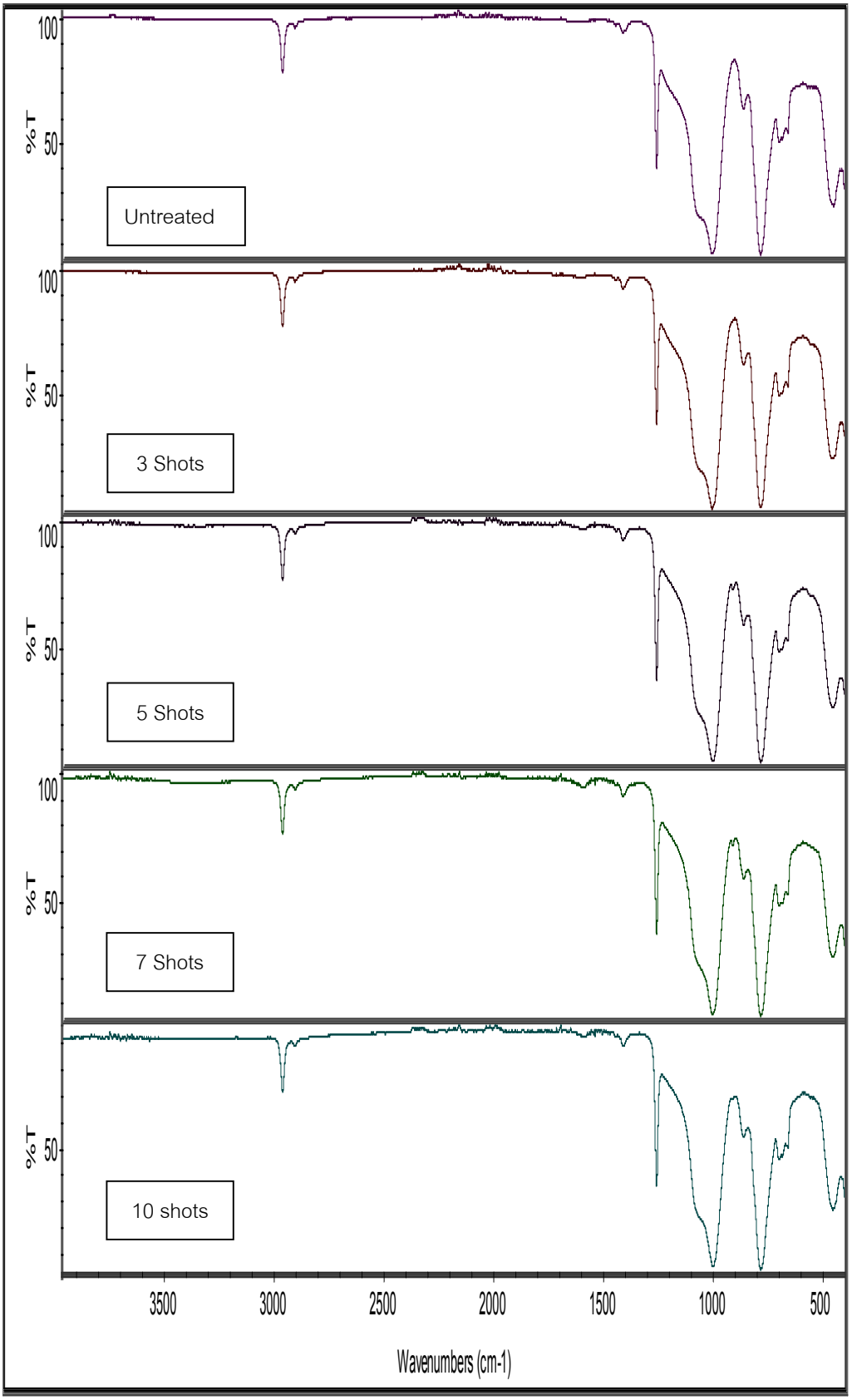

Figure 4.20 ATR-FTIR spectra of untreated silicone rubber and silicone rubber samples treated by nitrogen plasma placed at position 1

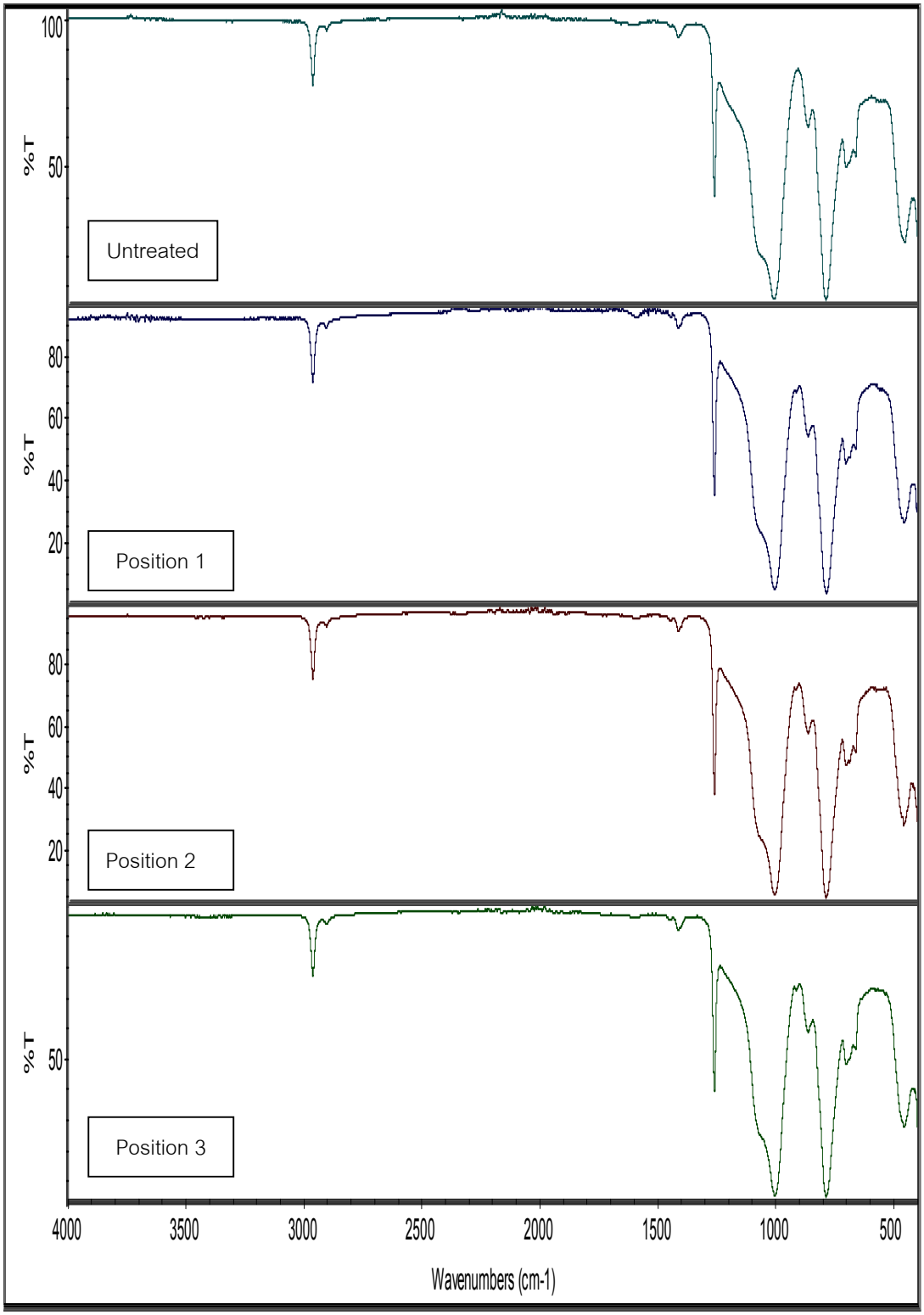

Figure 4.21 ATR-FTIR spectra of untreated silicone rubber and silicone rubber samples treated by 5 shots of nitrogen plasma

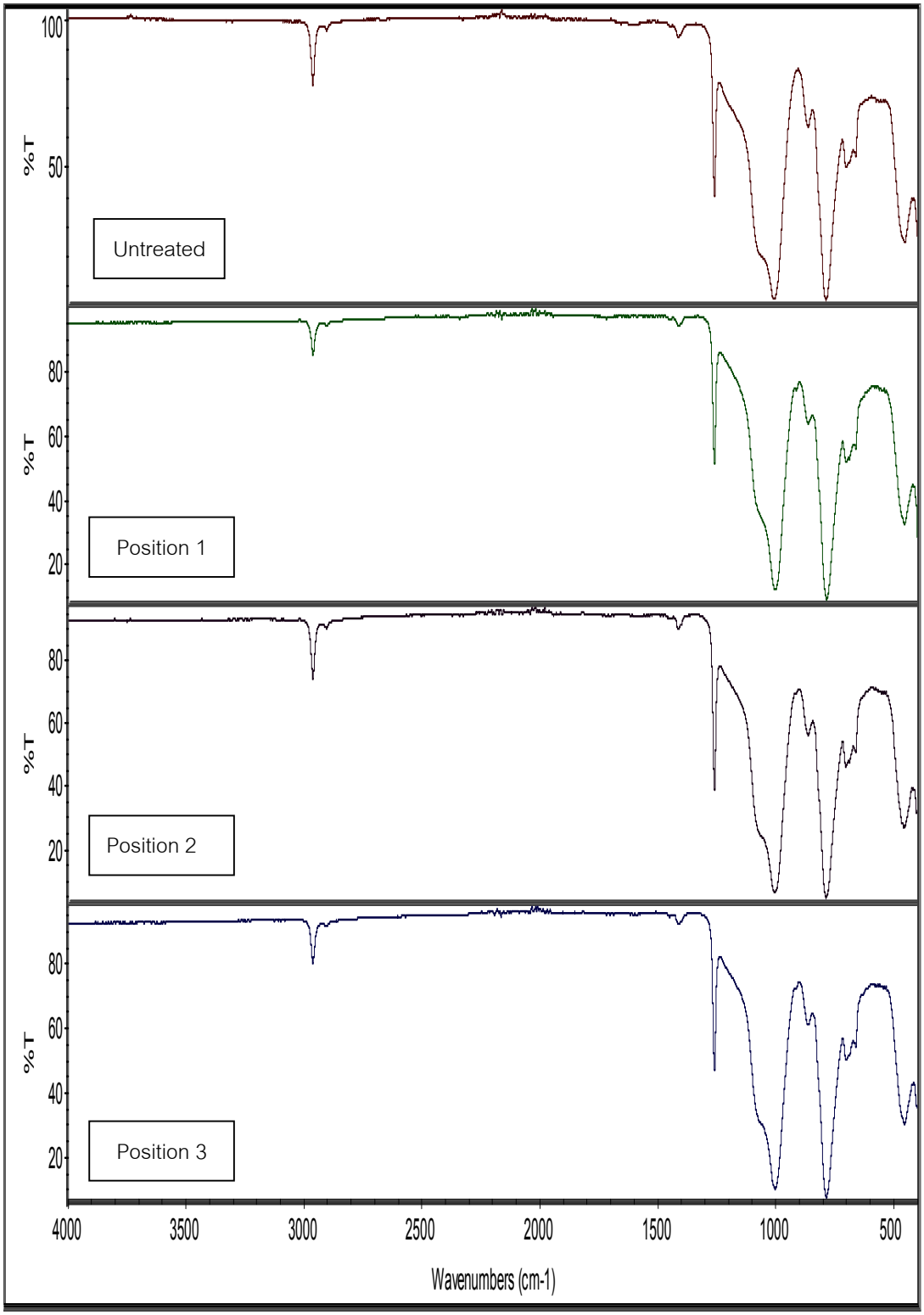

Figure 4.22 ATR-FTIR spectra of untreated silicone rubber and silicone rubber samples treated by 5 shots of oxygen plasma

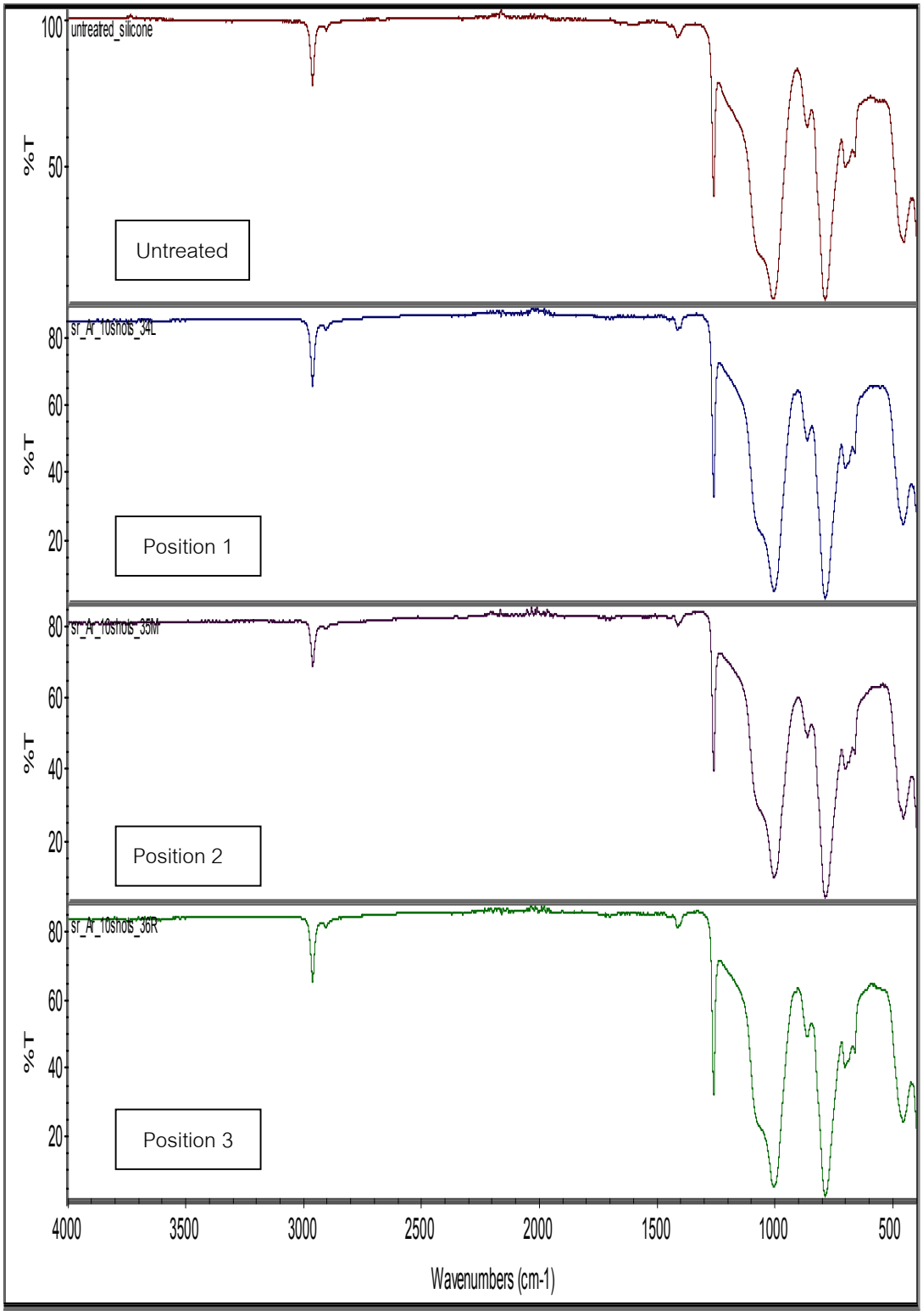

Figure 4.23 ATR-FTIR spectra of untreated silicone rubber and silicone rubber samples treated by 5 shots of argon plasma

4.2.4. Wettability

Figure 4.24 shows that the water contact angles of nitrogen plasma-treated silicon rubbers are lower than that of untreated silicone rubber which is 100°. This is a result of the formation of hydrophilic functional groups, the copper ion implantation and less surface roughness as previously presented. However, from Figure 4.25, oxygen plasma-treated samples also show a decrease in water contact angle even though the formation of hydrophilic functional groups is not clearly observed. This may be due to the roughness factor and the copper ion implantation. However, when the surface roughness is highest when 10 shots of oxygen plasma were applied, the surface becomes more hydrophobic than that of the untreated silicone rubber. Since no hydrophilic functional groups were formed and high surface roughness, argon plasma-treated samples exhibit higher water contact angle than the untreated one as shown in Figure 4.26.

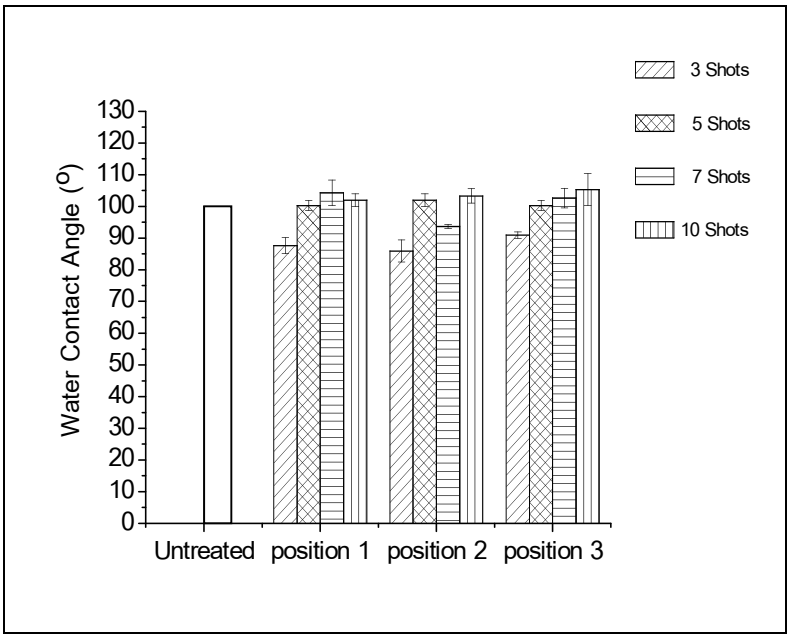

Figure 4.24 Water contact angle of silicone rubber samples treated by nitrogen plasma

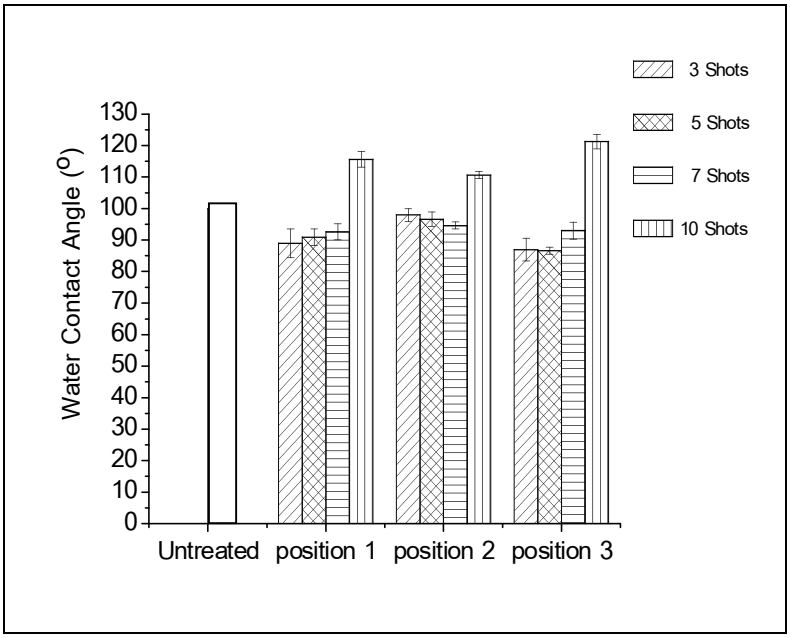

Figure 4.25 Water contact angle of silicone rubber samples treated by oxygen plasma

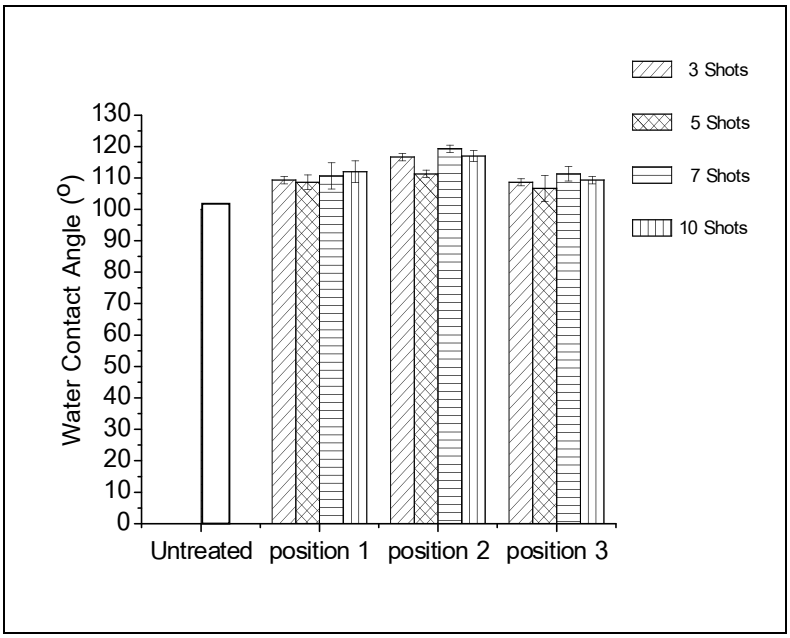

Figure 4.26 Water contact angle of silicone rubber samples treated by argon plasma

4.2.5. Antibacterial Property

The samples selected for antibacterial tests were the same as of PE. Table 4.9 shows that silicone rubber treated by nitrogen plasma at 3 shots has highest antibacterial efficiency against *S.aureus* due to its higher hydrophilic property and its lowest surface roughness. This is because increasing hydrophilic property causes the difficulty in the colony formation of the bacteria on the silicone rubber surface. On the other hand, for the treatment at 5, 7 and 10 shots, the copper content also affects this property as % reduction of *S.aureus* varies in according to the copper content. When considering the effect of the gas type, it can be seen from this table that at 5 shots, the copper content may be the main factor affecting the antibacterial efficiency since oxygen plasma-treated sample having lowest amount of copper implanted exhibits 0 % reduction of *S.aureus* while the others with higher copper contents show high % reduction of *S.aureus*.

However, the results from Table 4.10 indicate that *E. coli* has higher resistance to copper than *S. aureus*. This suggests that antibacterial efficiency also depends on the types of the bacteria and the metal used. This observation is in good agreement with that observed for PE.

Table 4.9 %Reduction of *S. aureus* of plasma-treated silicone rubber samples placed at position 1

Type of plasma	Shots	The number of bacteria CFU/mL	% reduction
Untreated	-	2.9×10^8	0
Nitrogen plasma	3	1.1×10^8	62.06
Nitrogen plasma	5	1.4×10^8	51.72
Nitrogen plasma	7	2.2×10^8	24.13
Nitrogen plasma	10	1.6×10^8	44.82
Oxygen plasma	5	4.4×10^8	0
Argon plasma	5	1.4×10^8	51.72

Table 4.10 %Reduction of *E. coli* of plasma-treated silicone rubber samples placed at position 1

Type of plasma	Shots	The number of bacteria CFU/mL	% reduction
Untreated	-	5.8×10^8	0
Nitrogen plasma	3	5.6×10^8	3.44
Nitrogen plasma	5	4.8×10^8	17.24
Nitrogen plasma	7	8.9×10^8	0
Nitrogen plasma	10	4.7×10^8	18.96
Oxygen plasma	5	6.4×10^8	0
Argon plasma	5	8.3×10^8	0

CHAPTER V
CONCLUSIONS AND RECOMMENDATIONS

5.1 Conclusions

In this research, PE and silicone rubber were treated by plasma generated from UNU/ICTP plasma focus device. The effects of the gas type, the number of plasma shots and the placement position of the sample in the plasma chamber were investigated. The results can be concluded as follows:

1. Three phenomena occurring during the plasma process were copper ion implantation, functionalization and etching.

2. The gas types significantly affected copper ion implantation. All results showed that higher copper contents were achieved from nitrogen plasma treatment for both PE and silicone rubber. On the other hand, due to higher etching effect in oxygen and argon plasma treatments, lower copper contents were observed in both cases.

3. Since copper ion implantation, functionalization and etching increased with increasing the number of plasma shots, the copper content and the functional groups formed in each condition depended on the dominance of each phenomenon at each shot.

4. Due to the principle of plasma generating process of a plasma focus device, it was found that the copper ion implantation favorably occurred at positions 1 and 3 whereas etching mostly occurred at position 2 causing the degradation at this position.

5. In this method, it was found that the surface roughness caused by copper ion implantation and etching was the main factors affecting antibacterial properties of both PE and silicone rubber. The types of bacteria and the type of metal also affect the antibacterial efficiency.

5.2 Recommendations

1. The effects of other types of gases, charging voltage and pressure on the characteristics and antibacterial properties of PE and silicone rubber should be studied.

2. Antibacterial property against *E.coli* should be studied by changing the type of metal but using the same method.

REFERENCES

[1] Kobayashi, T., Katou, R., Yokoto, T., Suzuki., Y., Iwaki, M., and Terai, T. Surface modification of silicone medical materials by plasma-based ion implantation. Nuclear Instruments and Methods in Physics Research B 257(2007): 128-131.

[2] An, Y. H., and Friedman, R. J. Concise review of mechanisms of bacterial adhesion to biomaterial surfaces. Biomed Mater Res (Appl Biomater) 43 (1998): 338-348.

[3] Zhang, W., and Chu, P.K. Enhancement of antibacterial and biocompatibility of polyethylene by silver and copper plasma immersion ion implantation. Surface & Coating Technology 203 (2008): 909-912.

[4] Greenwood, D., Finch, R., Oavey, P., and Wilcox, M. Antimicrobial chemotherapy, 5 edition. Oxford University Press, 2007.

[5] Alliance for the prudent use of antibiotics. Antibacterial agents [online] available from : http://www.tufts.edu/med/apua/Q&A/Q&A_antibacterials.html (acceessed on 21 April 2010)

[6] The Official Brand of the Worlds Most Effective Antimicrobial Touch Surface Material. Frequently Asked Questions about the most effective touch surface [online] available from : http://www.antimicrobialcopper.com/faq.aspx (acceessed on 21 April 2010)

[7] Thiel, T. Introduction to bacterial. Department of Biology. University of Missouri St. Louis: 1999.

[8] Honeyman, A.L., Friedman, H., and Bendinelli, M. Staphylococcus aureus infection and diseas. Kluwer Academic Publishers, New York: 2002.

[9] Logan, N. A. Bacterial systematics. Blackwell Scientific Publication: 1994.

[10] Todar ' s online textbook for bacteriology. Escherichia coli [online] available from : http://www.textbookofbacteriology.net/e.coli.html (accessed on 09/04/2010)

[11] Berg, H. C. *E. coli* in motion. United States of America : Springer-Verlag New York, Inc, 2004.

[12] University of California. E coli [online] available from : http://www.universityofcalifornia.edu/everyday/agriculture/images/e_coli.jpg (accessed on 09/04/2010)

[13] Tortora, G. J., Funke, B. R., and Case, L. C. Microbiology, An Introduction. Berlin: Benjamin Cummings, 2009.

[14] Donlan, R. M. Biofilms: Microbial Life on Surfaces. Emerging Infectious Diseases 8 (2002): 881-890.

[15] Hall-Stoodley, L., Costerton, J. W., and Stoodley, P. Bacterial biofilms: from the natural environment to infectious diseases. Microbiology 2 (2): 95–108 (2004).

[16] biofilmbook. hypertextbookshoop [online] Avilable from : http://biofilmbook.hypertextbookshoop.com/pulbic_version/contents/chapters /chapter001/section001/green/page001.html (acceessed on 21 April 2010)

[17] Vasile, C. and Pascu, M. Practical Guide to Polyethylene. Rapra Technology Limited

[18] Anderson, J. C., Leaver, K. K., Rawlings, R. D. and Alexander, J. M. Materials Science. Fourth edition, London, UK: Chapman&Hall 1994.

[19] Allcock, H. R., Lampe, F. W., and Mark, J. F. Contemporary polymer chemistry. Third edition, United States of America: Pearson Education Inc. 2003.

[20] Zhang, W., Zhang, Y., Ji, J., Zhao, J., Yan, Q., and Chu, P. K. Antimicrobial properties of copper plasma-modified polyethylene. Polymer Degradation and Stability 78 (2006): 257-262.

[21] LeVire, R. R., M. Harrison, C. R., Cook, R., and Lane, T. H. What is silicone?. Journal of Clinical Epidemiology 48 (1995): 513-517.

[22] Sperling, L. H. Introduction to physical polymer science. Fourth edition, United States of America : John Wiley & Sons, Inc, 2006.

[23] Bayston, R., Fisher, L. E., and Webber, K. An antimicrobial modified silicone peritoneal catheter with activity against both Gram positive and Gram negative bacteria, Biomaterials. 30 (2009): 3167-3173.

[24] Fullick, A, and McDuell, B. Edexcel A2 Chemistry. United States of America : Edexcel, 2009

[25] Zumdahl, S. S. Chemistry. Second edition, United States of America : Heath and Company, 1989

[26] John, P. I. Plasma sciences and the creation of wealth. India : TaTa McGraw-Hill, 2005.

[27] Rigden, J. S. (editor in chief). Macmillan encyclopidia of physics. United State of America: Simon & Schuster Macmillan, 1996.

[28] Fridman, A. Plasma chemistry. United State of America : Cambridge University Press, 2008.

[29] Goldson, R. J., and Rutherford, P. H. Introduction to plasma physics. United Kingdom: Plasma Physics Laboratory, Princeton University, 1995.

[30] Kobayashi, T., Katou, R., Yokota, T., Suzuki, Y., Iwaki, M. and Terai, T. Surface modification of silicone sheets and tubes using plasma-based ion implantation. Surface & Coating Technology 201(2007) : 8039-8042.

[31] Ngamrungroj, D. Plasma focus modification for material surface treatment. Master's thesis, Department of Physics, Faculty of Science, Chulalongkorn University, 2002.

[32] Lieberman, M.A. and Lichtenberg, A.J. Principles of plasma discharges and materials processing New York: John Wiley and Sons, Inc., 2005.

[33] The Naval Facilities Engineering Service Center (NAVFAC ESC). Ion implantation process. [online]. Available from : http://205.153.241.230/P2_Opportunity_Handbook/1_12.html [2010, May 17]

[34] Rimini, E. Ion implantation: basics to device fabrication. Norwell: Kluwer academic, 1995.

[35] Schiller, T.L., et al. Plasma immersion ion implantation (PIII) of poly(tetrafluoroethylene). Surface & Coatings Technology 177 (2004) : 483-488

[36] Ma, X., Wang, G. Yukimura, K., and Sun, M. Characteristics of copper oxide films deposited by PBII&D. Surface & Coatings Technology 201 (2007) : 6712-6714

[37] Egitto, D. F., Lyons, C.S., and Mittal, K. L. Plasma etching and modification of organic polymers. Pure & Applied Chemistry 62(1990) : 1699-1708.

[38] Strobel, M., Lyons, C.S., and Mittal, K. L. Plasma surface modification of polymers relevance to adhesion. netherlands : Koninklijke Wohrmann bv, Zutphen, 1994.

[39] Leech, P. W. Reactive ion etching of diamond in CF_4, O_2, O_2 and Ar-based mixtures. Materials Science 36 (2001) : 3453-3459

[40] Getty, J. How Plasma-Enhanced Surface Modification Improves the Production of Microelectronics and Optoelectronics. Chip Scale Review 2002: 72-75.

[41] V. Sˇvorcı´k et al. Ablation and water etching of poly(ethylene) modified by argon plasma. Polymer Degradation and Stability 92 (2007) : 1645-1649.

[42] H. Yasuda. Plasma for Modification of Polymers. Macromolecular Science 10 (1976) : 383-420.

[43] Inagaki, N., Tasaka, S., Ohkubo, J., and Kawai, H. Hydrophilic surface modification of polyethylene by plasma of nitrogen oxides. Journal of Polymer Science: Applied Polymer Symposiupm 46 (1990): 399-413.

[44] Khairallah, Y., Arefi, F., Amouroux, J., Leonard, D., and Bertrand, P. Surface fluorination of polyethylene films by different glow discharges. effects of frequency and electrode configuration. Plasma Surface Modification of Polymer 241 (1994): 295-300.

[45] Williams, R. L., Wilson, D. J., and Rhodes, N. P. Stability of plasma-treated silicone rubber and its influence on the interfacial aspects of blood compatibility, Biomaterials 25 (2004): 4659-4673.

[46] Jumpa, P. Mechanical property enhancement of polypropylene and polyester/cotton composites using a plasma focus device. Master's thesis, Department of Materials Science, Faculty of Science, Chulalongkorn University, 2005.

[47] Kamsing, P. A study of coating method for polymer by using plasma focus device. Bachelor Report, Department of Physics, Faculty of Science, Chulalongkorn University, 2000.

[48] Kulkoulprakar, T. Investigation of x-ray emission from a small plasma focus device. Master's thesis, Department of Physics, Faculty of Science, Chulalongkorn University, 2005.

[44] Srisawat, J. Surface modification of polypropylene nonwoven using a plasma focus device for lamination with polyester and cotton nonwoven. Master's Thesis, Department of Materials Science, Faculty of Science, Chulalongkorn University, 2004.

APPENDICES

APPENDIX A

Water Contact Angle of Polyethylene and Silicone Rubber

1. Water Contact Angle of Polyethylene

Table A-1 Water contact angle of PE sample treated by nitrogen plasma at position 1

Measurement	Number of plasma shots				
	untreated	3 shots	5 shots	7 shots	10 shots
1	80	78	66	62	66
2	80	80	68	70	72
3	80	78	72	70	74
Mean	80	78.67	68.67	67.33	70.67
SD	0	1.15	3.06	4.62	4.16

Table A-2 Water contact angle of PE sample treated by nitrogen plasma at position 2

Measurement	Number of plasma shots				
	untreated	3 shots	5 shots	7 shots	10 shots
1	80	78	70	70	68
2	80	82	68	70	72
3	80	80	62	70	70
Mean	80	80.00	66.67	70.00	70.00
SD	0	2.00	4.16	0.00	2.00

Table A-3 Water contact angle of PE sample treated by nitrogen plasma at position 3

Measurement	Number of plasma shots				
	untreated	3 shots	5 shots	7 shots	10 shots
1	80	86	60	80	60
2	80	68	60	80	60
3	80	70	60	80	60
Mean	80	74.67	60.00	80.00	60.00
SD	0	9.87	0.00	0.00	0.00

Table A-4 Water contact angle of PE sample treated by oxygen plasma at position 1

Measurement	Number of plasma shots				
	untreated	3 shots	5 shots	7 shots	10 shots
1	80	58	80	86	83
2	80	58	75	86	83
3	80	57	76	81	77
Mean	80	57.67	77.00	84.33	81.00
SD	0	0.58	2.65	2.89	3.46

Table A-5 Water contact angle of PE sample treated by oxygen plasma at position 2

Measurement	Number of plasma shots				
	untreated	3 shots	5 shots	7 shots	10 shots
1	80	58	76	83	73
2	80	60	79	83	81
3	80	60	74	83	80
Mean	80	59.33	76.33	83.00	78.00
SD	0	1.15	2.52	0.00	4.36

Table A-6 Water contact angle of PE sample treated by oxygen plasma at position 3

Measurement	Number of plasma shots				
	untreated	3 shots	5 shots	7 shots	10 shots
1	80	54	69	88	82
2	80	58	79	90	90
3	80	55	79	88	85
Mean	80	55.67	75.67	88.67	85.67
SD	0	2.08	5.77	1.15	4.04

Table A-7 Water contact angle of PE sample treated by argon plasma at position 1

Measurement	Number of plasma shots				
	untreated	3 shots	5 shots	7 shots	10 shots
1	80	84	86	88	88
2	80	88	84	86	88
3	80	88	88	86	88
Mean	80	86.67	86.00	86.67	88.00
SD	0	2.31	2.00	1.15	0.00

Table A-8 Water contact angle of PE sample treated by argon plasma at position 2

Measurement	Number of plasma shots				
	untreated	3 shots	5 shots	7 shots	10 shots
1	80	82	84	88	90
2	80	82	82	88	90
3	80	84	82	90	88
Mean	80	82.67	82.67	88.67	89.33
SD	0	1.15	1.15	1.15	1.15

Table A-9 Water contact angle of PE sample treated by argon plasma at position 3

Measurement	Number of plasma shots				
	untreated	3 shots	5 shots	7 shots	10 shots
1	80	84	90	90	90
2	80	84	90	90	90
3	80	88	90	90	90
Mean	80	85.33	90.00	90.00	90.00
SD	0	2.31	0.00	0.00	0.00

2. **Water Contact Angle of Silicone Rubber**

Table A-10 Water contact angle of silicone rubber sample treated by nitrogen plasma at position 1

Measurement	Number of plasma shots				
	untreated	3 shots	5 shots	7 shots	10 shots
1	100	88	100	100	104
2	100	85	99	105	102
3	100	90	102	108	100
Mean	100	87.67	100.33	104.33	102.00
SD	0	2.52	1.53	4.04	2.00

Table A-11 Water contact angle of silicone rubber sample treated by nitrogen plasma at position 2

Measurement	Number of plasma shots				
	untreated	3 shots	5 shots	7 shots	10 shots
1	100	84	104	94	102
2	100	84	100	94	102
3	100	90	102	94	106
Mean	100	86.00	102.00	94.00	103.33
SD	0	3.46	2.00	0.00	2.31

Table A-12 Water contact angle of silicone rubber sample treated by nitrogen plasma at position 3

Measurement	Number of plasma shots				
	untreated	3 shots	5 shots	7 shots	10 shots
1	100	90	102	100	106
2	100	90	100	106	110
3	100	90	99	102	100
Mean	100	90.00	100.33	102.67	105.33
SD	0	0.00	1.53	3.06	5.03

Table A-13 Water contact angle of silicone rubber sample treated by oxygen plasma at position 1

Measurement	Number of plasma shots				
	untreated	3 shots	5 shots	7 shots	10 shots
1	100	88	90	90	118
2	100	85	89	93	116
3	100	94	94	95	113
Mean	100	89.00	91.00	92.67	115.67
SD	0	4.58	2.65	2.52	2.52

Table A-14 Water contact angle of silicone rubber sample treated by oxygen plasma at position 2

Measurement	Number of plasma shots				
	untreated	3 shots	5 shots	7 shots	10 shots
1	100	96	94	96	110
2	100	98	98	94	110
3	100	100	98	94	110
Mean	100	98.00	96.67	94.67	110.00
SD	0	2.00	2.31	1.15	0.00

Table A-15 Water contact angle of silicone rubber sample treated by oxygen plasma at position 3

Measurement	Number of plasma shots				
	untreated	3 shots	5 shots	7 shots	10 shots
1	100	90	86	90	120
2	100	83	88	94	120
3	100	88	86	95	120
Mean	100	87.00	86.67	93.00	120.00
SD	0	3.61	1.15	2.65	0.00

Table A-16 Water contact angle of silicone rubber sample treated by argon plasma at position 1

Measurement	Number of plasma shots				
	untreated	3 shots	5 shots	7 shots	10 shots
1	100	108	106	106	110
2	100	110	110	112	110
3	100	110	110	114	116
Mean	100	109.33	108.67	110.67	112.00
SD	0	1.15	2.31	4.16	3.46

Table A-17 Water contact angle of silicone rubber sample treated by argon plasma at position 2

Measurement	Number of plasma shots				
	untreated	3 shots	5 shots	7 shots	10 shots
1	100	118	110	120	118
2	100	116	112	118	118
3	100	116	112	120	118
Mean	100	116.67	111.33	119.33	118.00
SD	0	1.15	1.15	1.15	0.00

Table A-18 Water contact angle of silicone rubber sample treated by argon plasma at position 3

Measurement	Number of plasma shots				
	untreated	3 shots	5 shots	7 shots	10 shots
1	100	110	110	114	110
2	100	108	108	110	110
3	100	108	102	110	108
Mean	100	108.67	106.67	111.33	109.33
SD	0	1.15	4.16	2.31	1.15

Copper Content of Polyethylene and Silicone Rubber

1. Copper Content of Polyethylene

Table A-19 Copper content of PE sample treated by nitrogen plasma

Nitrogen plasma	Copper Content (ppm)		
	Position1	Position2	Position3
3 Shots	0.261	0.221	0.273
5 Shots	2.245	1.455	2.597
7 Shots	2.542	1.913	2.989
10 Shots	3.593	2.483	3.034

Table A-20 Copper content of PE sample treated by oxygen plasma

Nitrogen plasma	Copper Content (ppm)	
	Position1	Position 2
3 Shots	0.379	0.148
5 Shots	1.043	0.76
7 Shots	1.497	1.604
10 Shots	1.474	1.063

Table A-21 Copper content of PE sample treated by argon plasma

Nitrogen plasma	Copper Content (ppm)	
	Position1	Position 2
3 Shots	0.258	0.293
5 Shots	1.263	0.484
7 Shots	0.325	0.647
10 Shots	0..780	1.264

2. Copper Content of Silicone Rubber

Table A-22 Copper content of silicone rubber sample treated by nitrogen plasma

Nitrogen plasma	Copper Content (ppm)	
	Position1	Position2
3 Shots	0.156	0.134
5 Shots	1.069	0.988
7 Shots	0.453	0.366
10 Shots	0.547	0.476

Table A-23 Copper content of silicone rubber sample treated by oxygen plasma

Nitrogen plasma	Copper Content (ppm)	
	Position1	Position 2
3 Shots	0.181	0.231
5 Shots	0.366	0.322
7 Shots	0.129	0.328
10 Shots	0.516	0.624

Table A-24 Copper content of silicone rubber sample treated by argon plasma

Nitrogen plasma	Copper Content (ppm)	
	Position1	Position 2
3 Shots	0.205	0.330
5 Shots	0.617	0.563
7 Shots	0.242	0.469
10 Shots	0.694	0.3

APPENDIX B

ATR/FT-IR Spectra of Polyethylene and Silicone Rubber

1. ATR/FTIR Spectra of Polyethylene

ATR/FT-IR spectrum of untreated PE

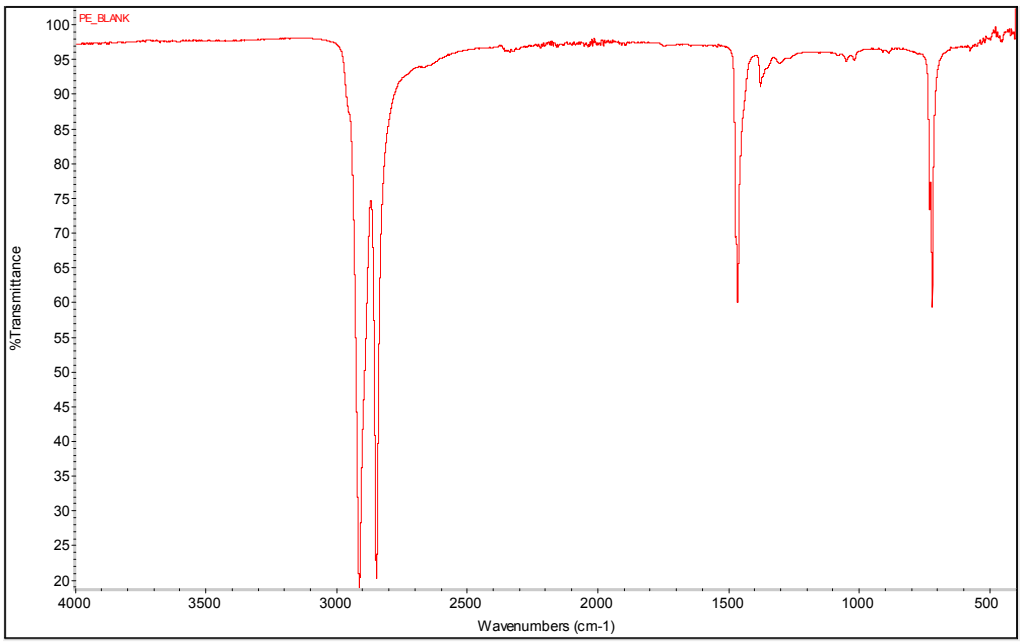

ATR/FT-IR spectrum of PE sample treated by 3 shots of nitrogen plasma at position 1

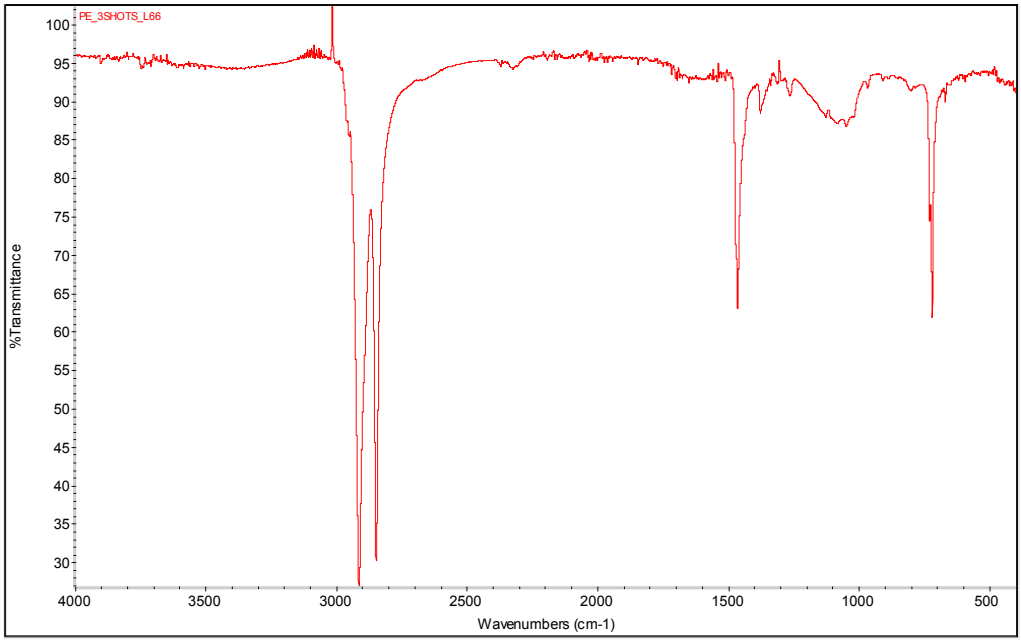

ATR/FT-IR spectrum of PE sample treated by 3 shots of nitrogen plasma at position 2

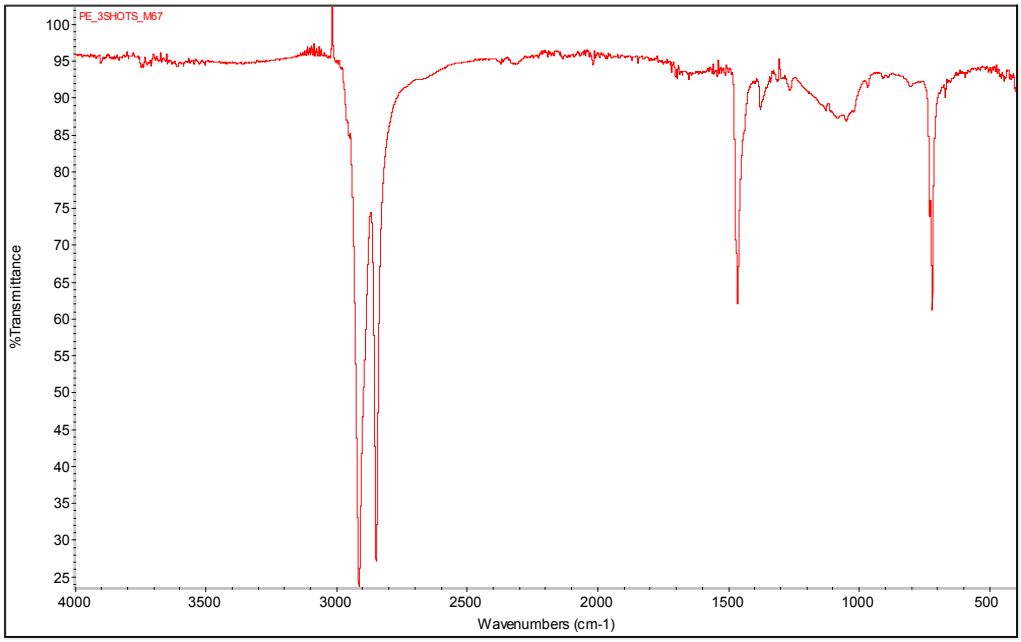

ATR/FT-IR spectrum of PE sample treated by 3 shots of nitrogen plasma at position 3

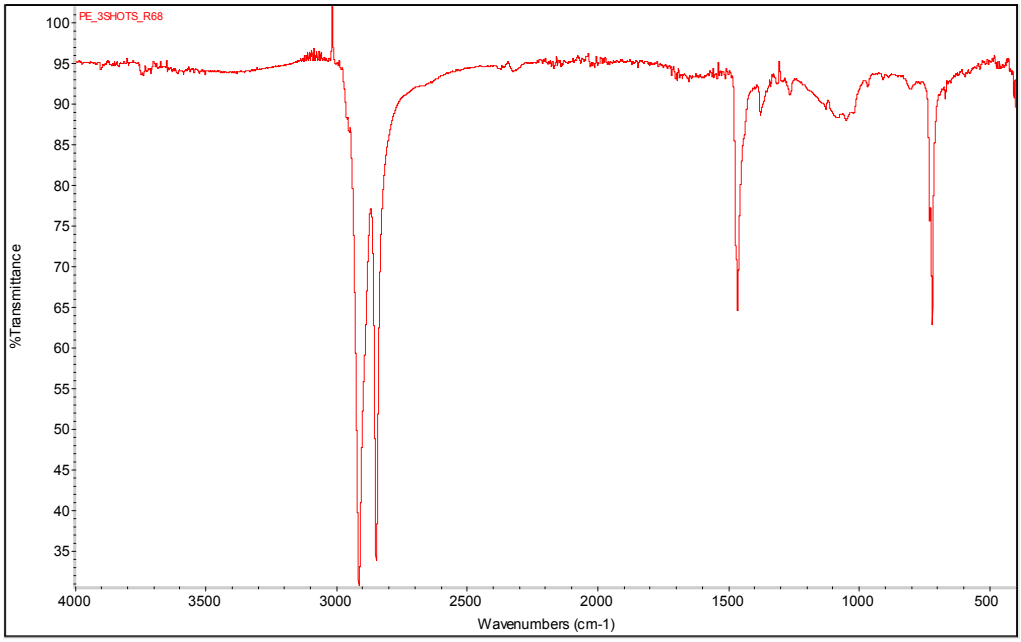

ATR/FT-IR spectrum of PE sample treated by 5 shots of nitrogen plasma at position 1

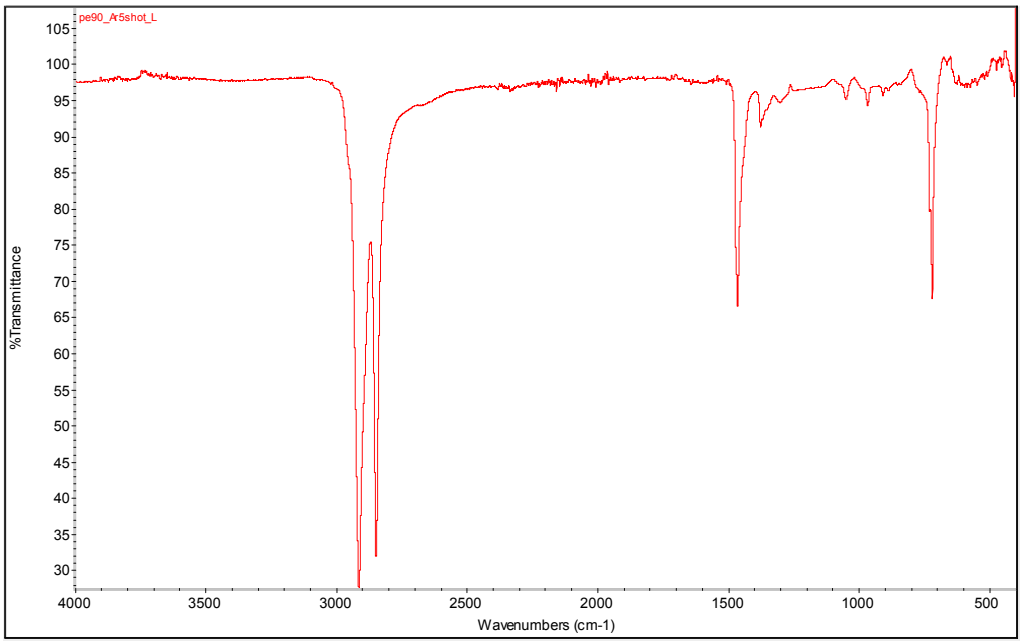

ATR/FT-IR spectrum of PE sample treated by 5 shots of nitrogen plasma at position 2

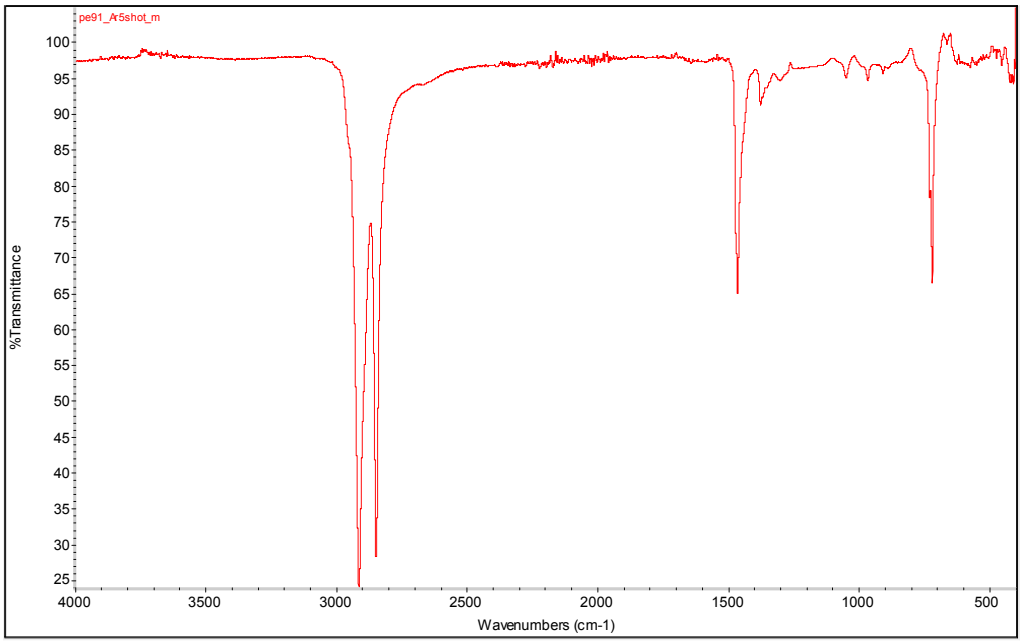

ATR/FT-IR spectrum of PE sample treated by 5 shots of nitrogen plasma at position 3

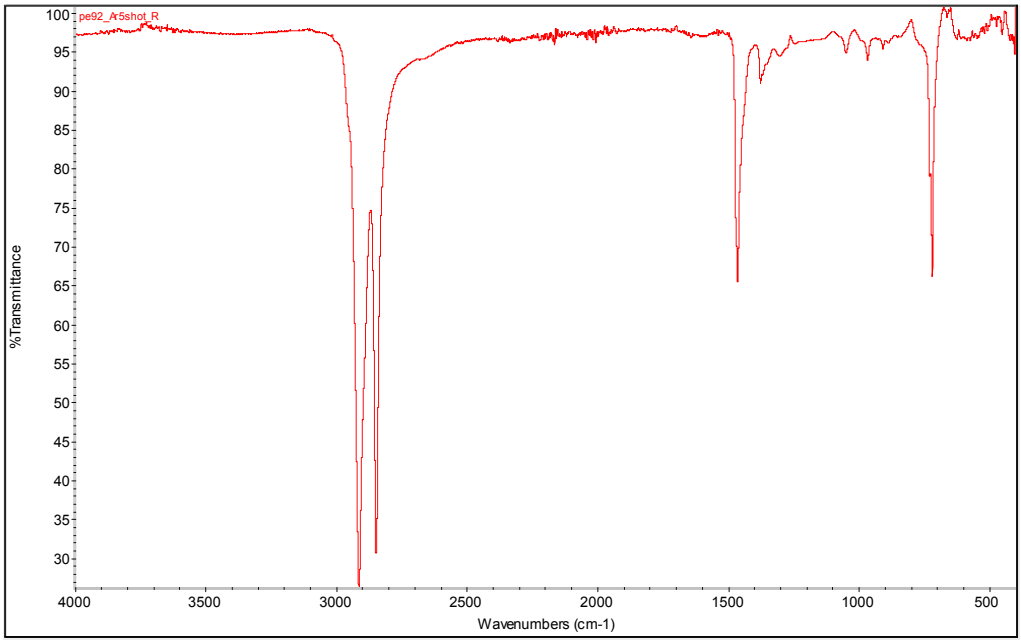

ATR/FT-IR spectrum of PE sample treated by 7 shots of nitrogen plasma at position 1

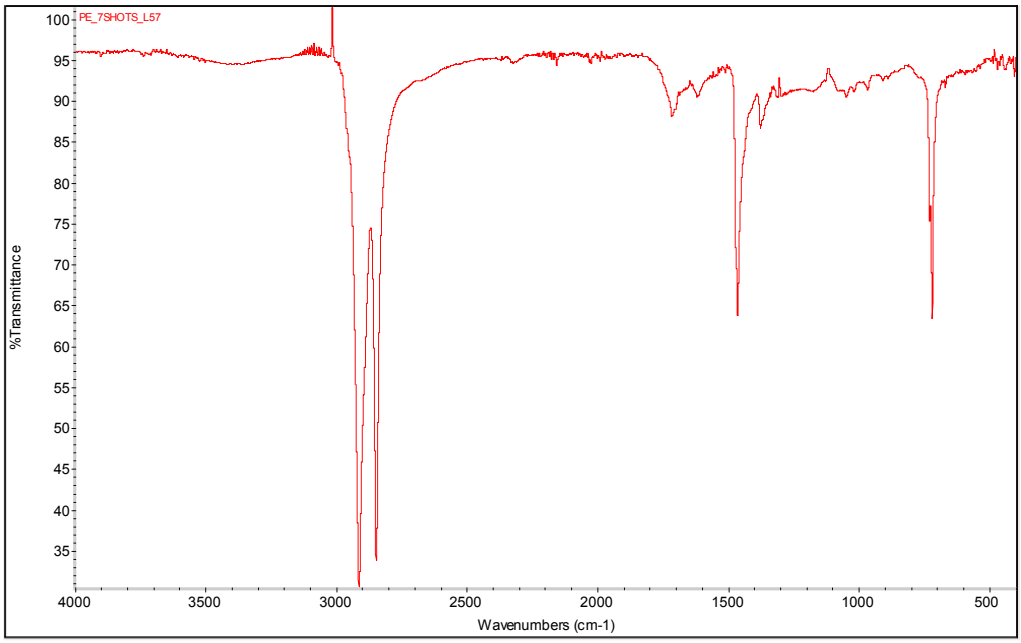

ATR/FT-IR spectrum of PE sample treated by 7 shots of nitrogen plasma at position 2

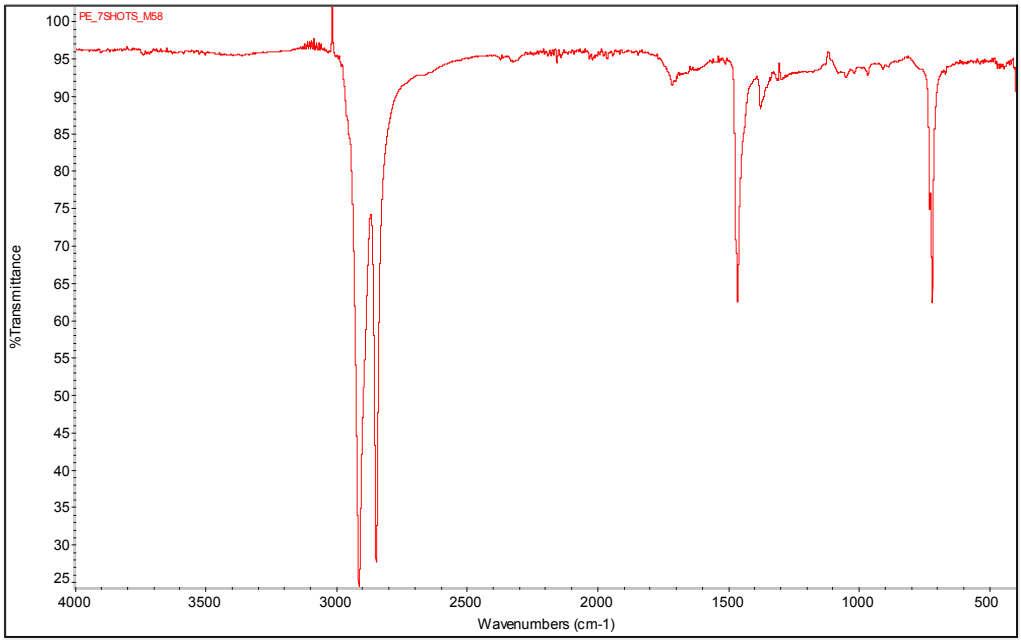

ATR/FT-IR spectrum of PE sample treated by 7 shots of nitrogen plasma at position 3

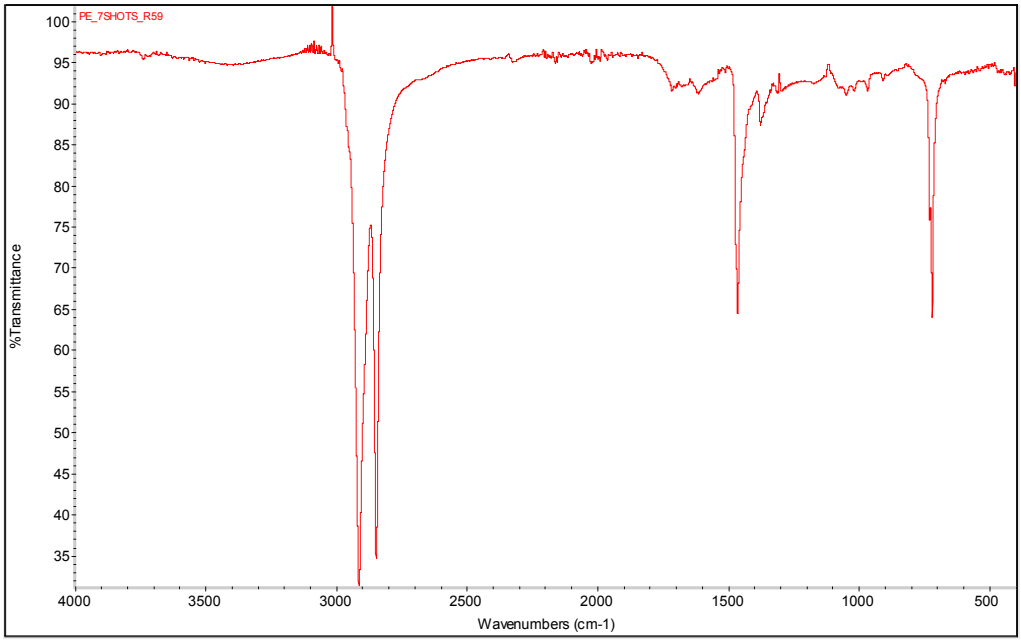

ATR/FT-IR spectrum of PE sample treated by 10 shots of nitrogen plasma at position 1

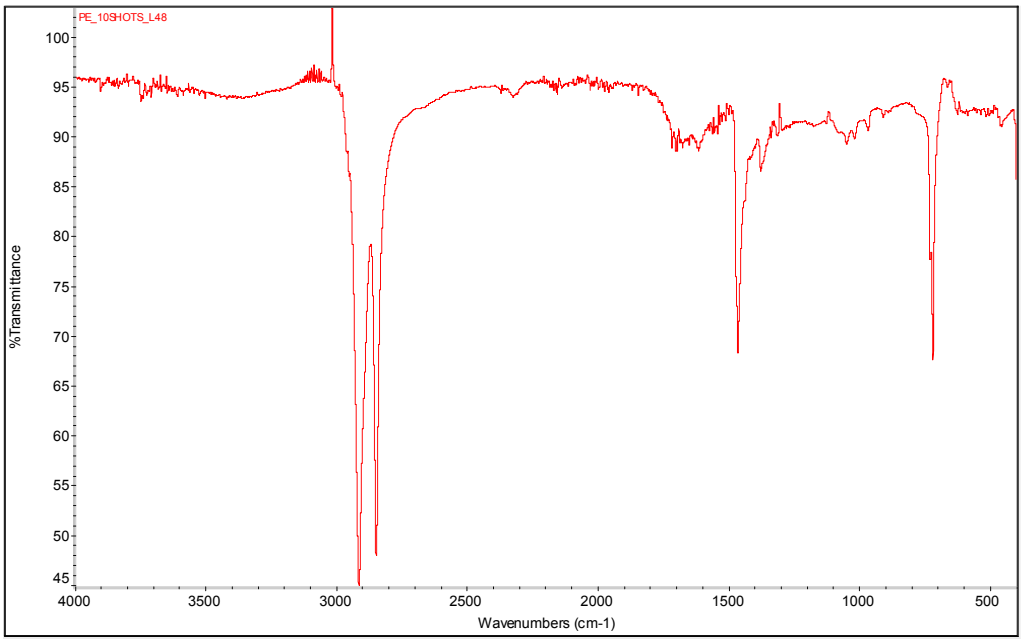

ATR/FT-IR spectrum of PE sample treated by 10 shots of nitrogen plasma at position 2

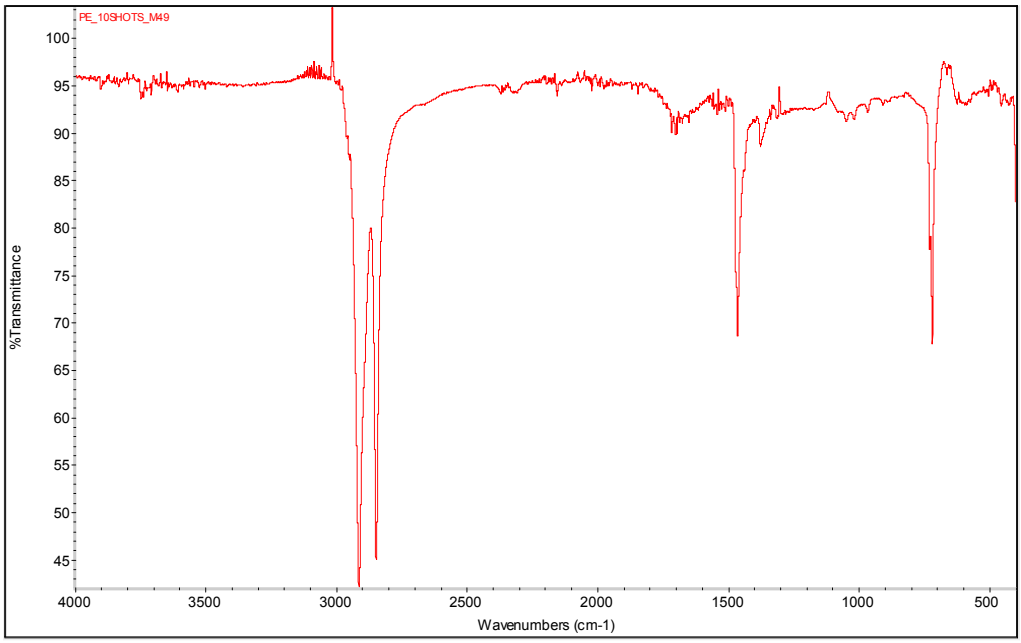

ATR/FT-IR spectrum of PE sample treated by 10 shots of nitrogen plasma at position 3

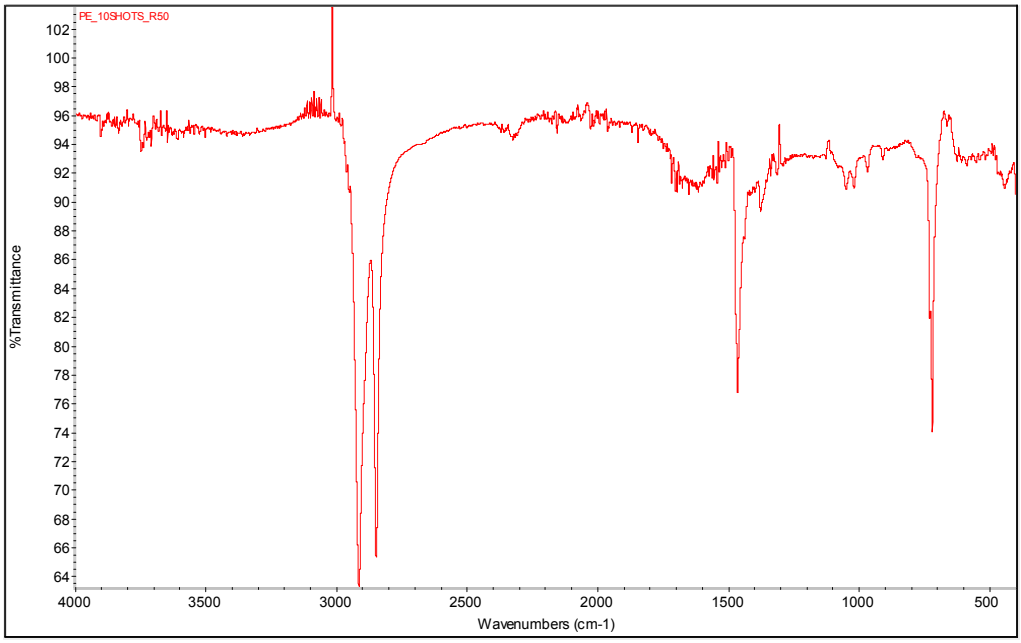

ATR/FT-IR spectrum of PE sample treated by 3 shots of oxygen plasma at position 1

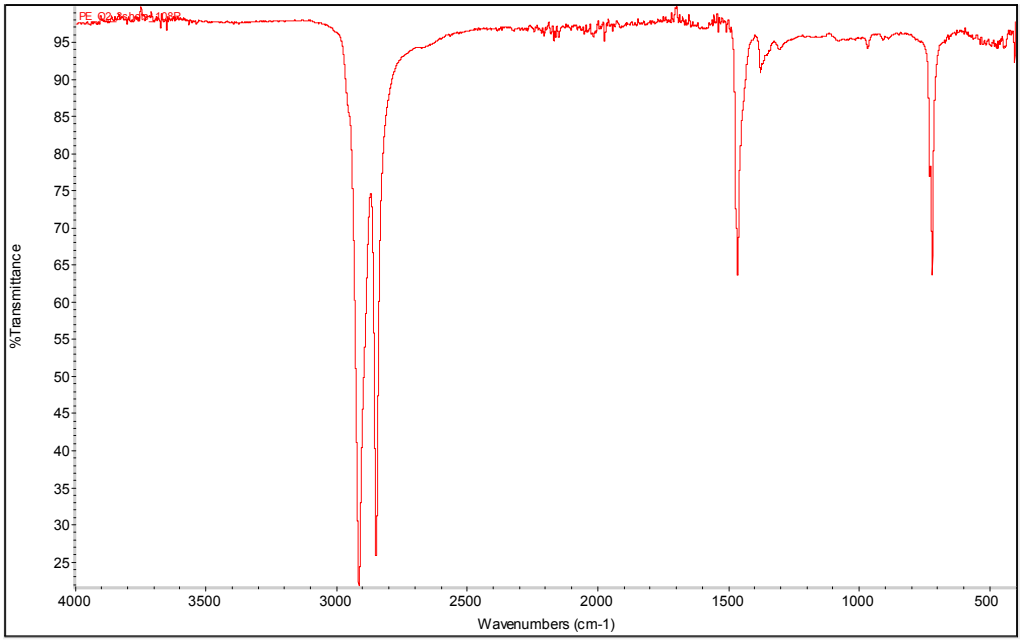

ATR/FT-IR spectrum of PE sample treated by 3 shots of oxygen plasma at position 2

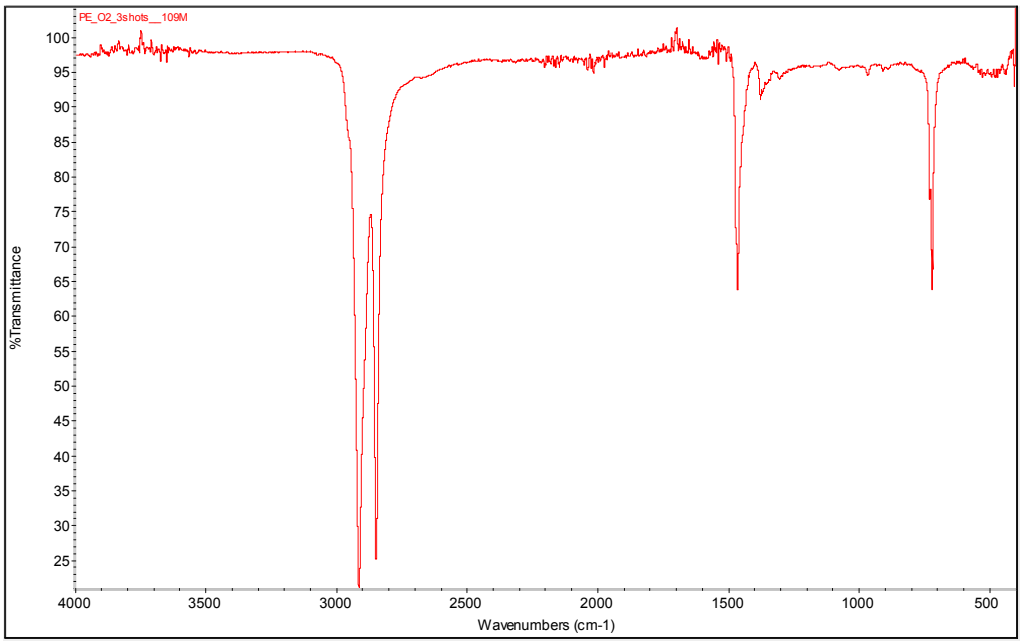

ATR/FT-IR spectrum of PE sample treated by 3 shots of oxygen plasma at position 3

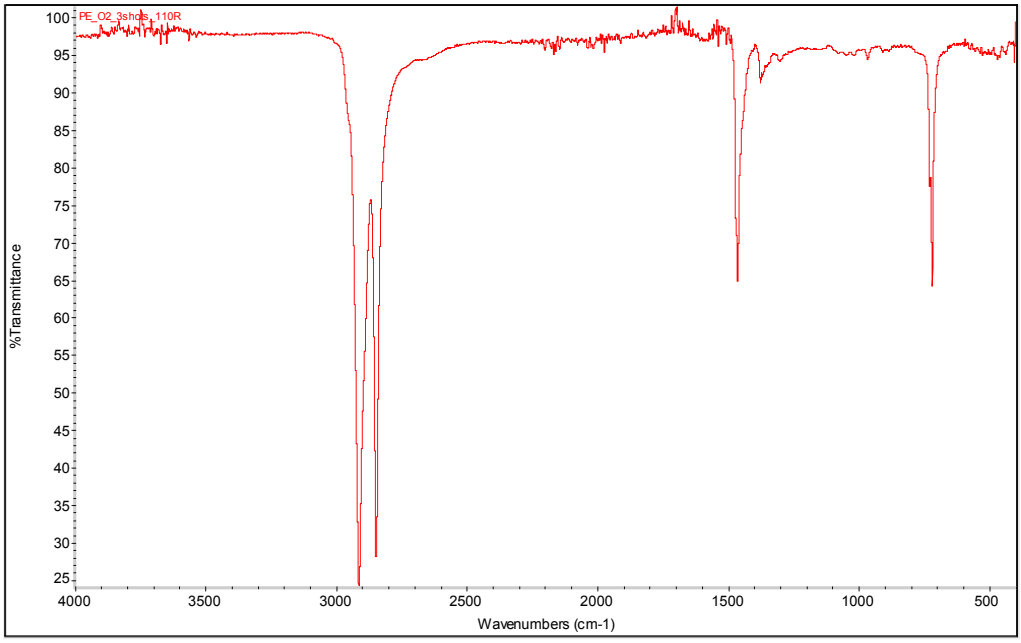

ATR/FT-IR spectrum of PE sample treated by 5 shots of oxygen plasma at position 1

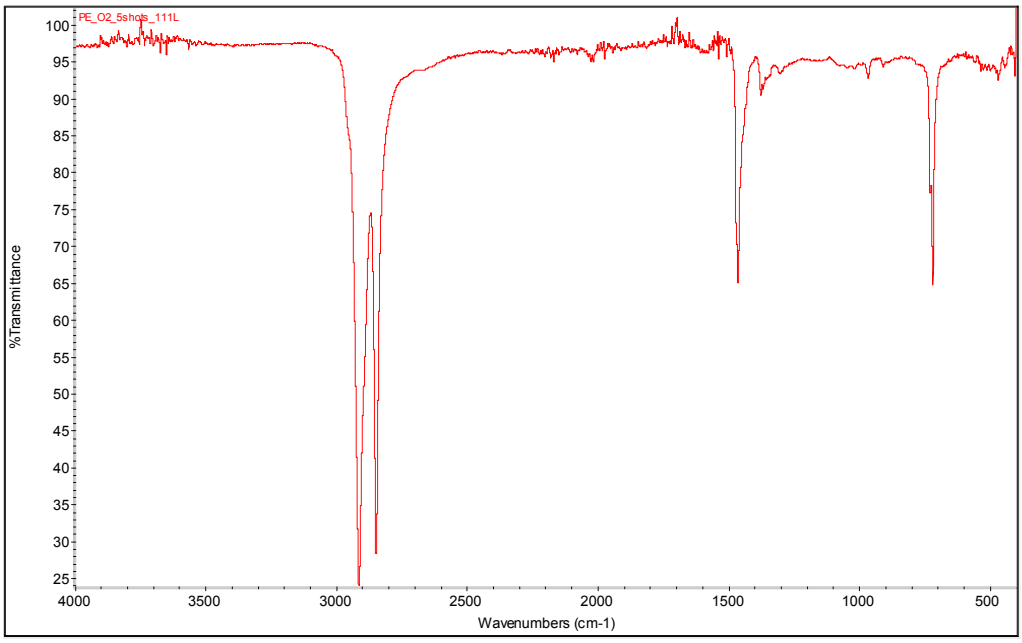

ATR/FT-IR spectrum of PE sample treated by 5 shots of oxygen plasma at position 2

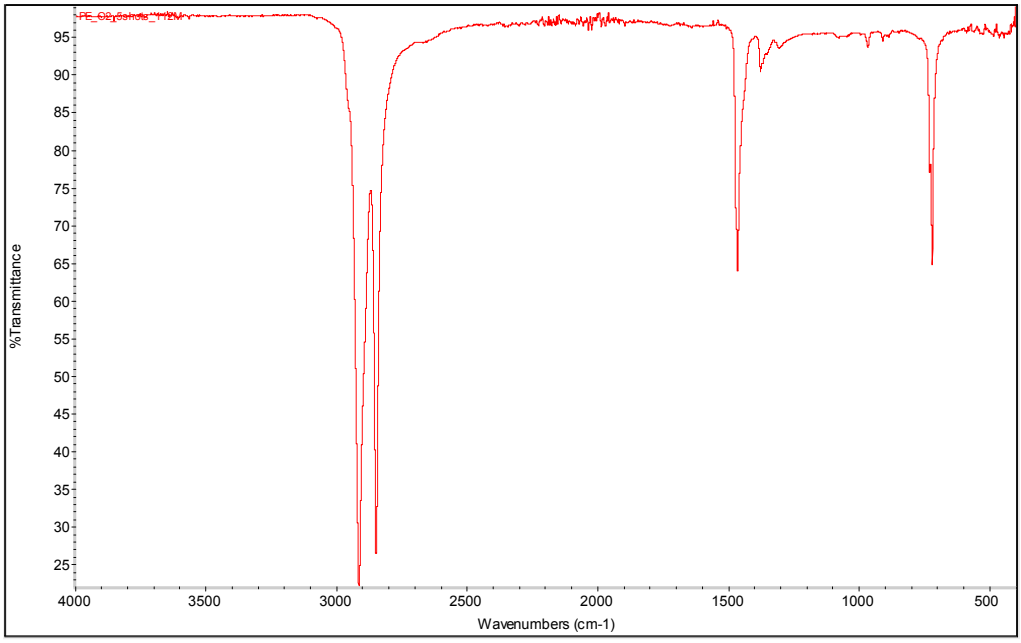

ATR/FT-IR spectrum of PE sample treated by 5 shots of oxygen plasma at position 3

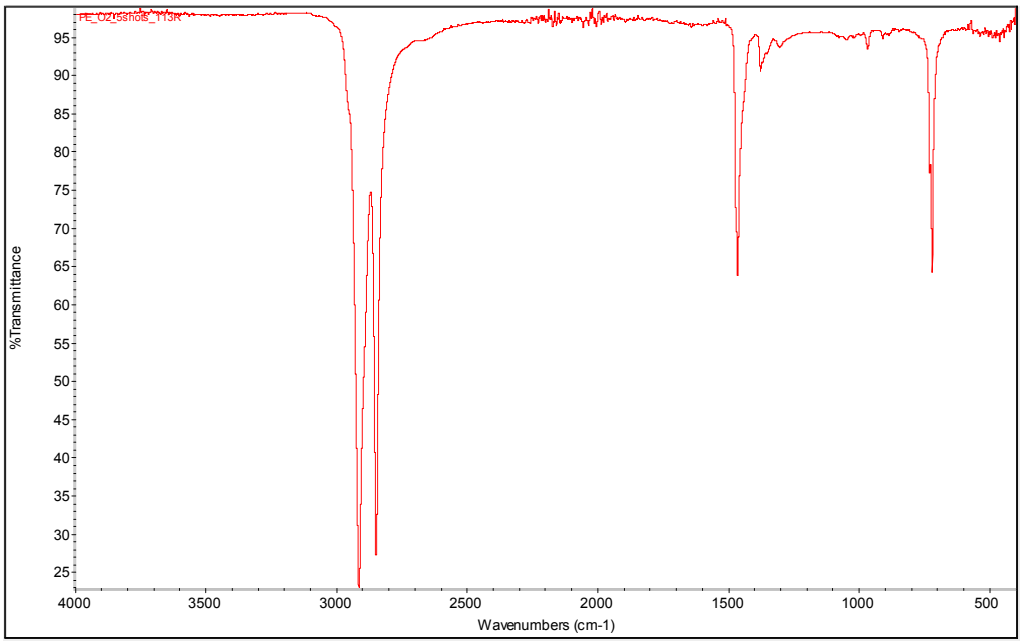

ATR/FT-IR spectrum of PE sample treated by 7 shots of oxygen plasma at position 1

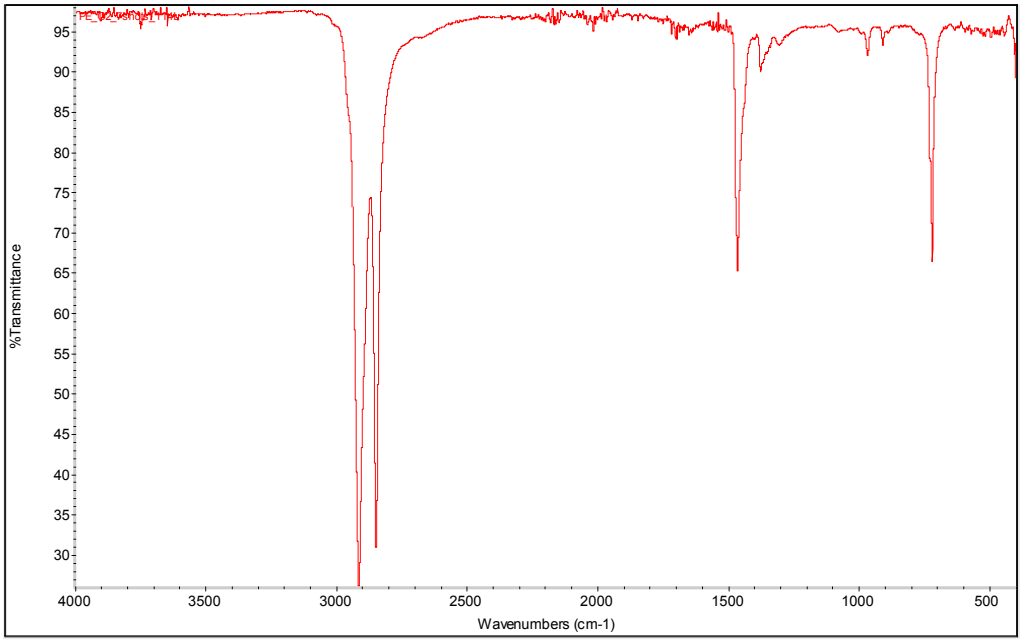

ATR/FT-IR spectrum of PE sample treated by 7 shots of oxygen plasma at position 2

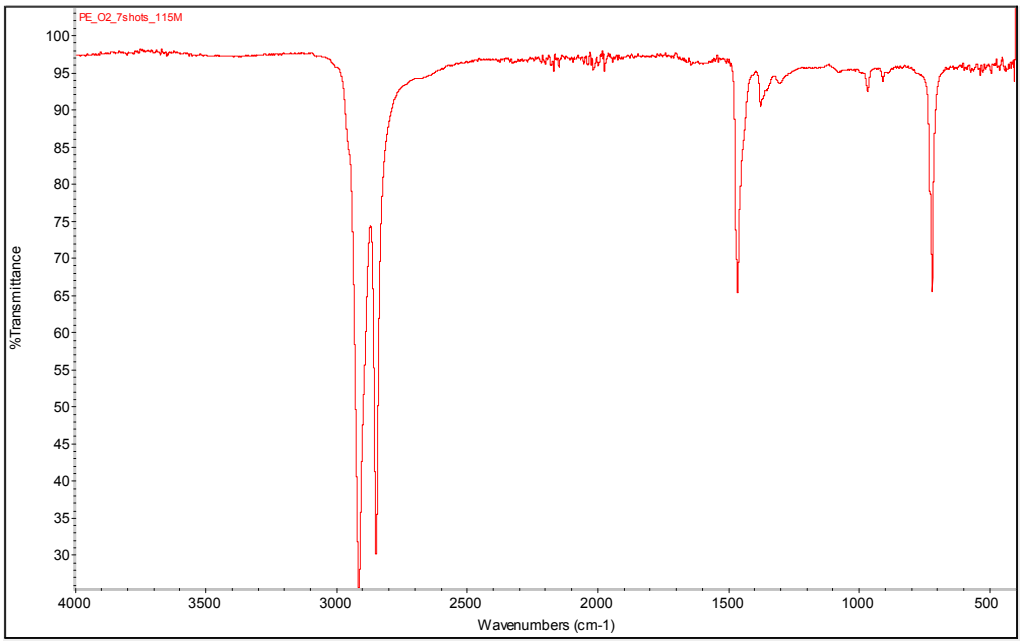

ATR/FT-IR spectrum of PE sample treated by 7 shots of oxygen plasma at position 3

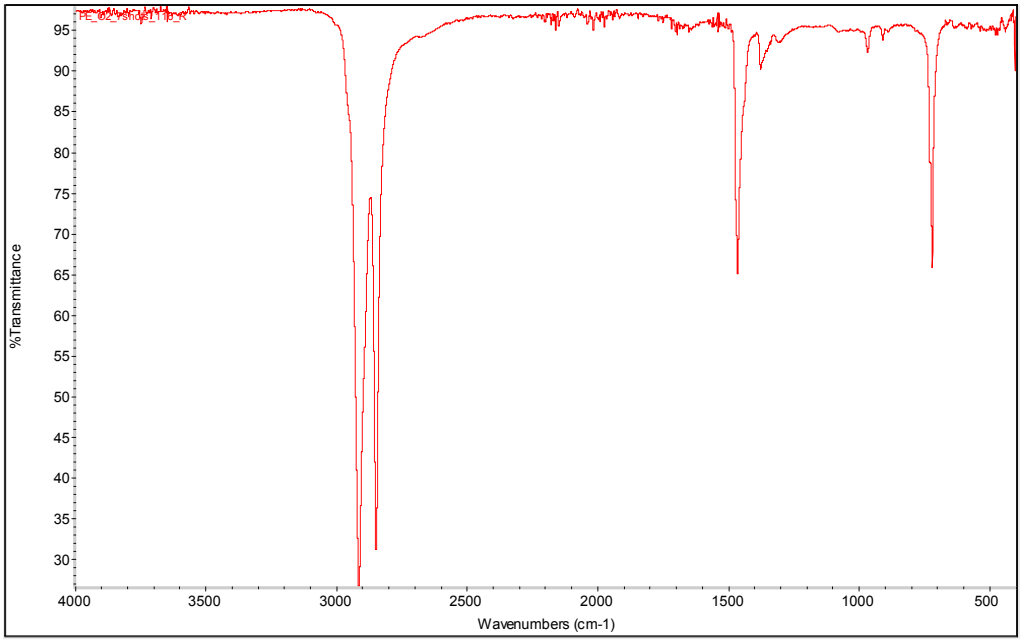

ATR/FT-IR spectrum of PE sample treated by 10 shots of oxygen plasma at position 1

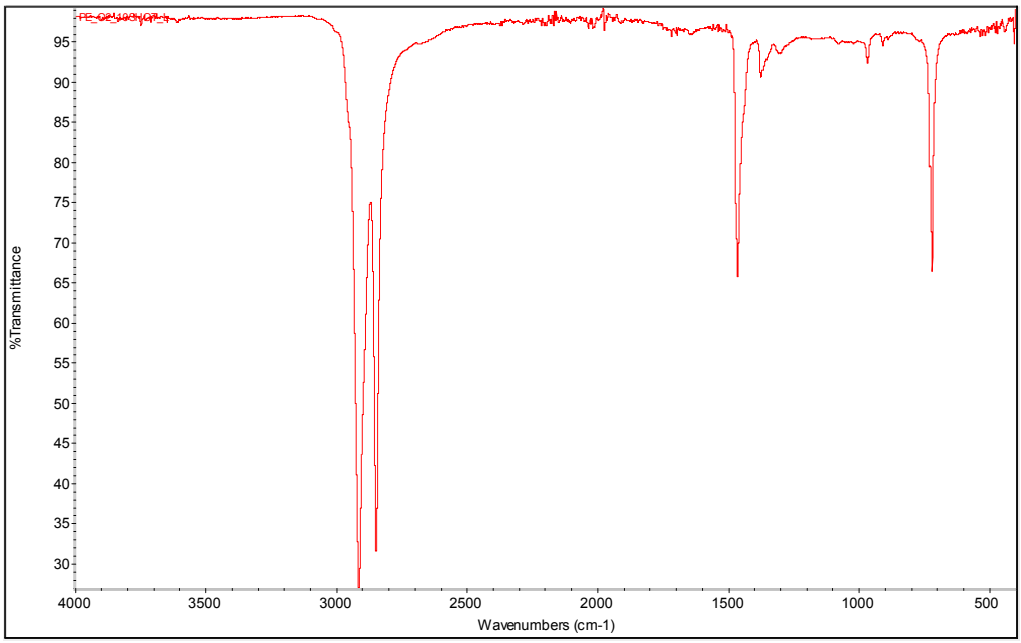

ATR/FT-IR spectrum of PE sample treated by 10 shots of oxygen plasma at position 2

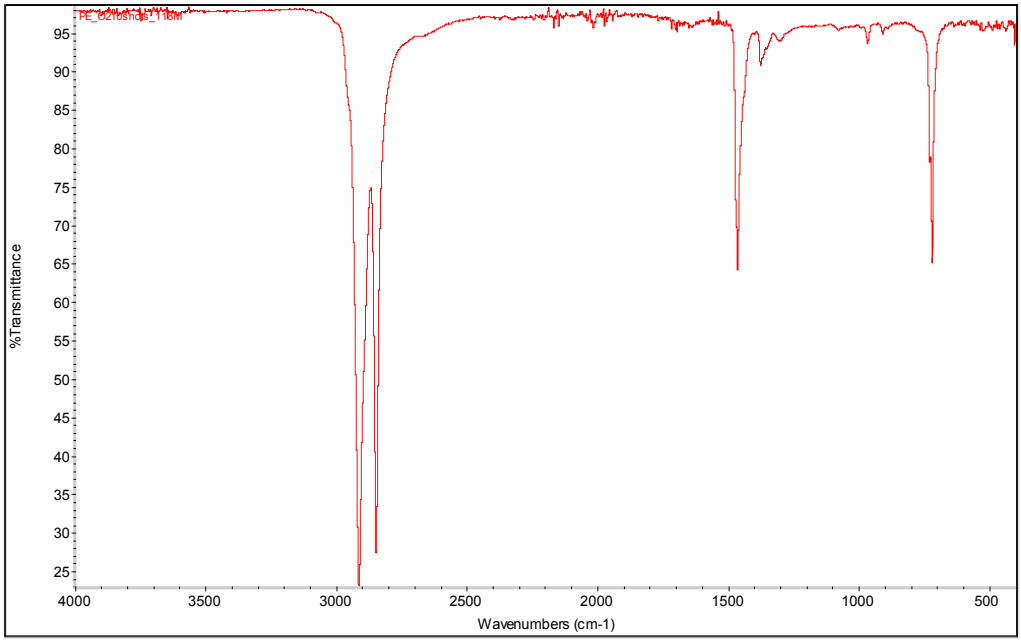

ATR/FT-IR spectrum of PE sample treated by 10 shots of oxygen plasma at position 3

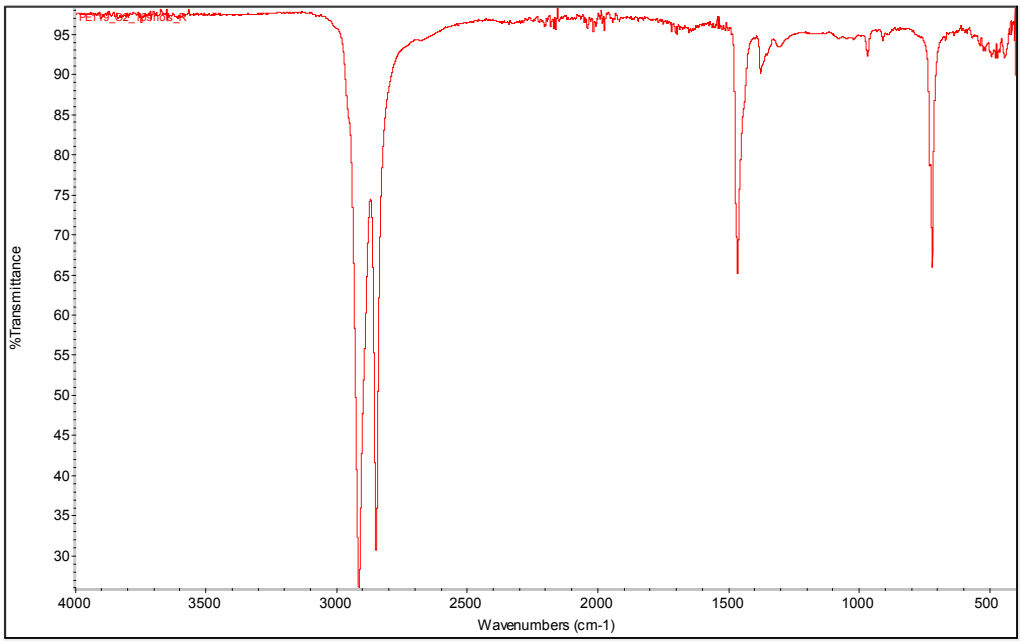

ATR/FT-IR spectrum of PE sample treated by 3 shots of argon plasma at position 1

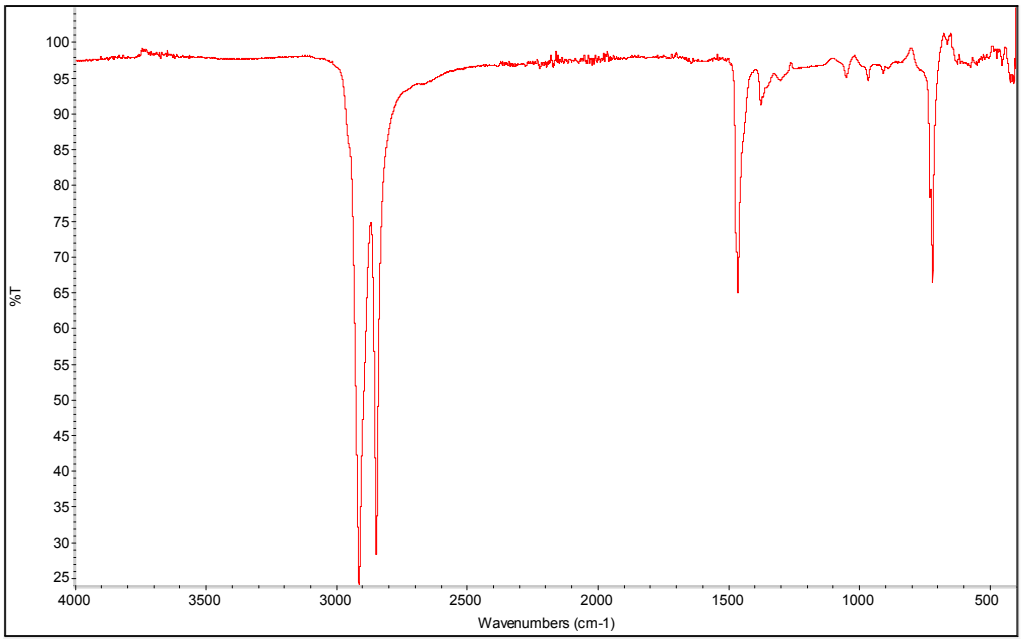

ATR/FT-IR spectrum of PE sample treated by 3 shots of argon plasma at position 2

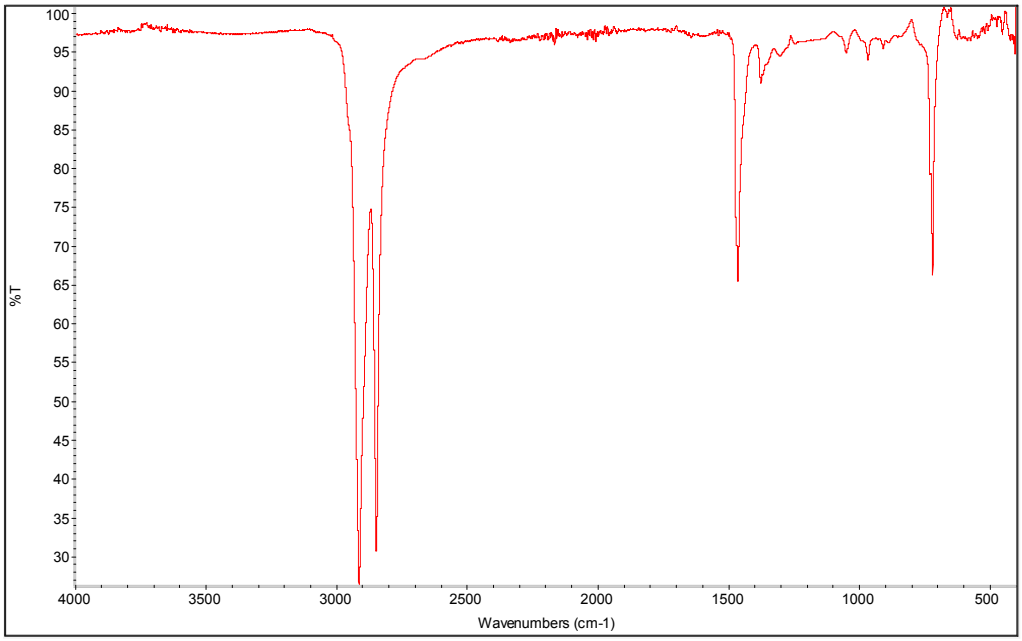

ATR/FT-IR spectrum of PE sample treated by 3 shots of argon plasma at position 3

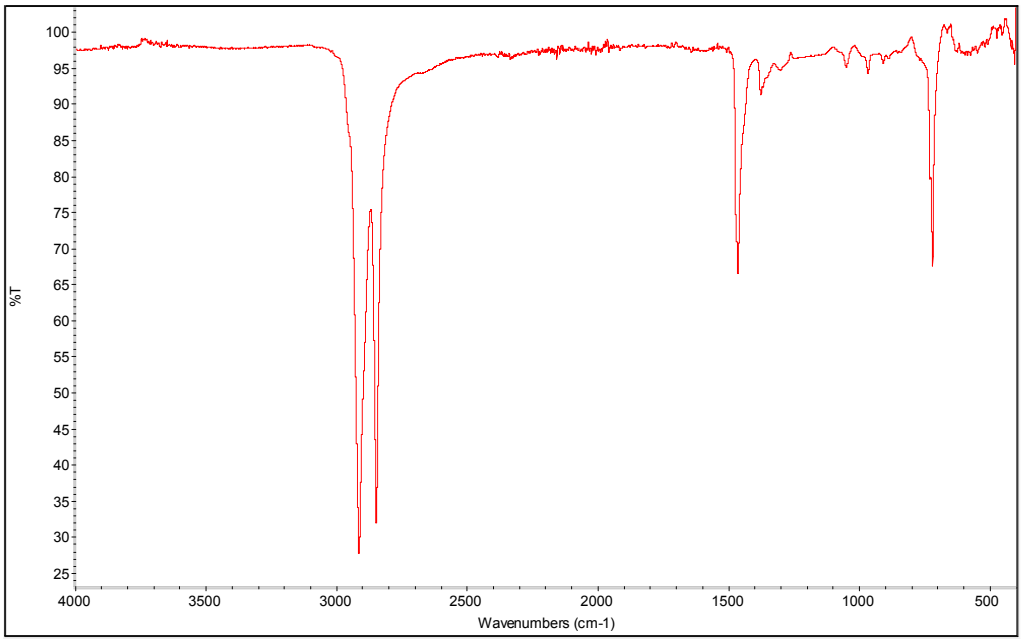

ATR/FT-IR spectrum of PE sample treated by 5 shots of argon plasma at position 1

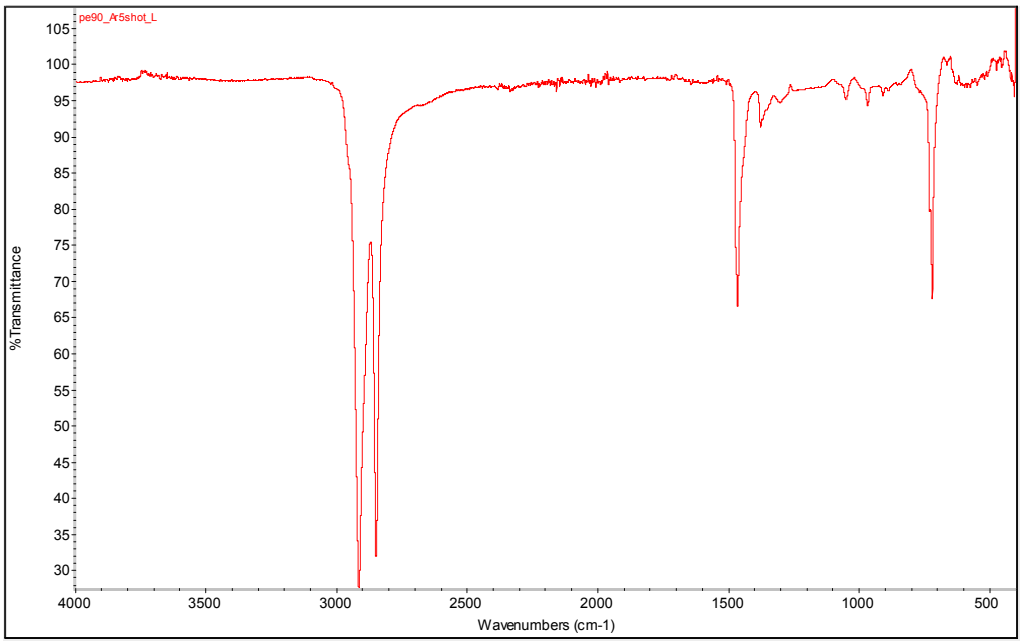

ATR/FT-IR spectrum of PE sample treated by 5 shots of argon plasma at position 2

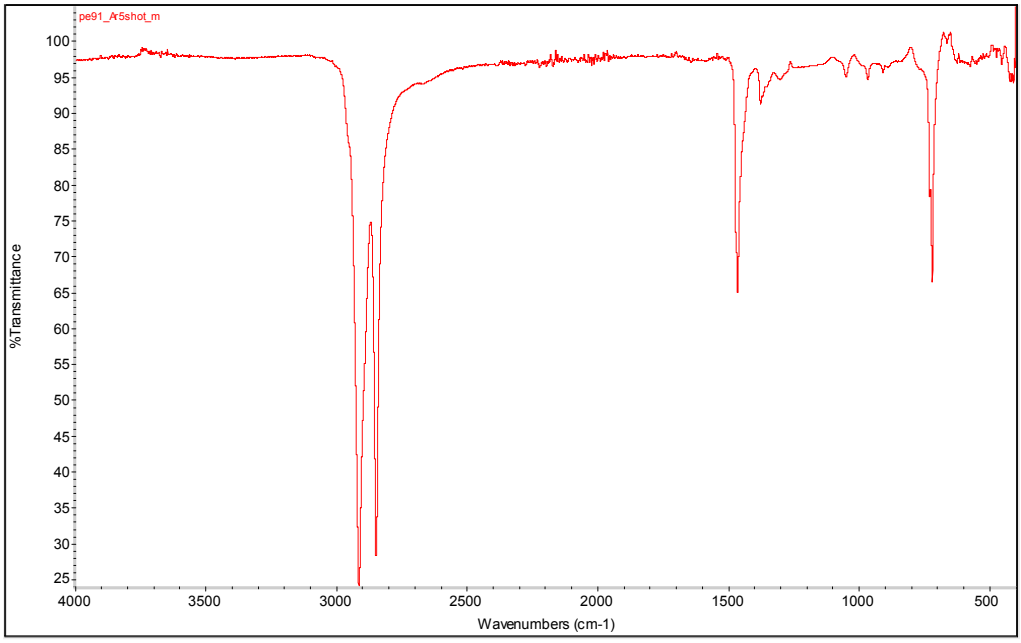

ATR/FT-IR spectrum of PE sample treated by 5 shots of argon plasma at position 3

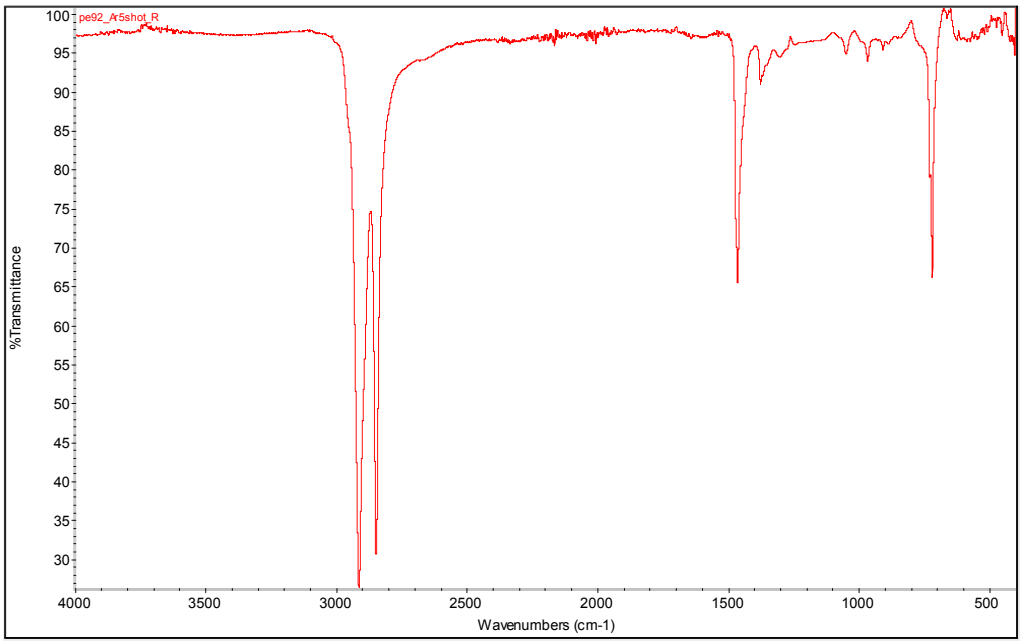

ATR/FT-IR spectrum of PE sample treated by 7 shots of argon plasma at position 1

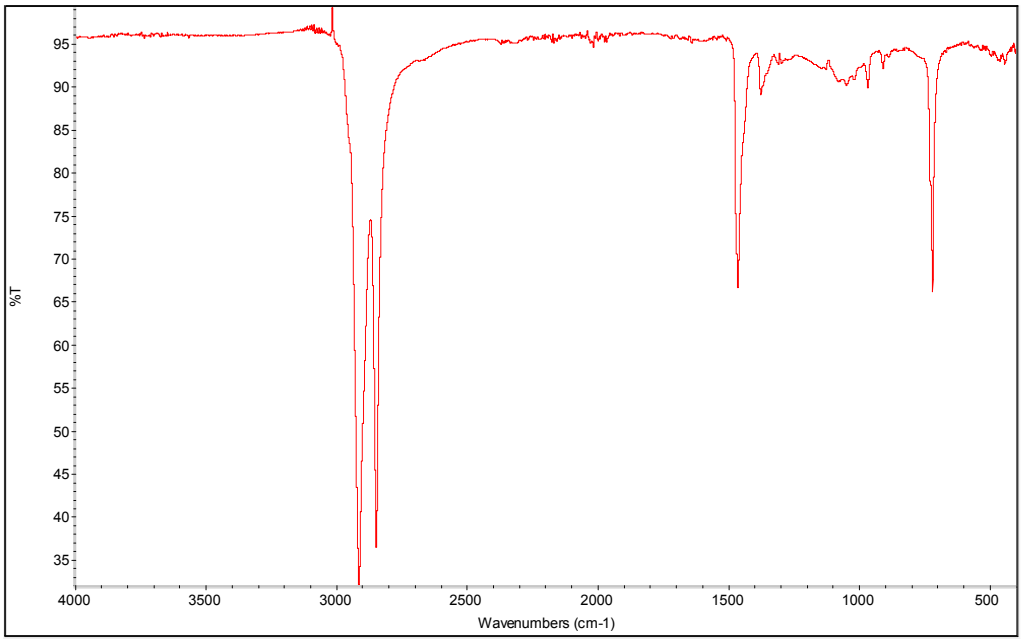

ATR/FT-IR spectrum of PE sample treated by 7 shots of argon plasma at position 2

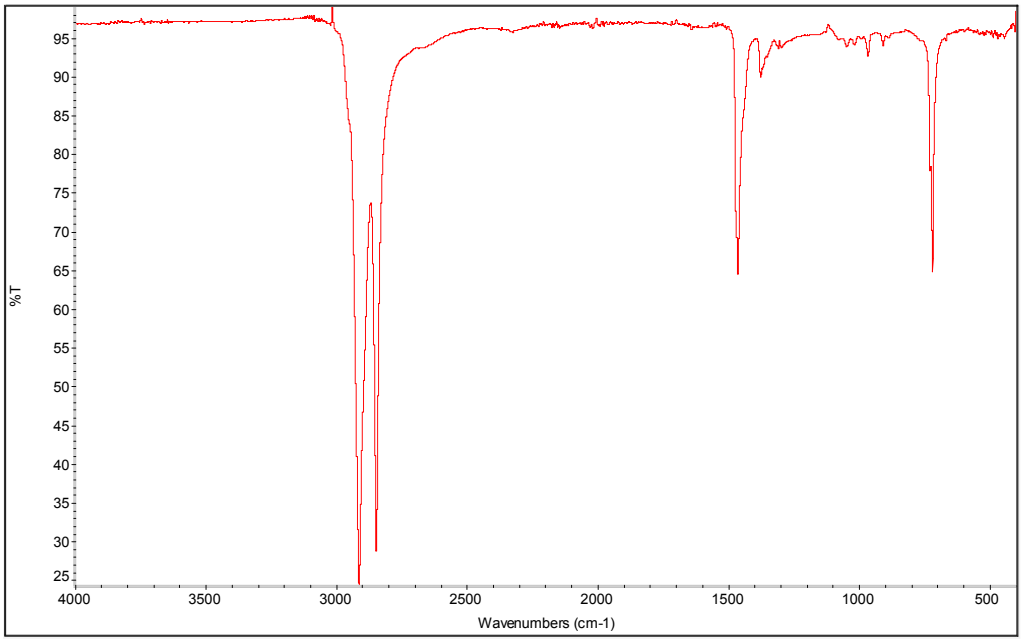

ATR/FT-IR spectrum of PE sample treated by 7 shots of argon plasma at position 3

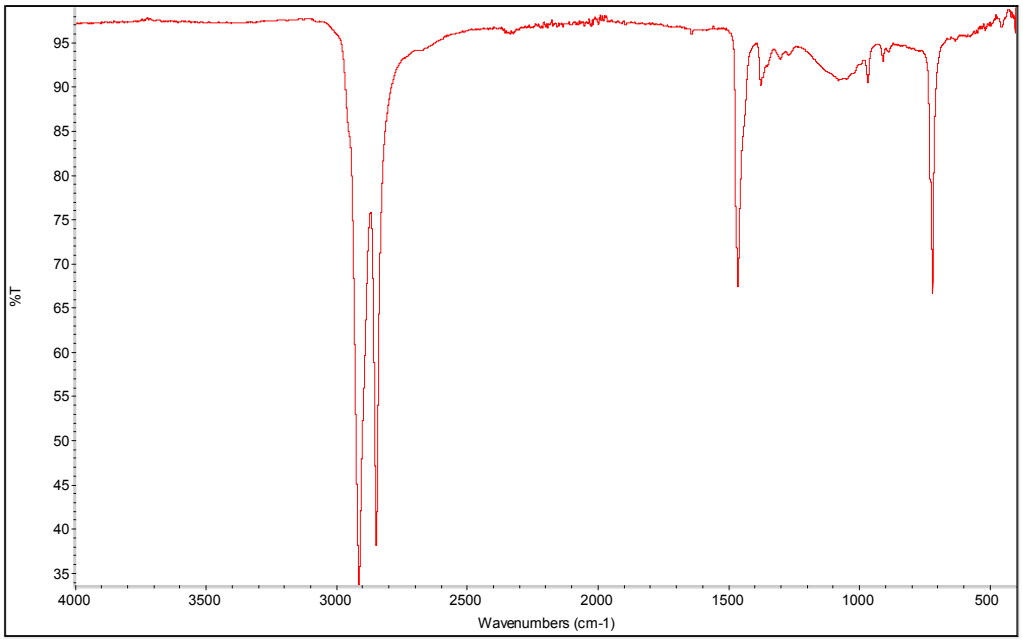

ATR/FT-IR spectrum of PE sample treated by 10 shots of argon plasma at position 1

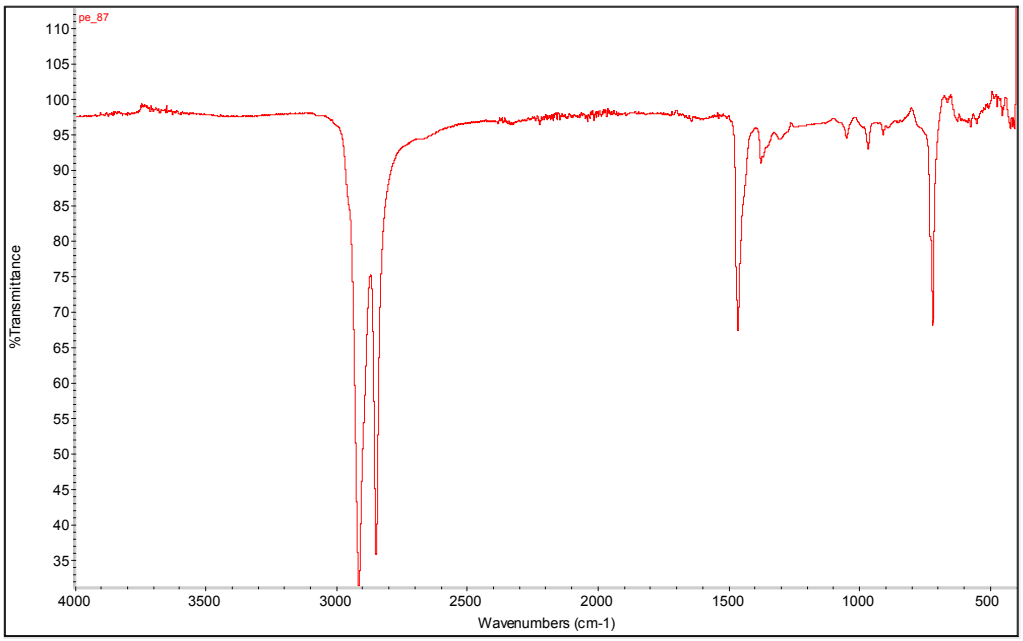

ATR/FT-IR spectrum of PE sample treated by 10 shots of argon plasma at position 2

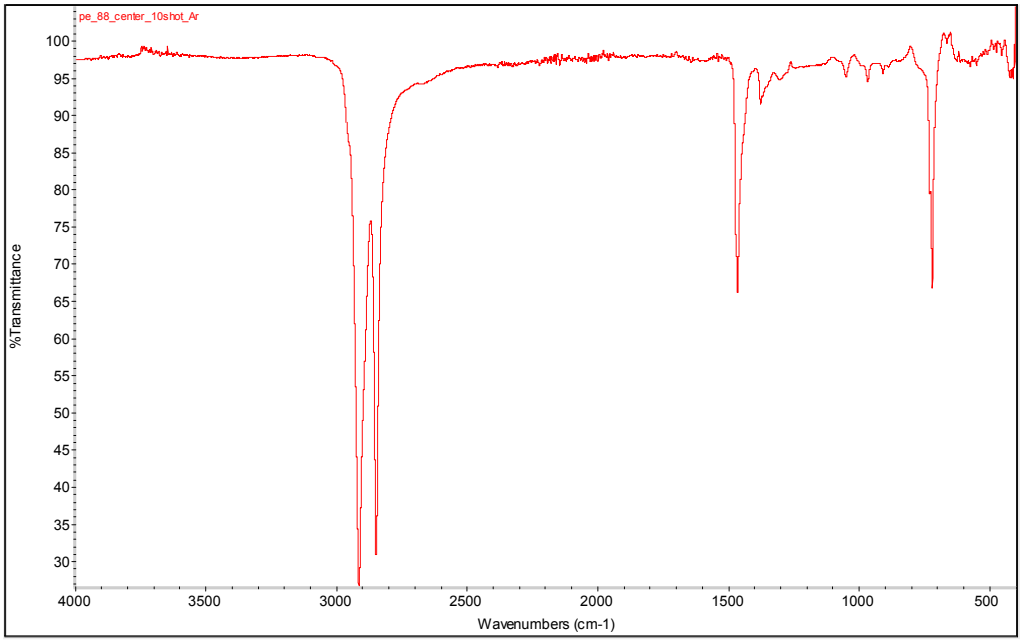

ATR/FT-IR spectrum of PE sample treated by 10 shots of argon plasma at position 3

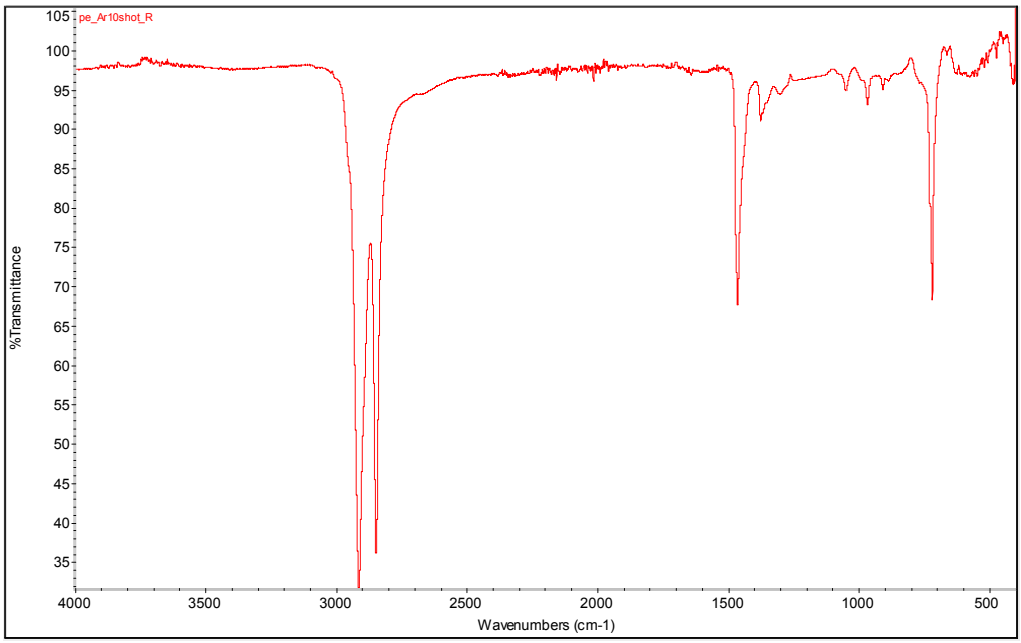

2. ATR/FTIR Spectra of Silicone Rubber

ATR/FT-IR spectrum of untreated silicone rubber

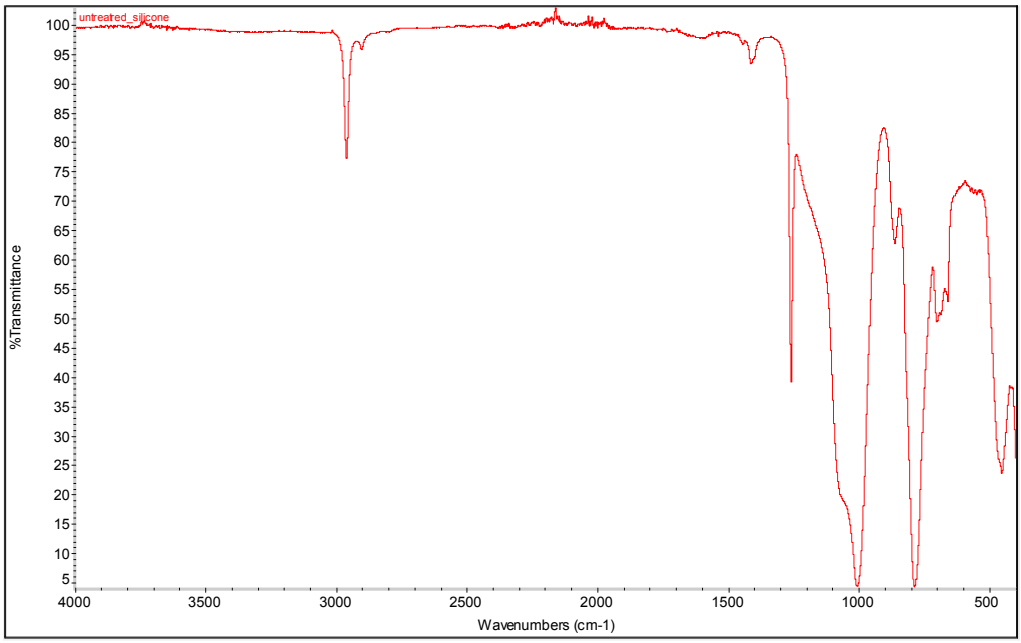

ATR/FT-IR spectrum of silicone rubber sample treated by 3 shots of nitrogen plasma at position 1

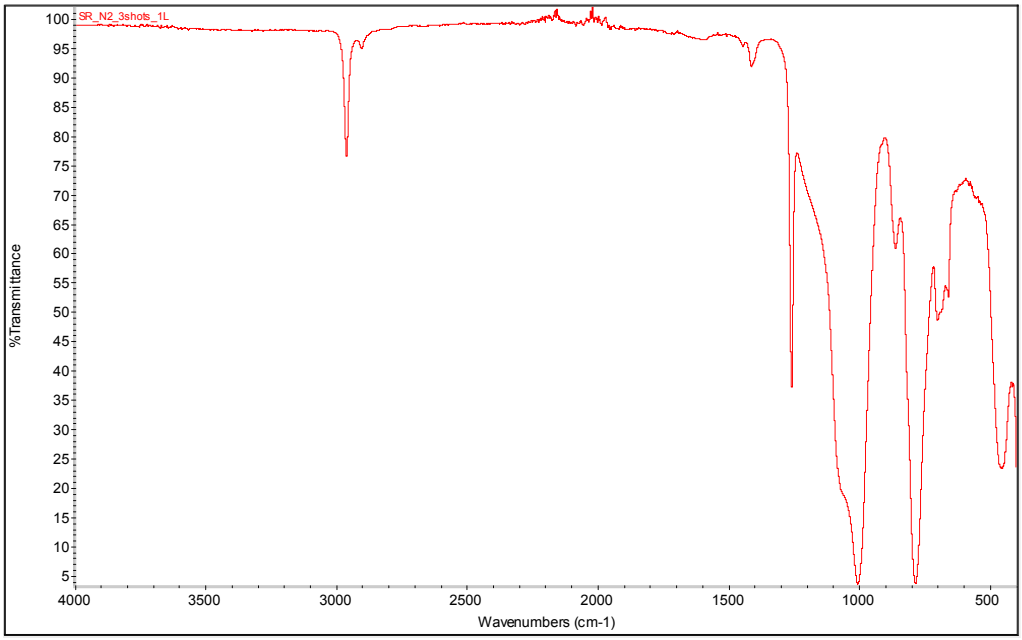

ATR/FT-IR spectrum of silicone rubber sample treated by 3 shots of nitrogen plasma at position 2

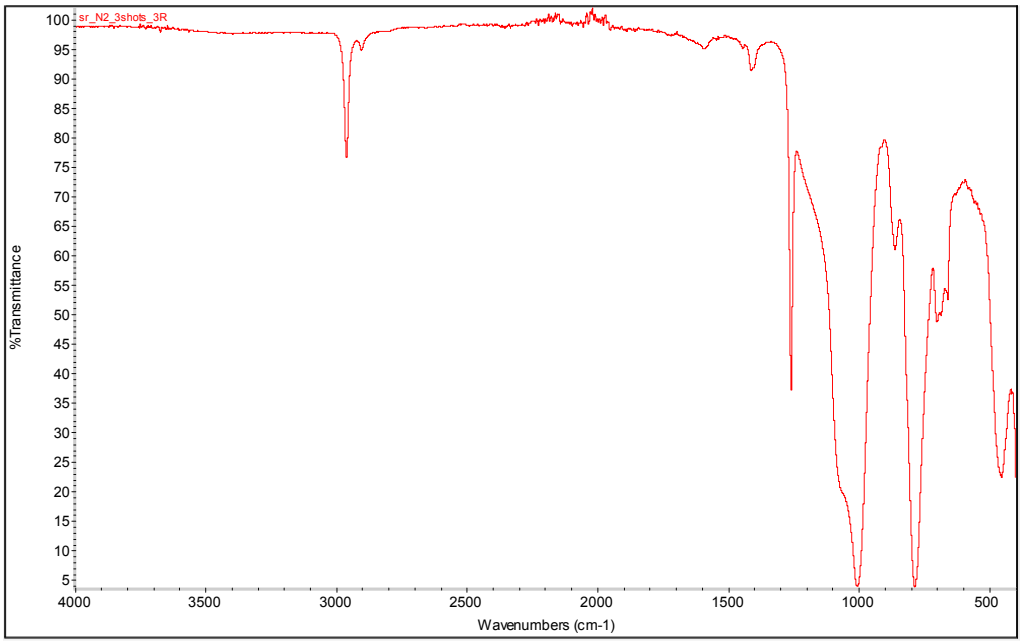

ATR/FT-IR spectrum of silicone rubber sample treated by 3 shots of nitrogen plasma at position 3

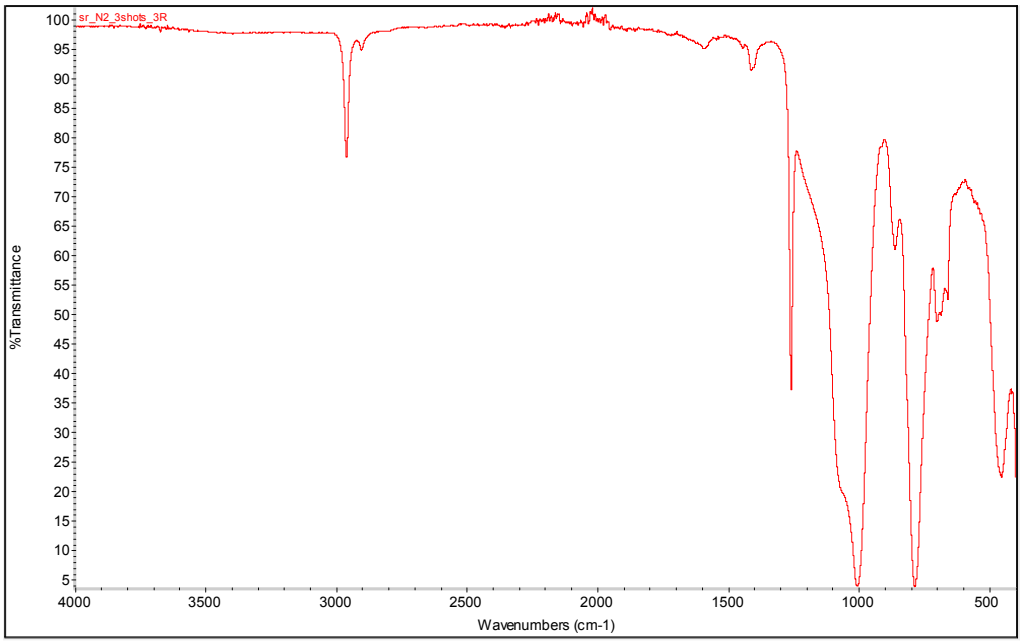

ATR/FT-IR spectrum of silicone rubber sample treated by 5 shots of nitrogen plasma at position 1

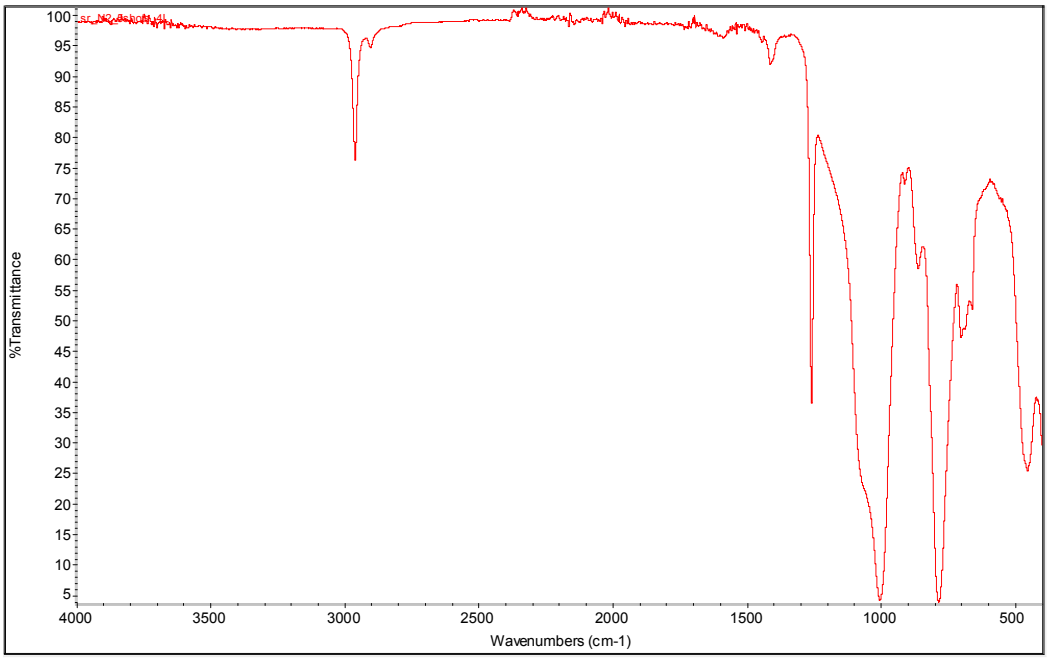

ATR/FT-IR spectrum of silicone rubber sample treated by 5 shots of nitrogen plasma at position 2

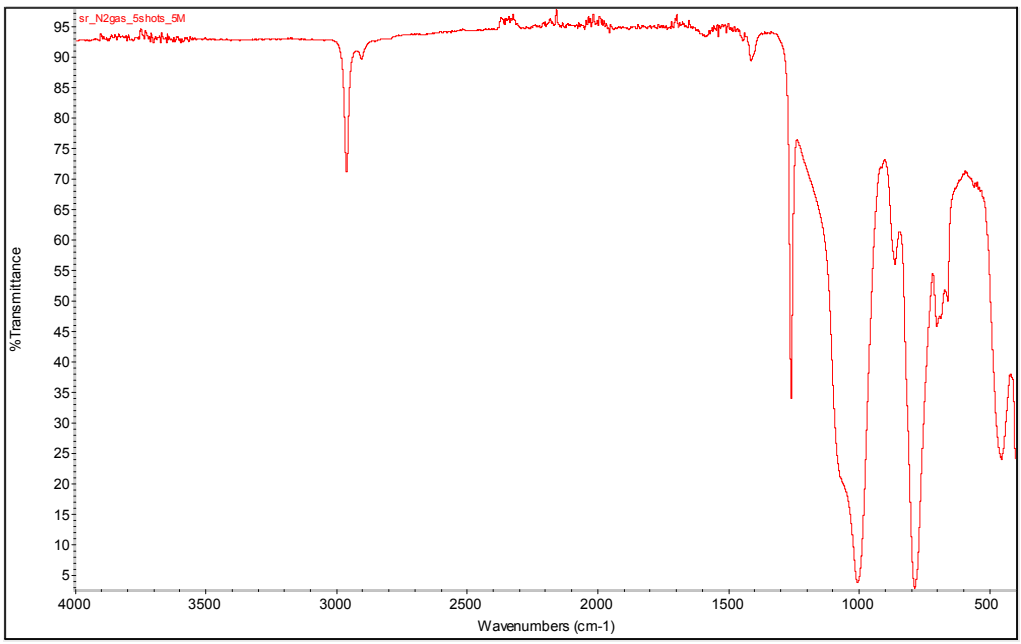

ATR/FT-IR spectrum of silicone rubber sample treated by 5 shots of nitrogen plasma at position 3

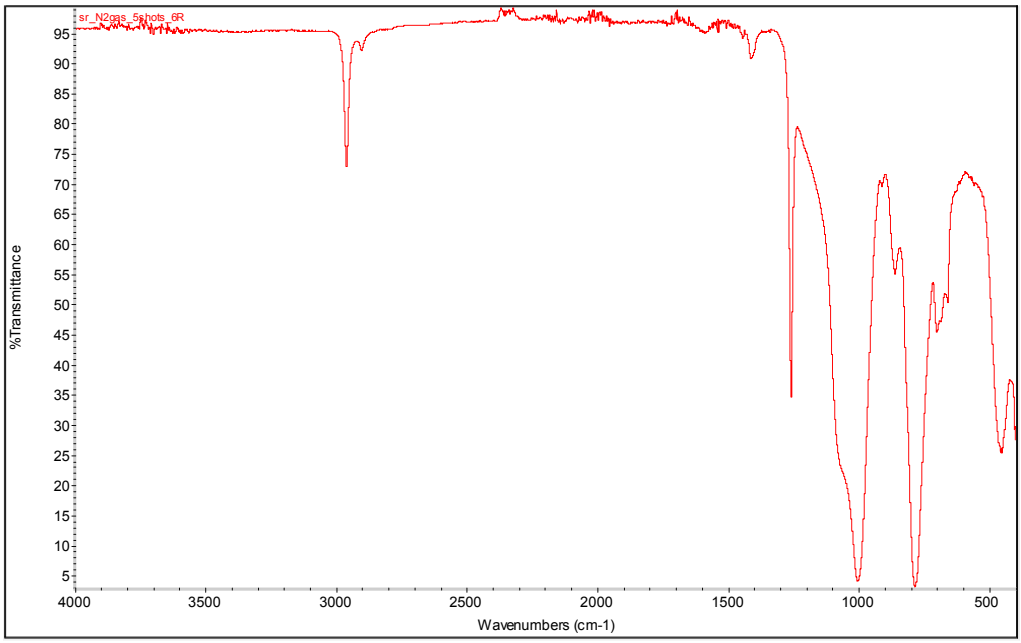

ATR/FT-IR spectrum of silicone rubber sample treated by 7 shots of nitrogen plasma at position 1

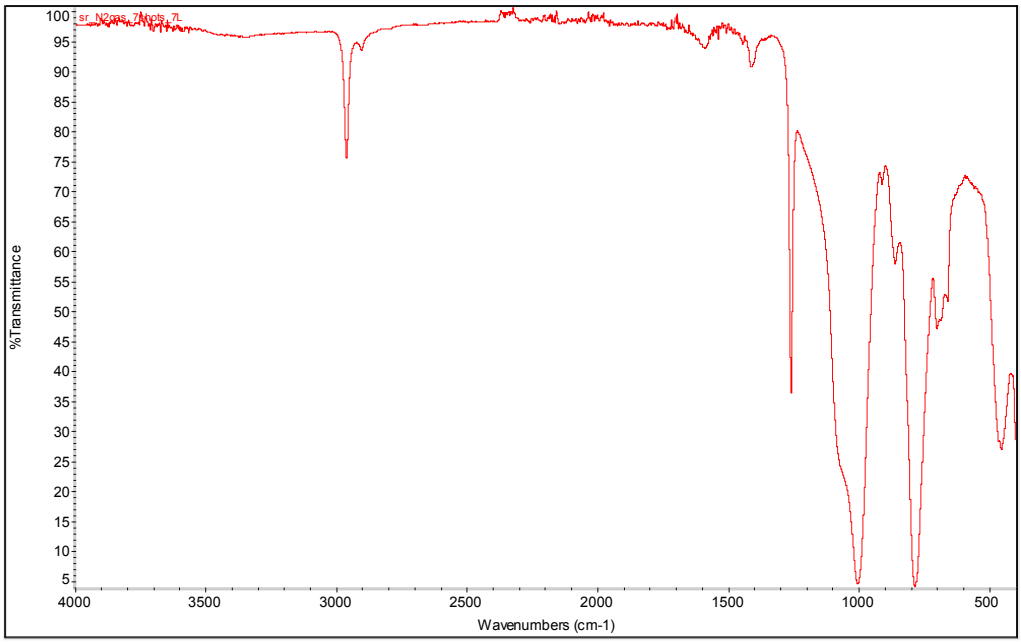

ATR/FT-IR spectrum of silicone rubber sample treated by 7 shots of nitrogen plasma at position 2

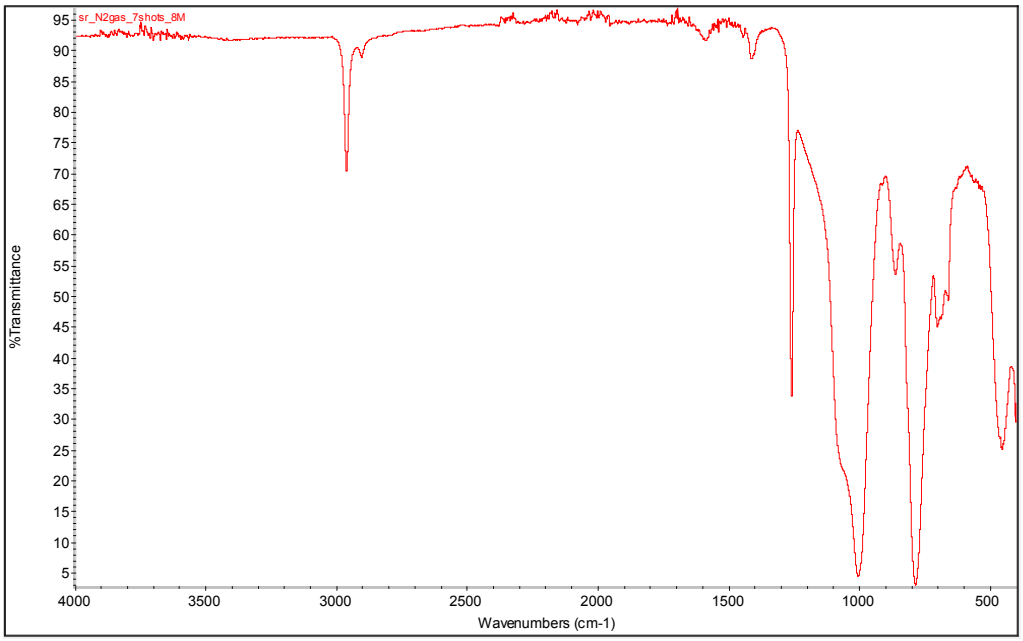

ATR/FT-IR spectrum of silicone rubber sample treated by 7 shots of nitrogen plasma at position 3

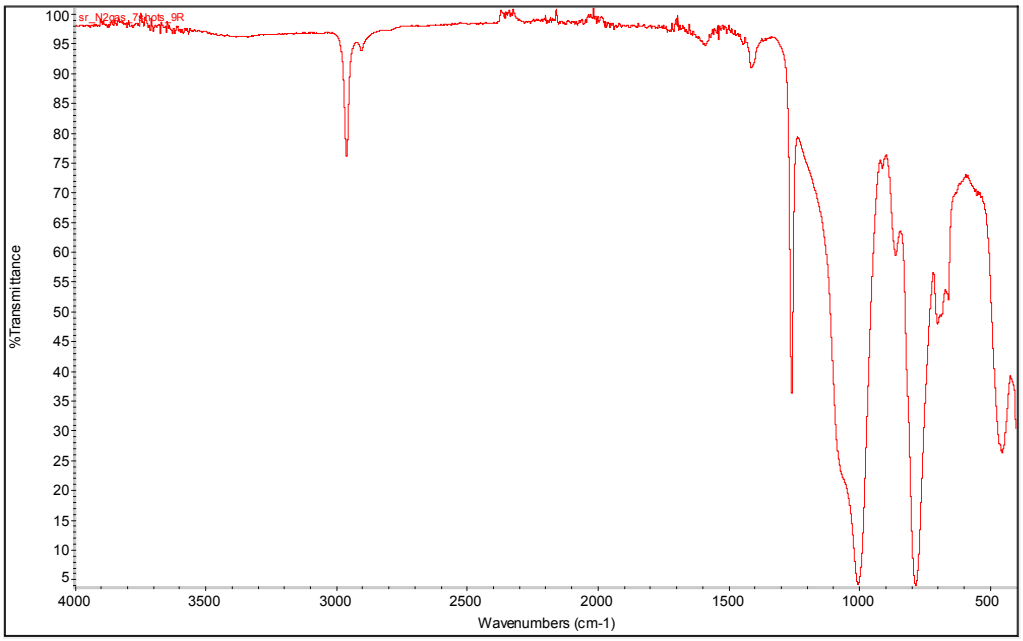

ATR/FT-IR spectrum of silicone rubber sample treated by 10 shots of nitrogen plasma at position 1

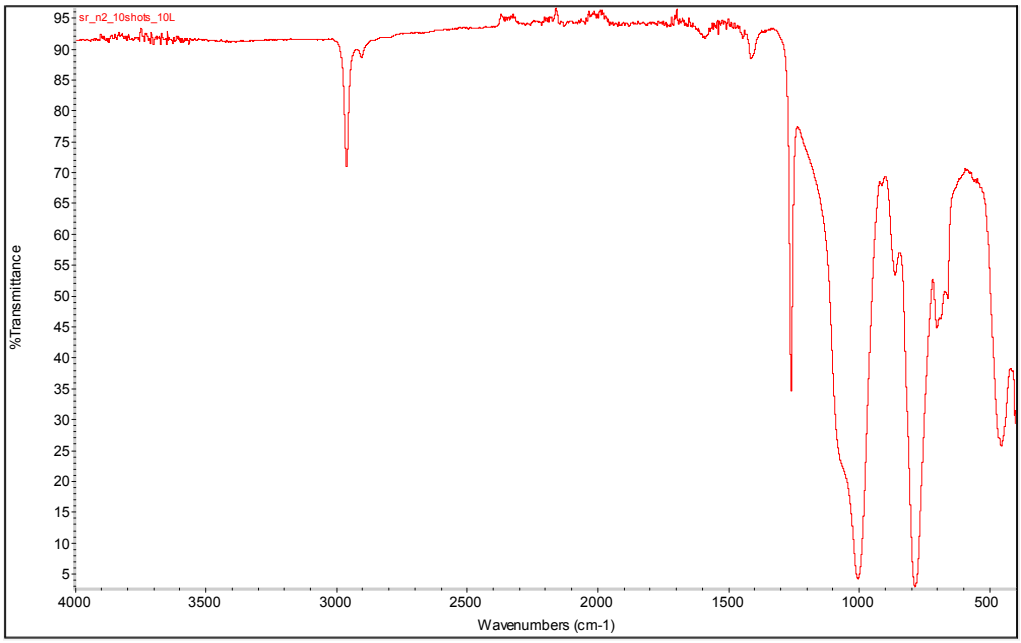

ATR/FT-IR spectrum of silicone rubber sample treated by 10 shots of nitrogen plasma at position 2

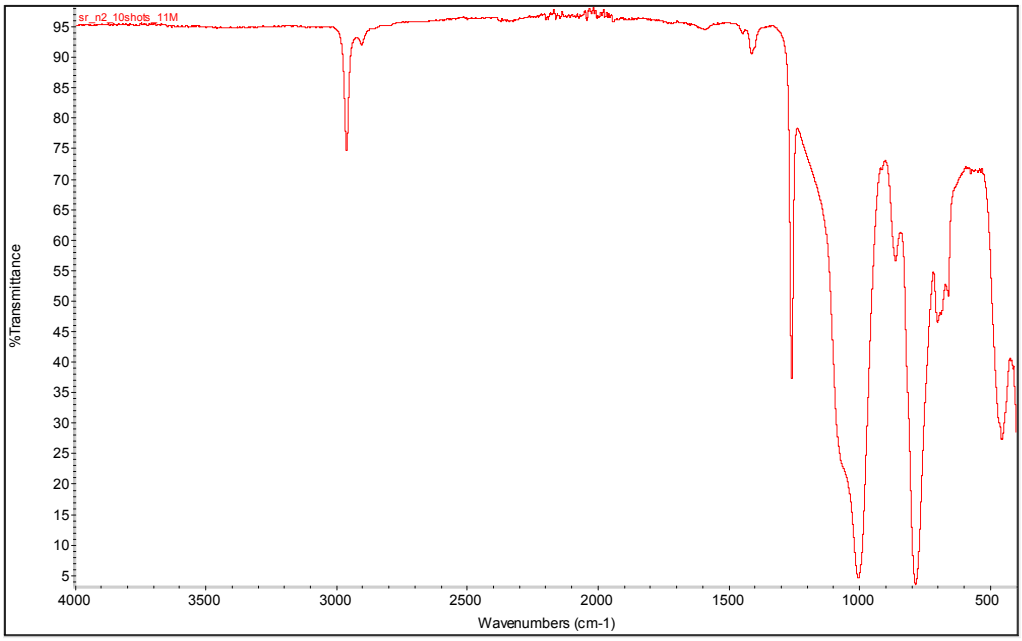

ATR/FT-IR spectrum of silicone rubber sample treated by 10 shots of nitrogen plasma at position 3

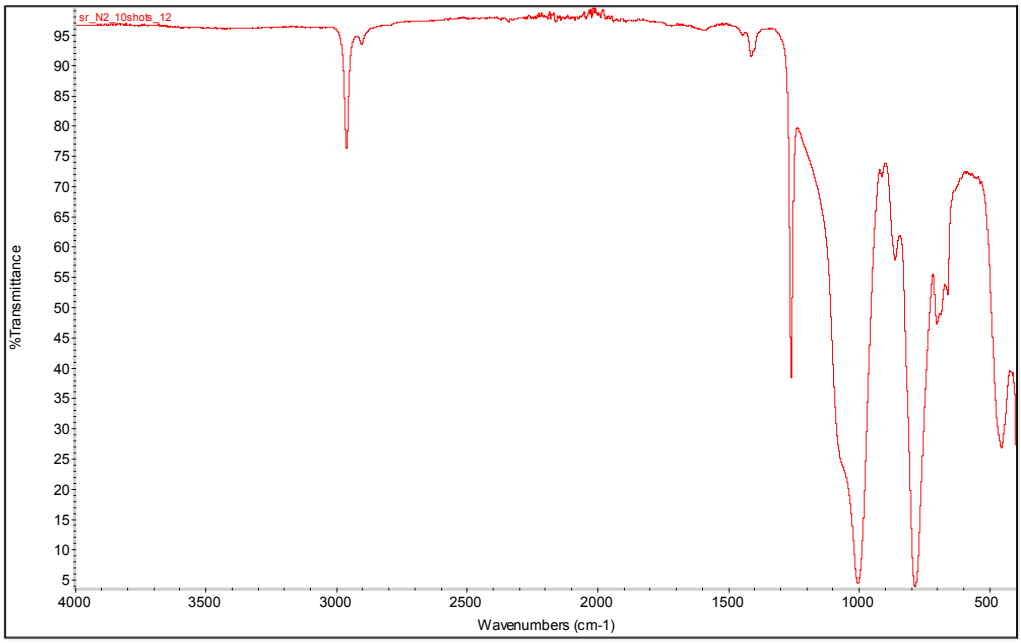

ATR/FT-IR spectrum of silicone rubber sample treated by 3 shots of oxygen plasma at position 1

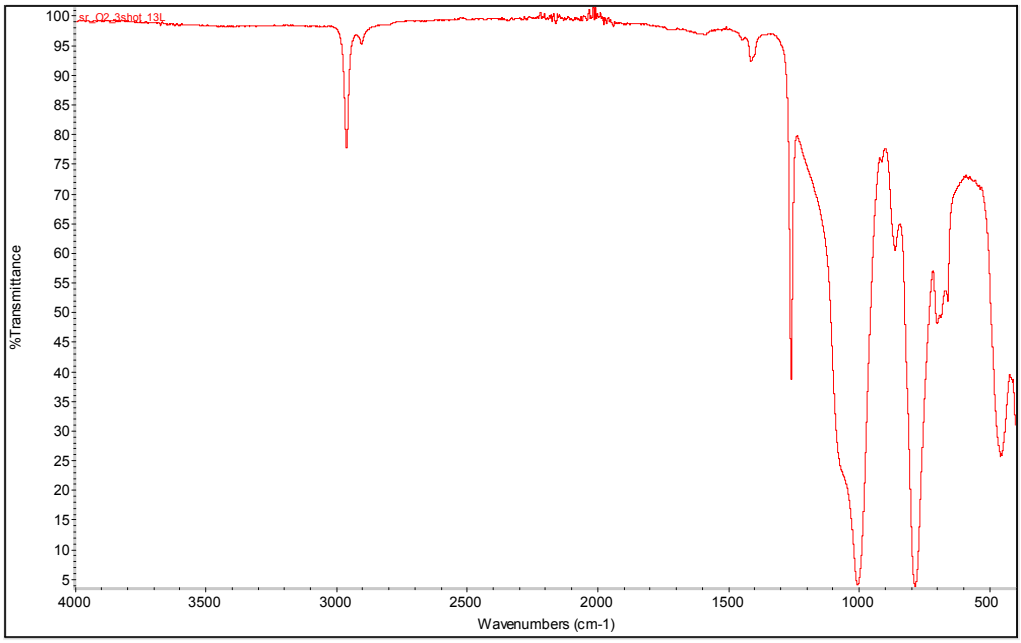

ATR/FT-IR spectrum of silicone rubber sample treated by 3 shots of oxygen plasma at position 2

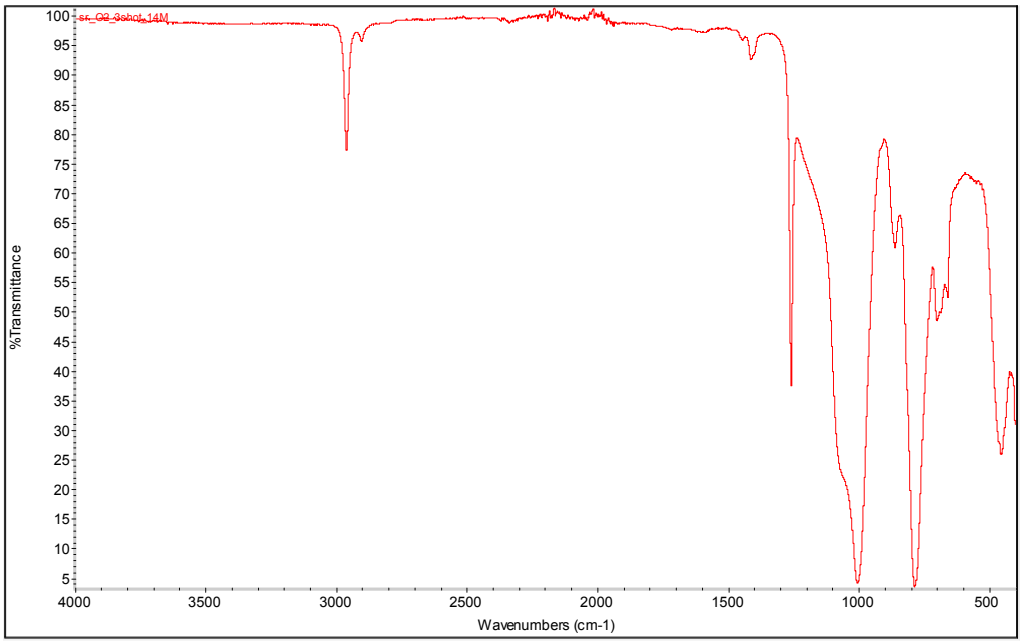

ATR/FT-IR spectrum of silicone rubber sample treated by 3 shots of oxygen plasma at position 3

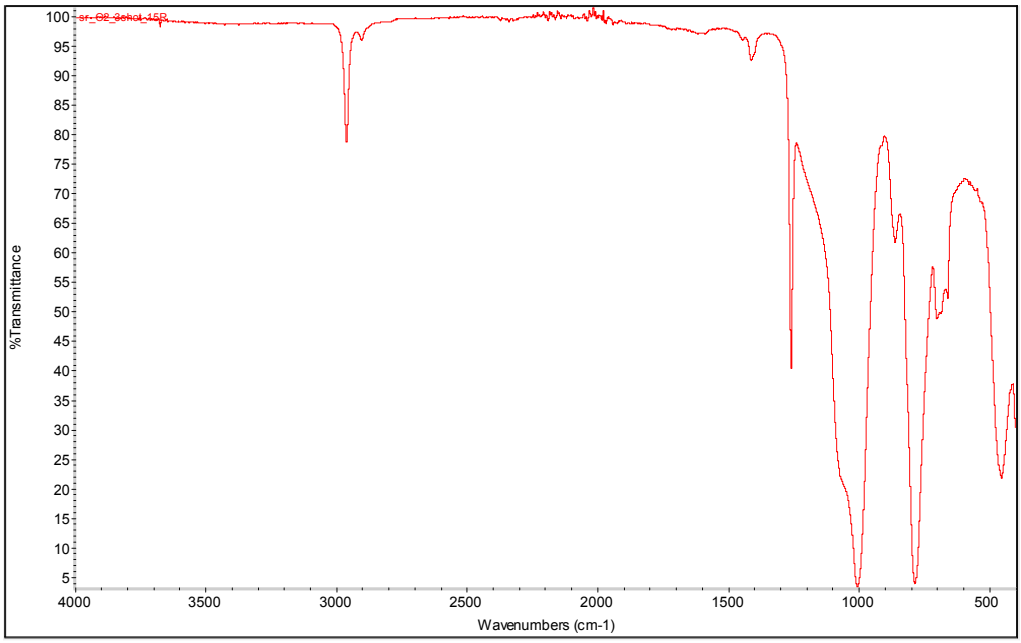

ATR/FT-IR spectrum of silicone rubber sample treated by 5 shots of oxygen plasma at position 1

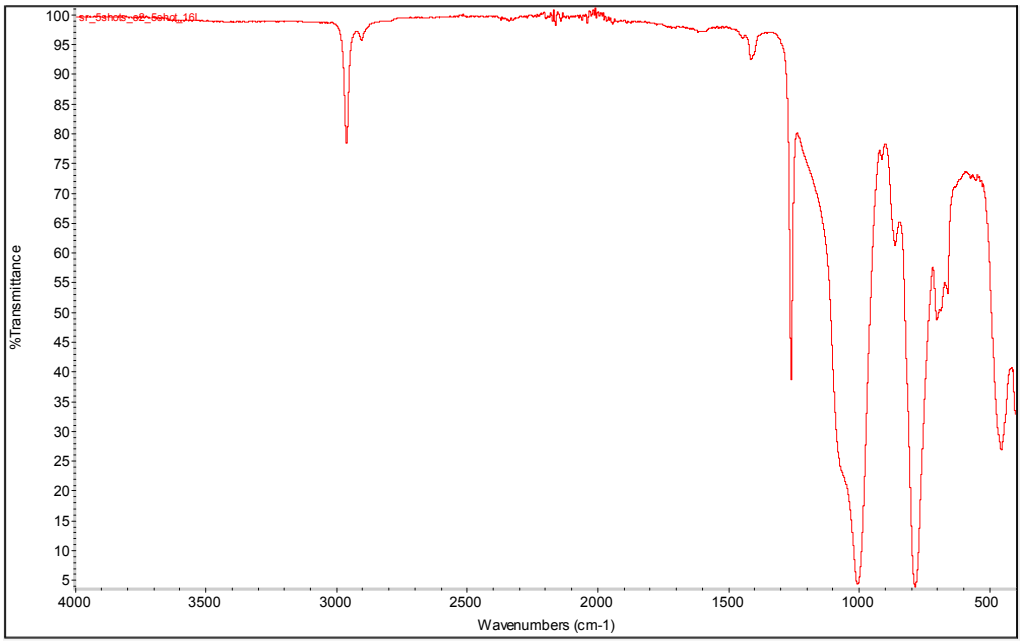

ATR/FT-IR spectrum of silicone rubber sample treated by 5 shots of oxygen plasma at position 2

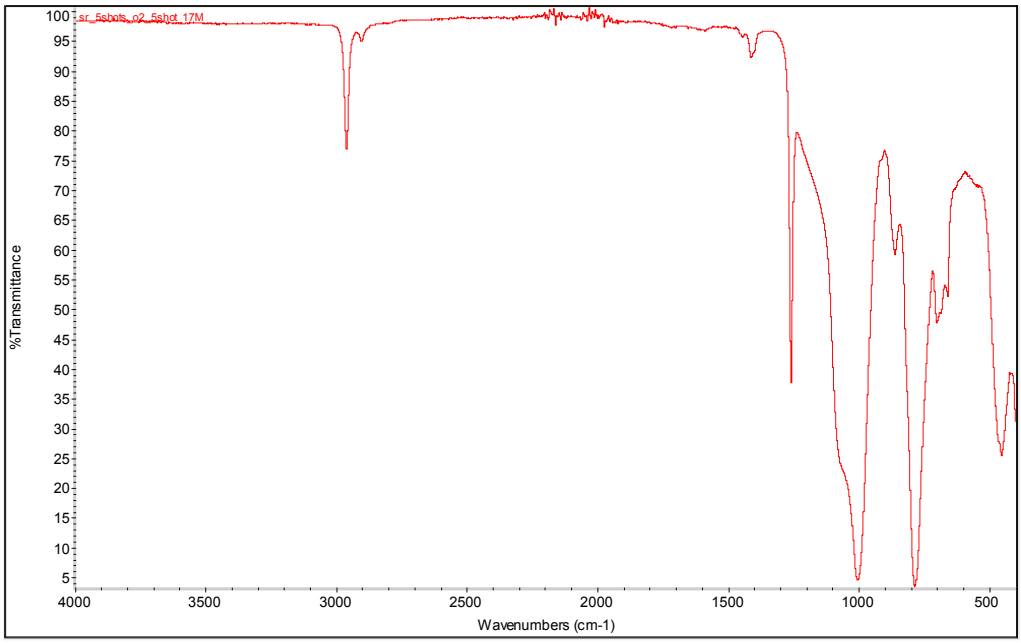

ATR/FT-IR spectrum of silicone rubber sample treated by 5 shots of oxygen plasma at position 3

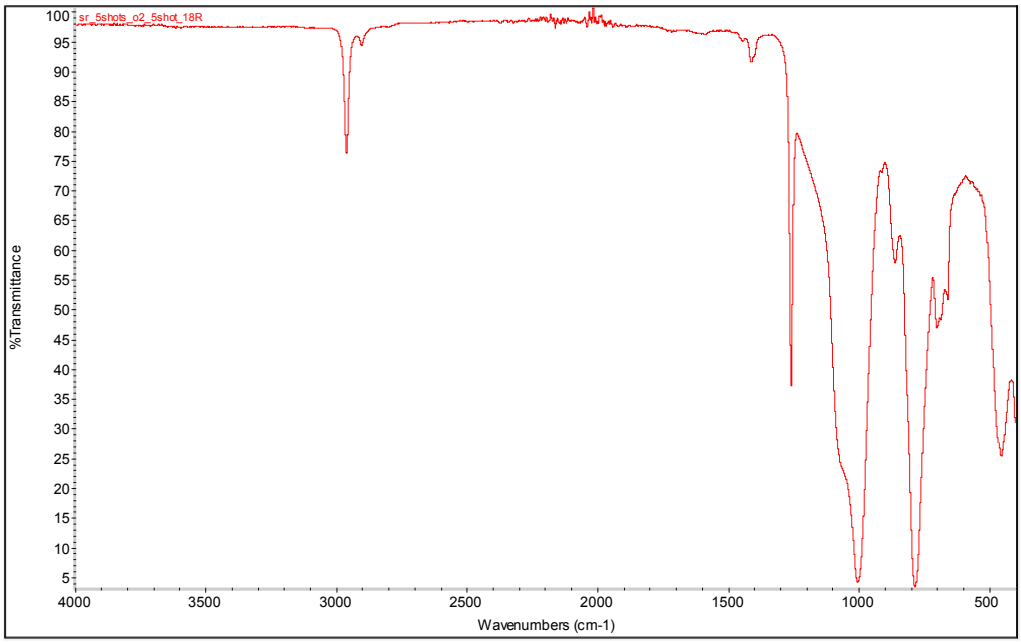

ATR/FT-IR spectrum of silicone rubber sample treated by 7 shots of oxygen plasma at position 1

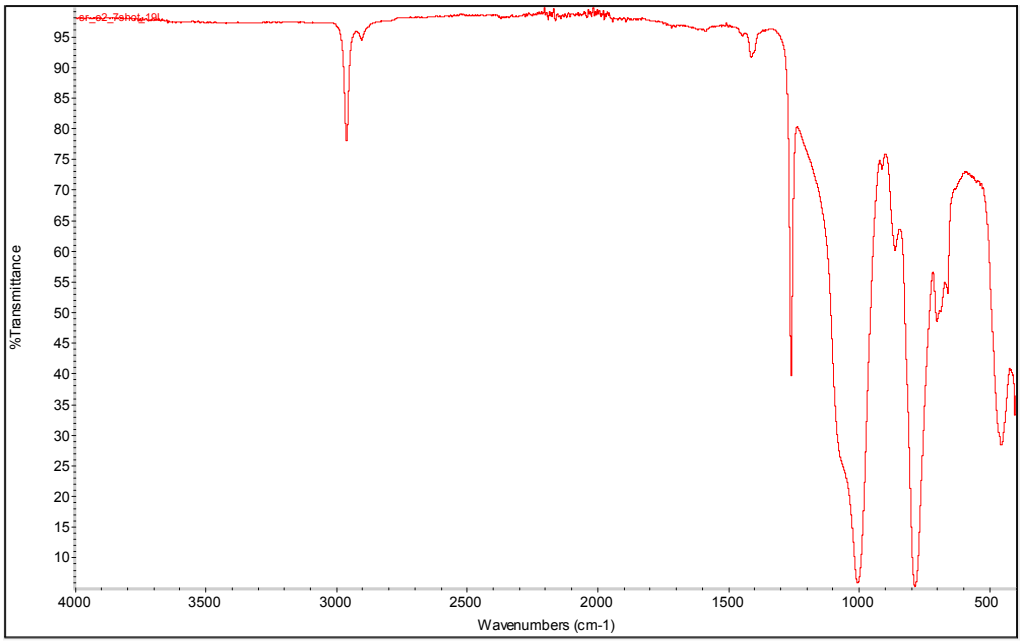

ATR/FT-IR spectrum of silicone rubber sample treated by 7 shots of oxygen plasma at position 2

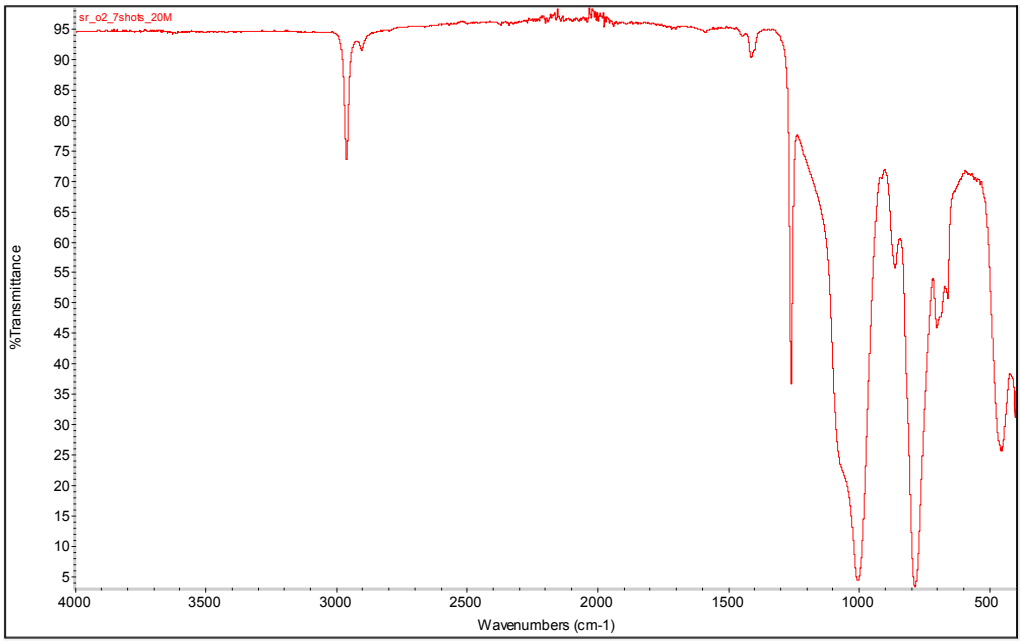

ATR/FT-IR spectrum of silicone rubber sample treated by 7 shots of oxygen plasma at position 3

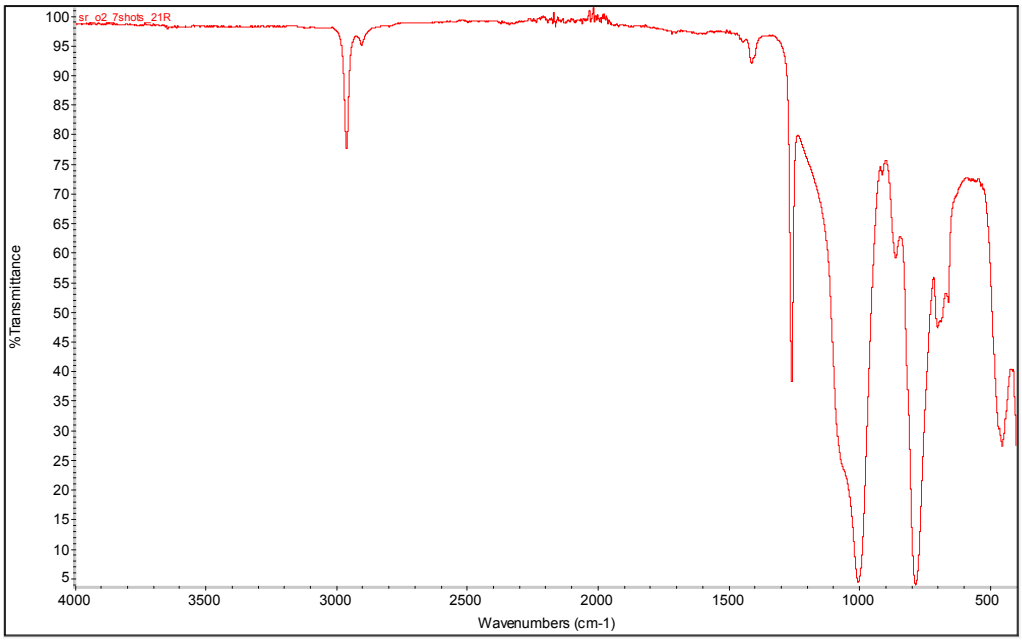

ATR/FT-IR spectrum of silicone rubber sample treated by 10 shots of oxygen plasma at position 1

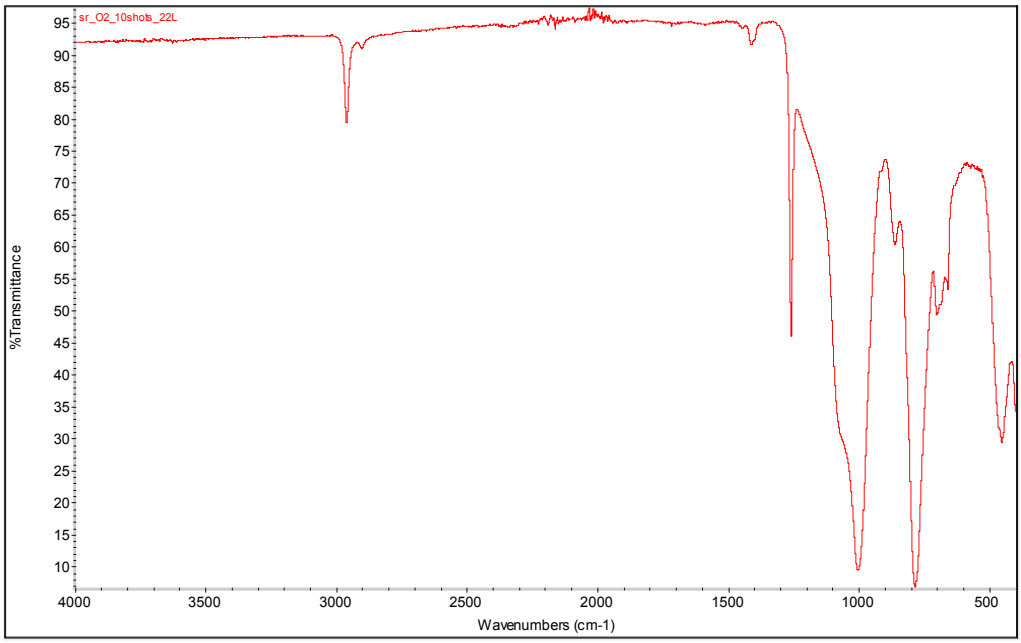

ATR/FT-IR spectrum of silicone rubber sample treated by 10 shots of oxygen plasma at position 2

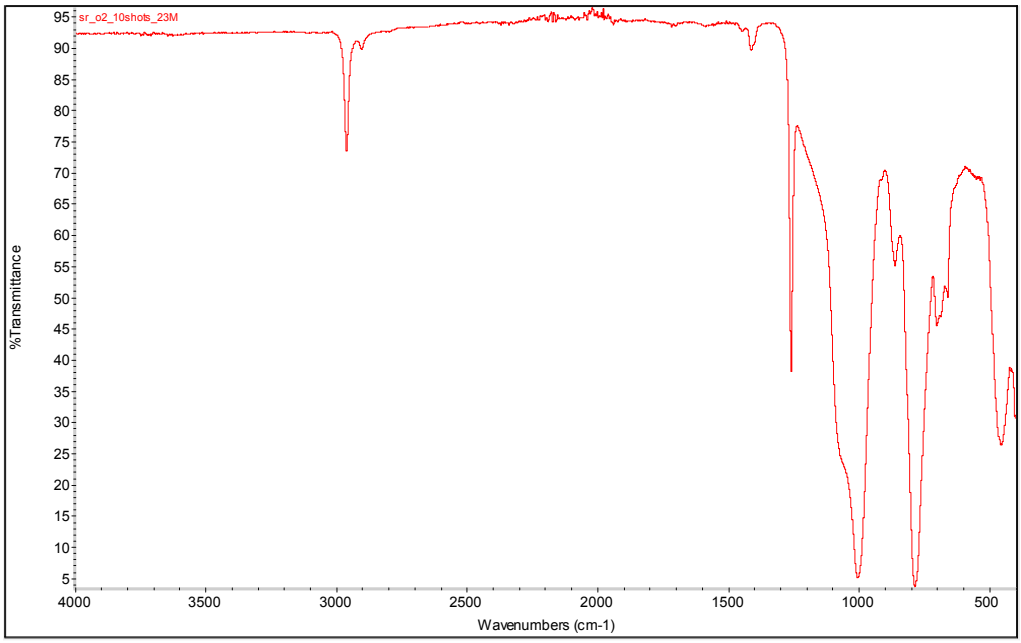

ATR/FT-IR spectrum of silicone rubber sample treated by 10 shots of oxygen plasma at position 3

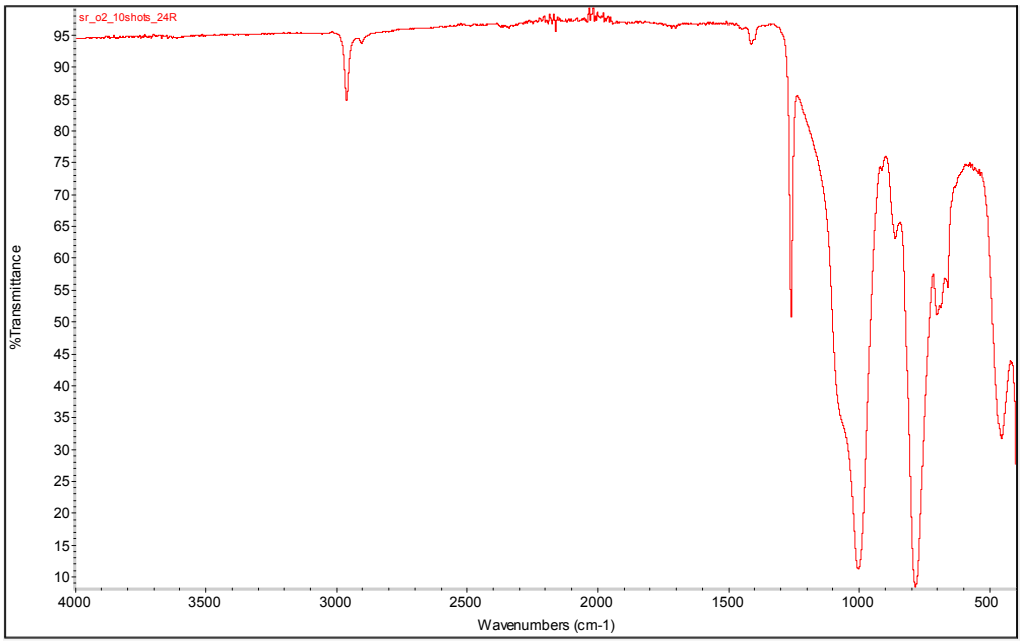

ATR/FT-IR spectrum of silicone rubber sample treated by 3 shots of argon plasma at position 1

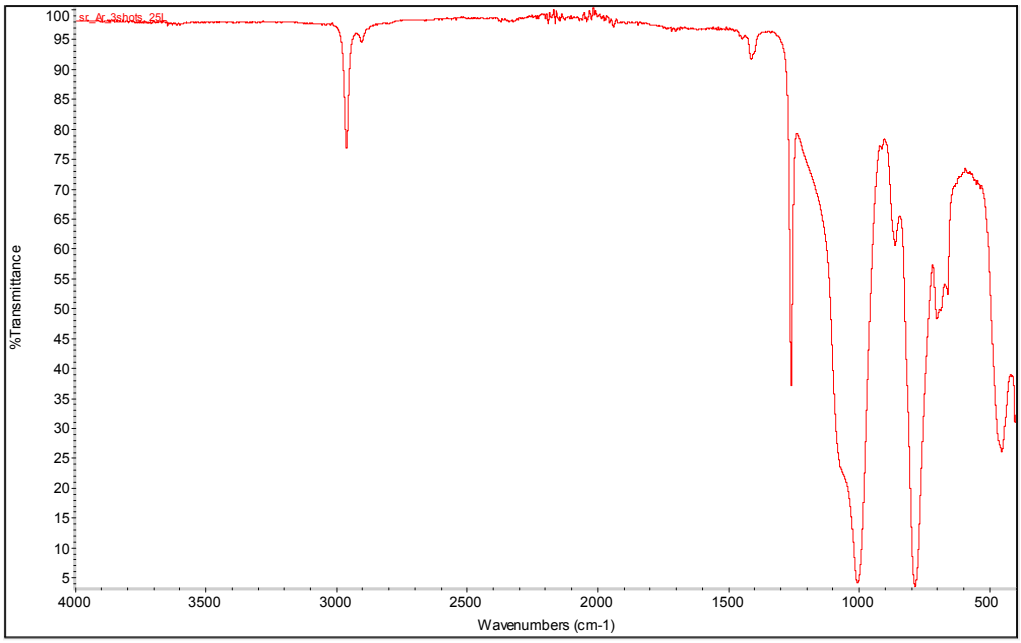

ATR/FT-IR spectrum of silicone rubber sample treated by 3 shots of argon plasma at position 2

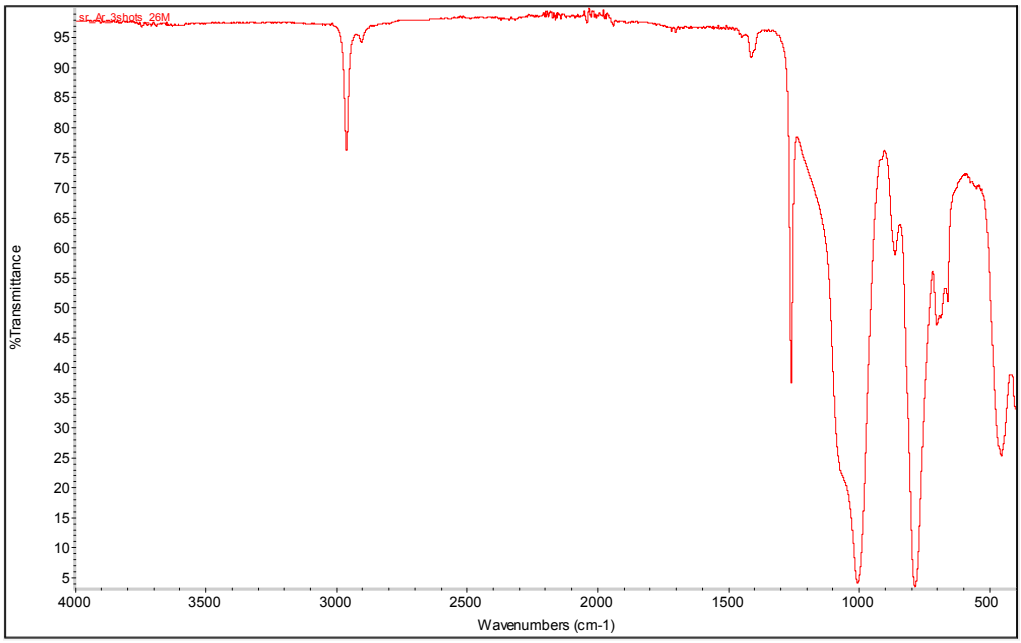

ATR/FT-IR spectrum of silicone rubber sample treated by 3 shots of argon plasma at position 3

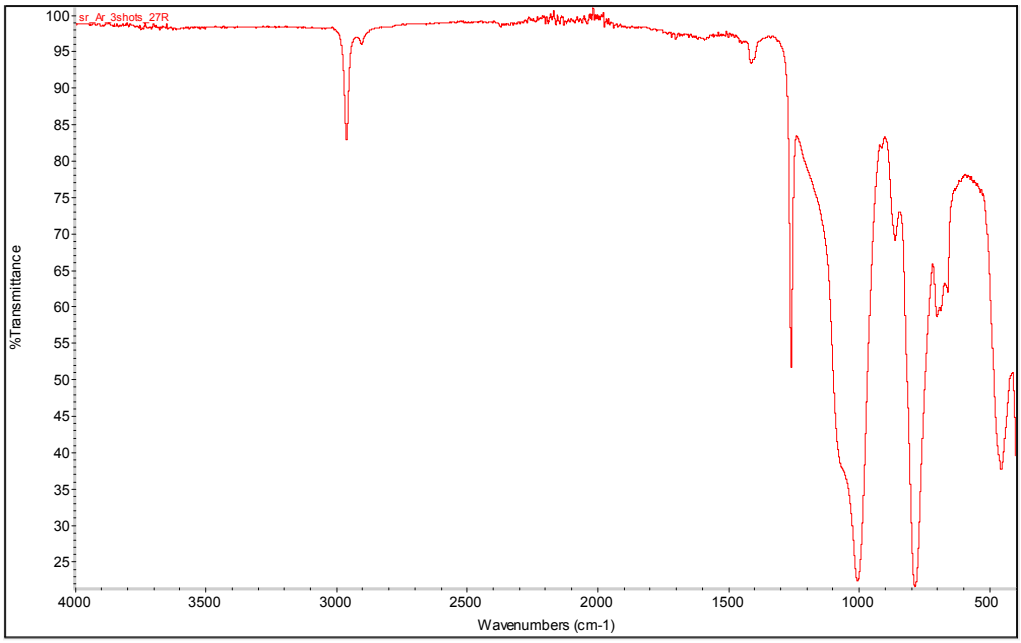

ATR/FT-IR spectrum of silicone rubber sample treated by 5 shots of argon plasma at position 1

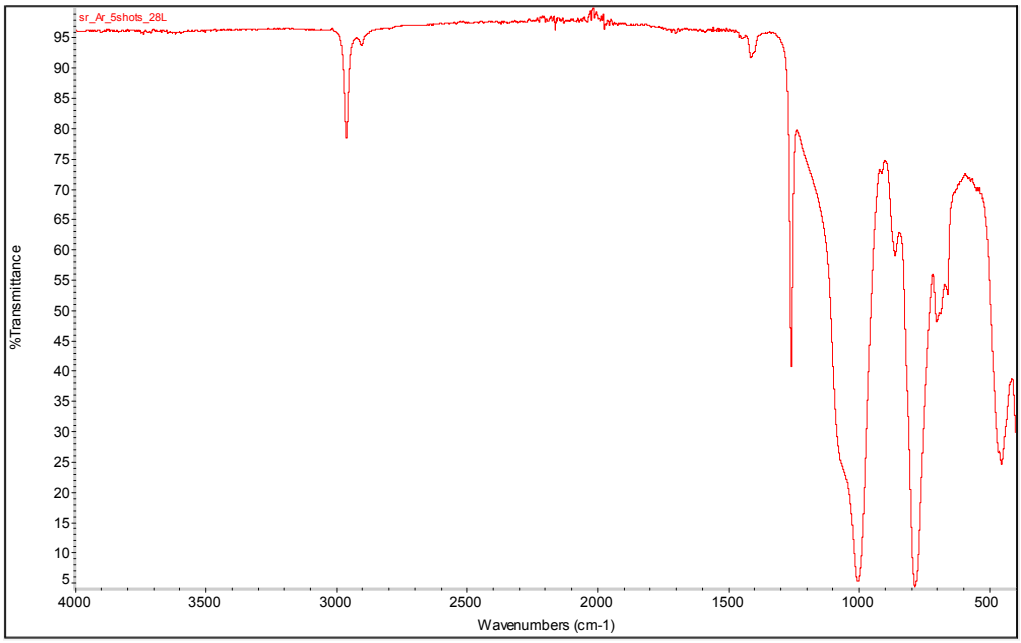

ATR/FT-IR spectrum of silicone rubber sample treated by 5 shots of argon plasma at position 2

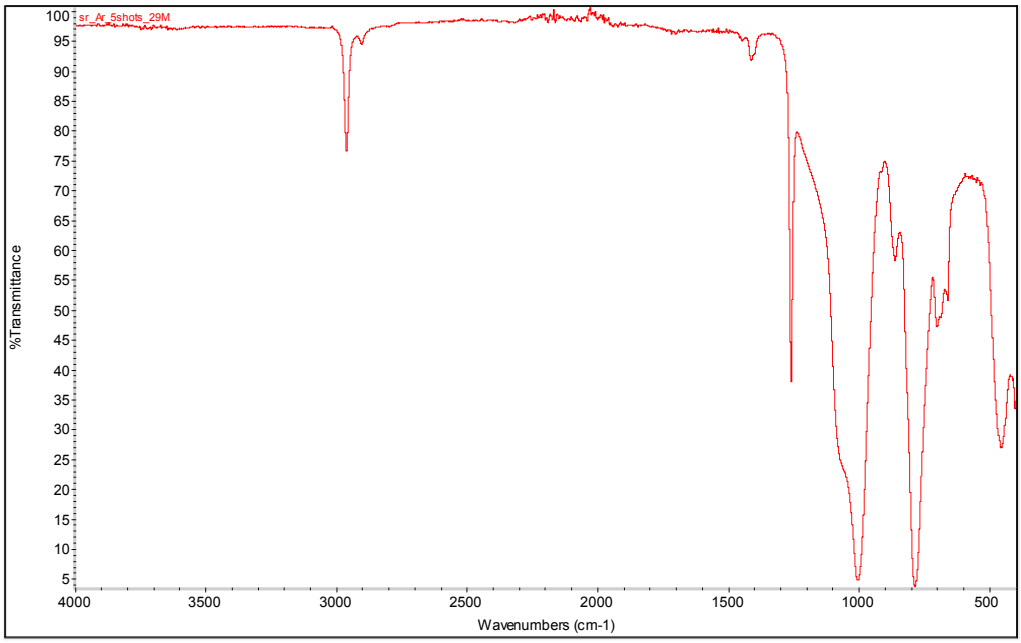

ATR/FT-IR spectrum of silicone rubber sample treated by 5 shots of argon plasma at position 3

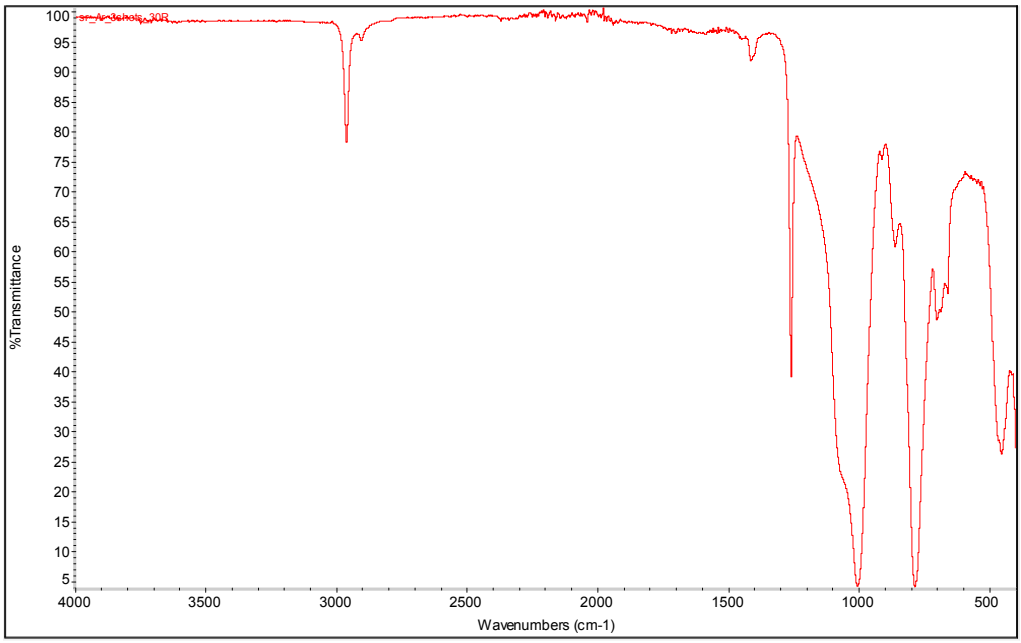

ATR/FT-IR spectrum of silicone rubber sample treated by 7 shots of argon plasma at position 1

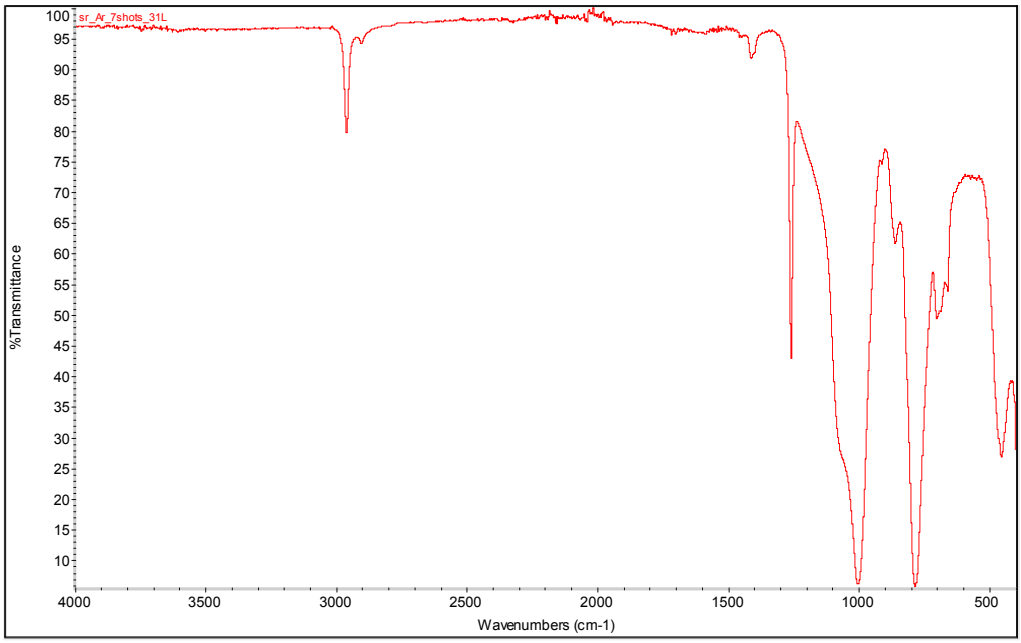

ATR/FT-IR spectrum of silicone rubber sample treated by 7 shots of argon plasma at position 2

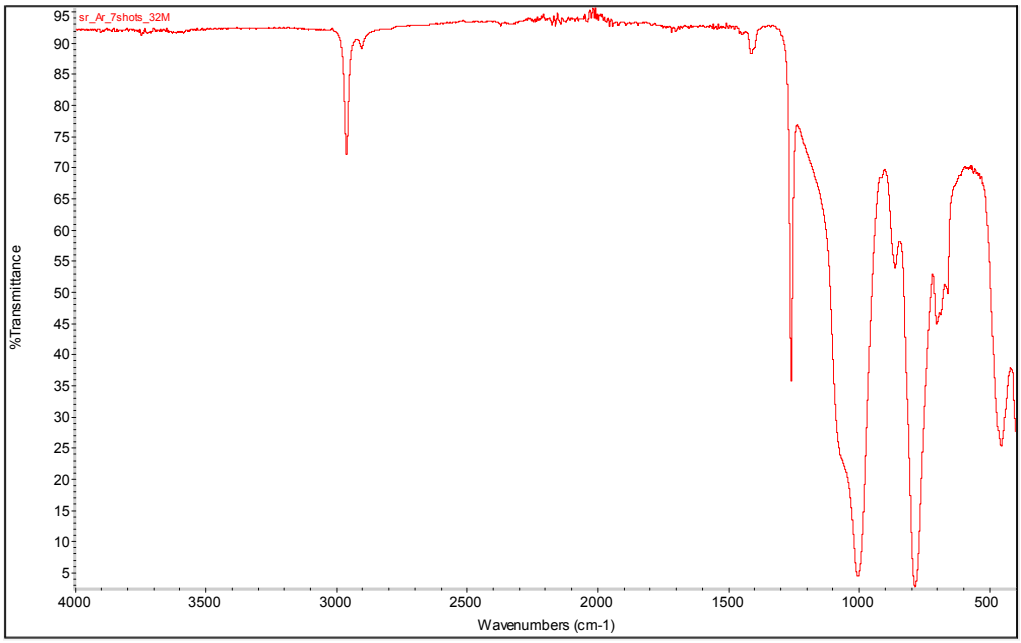

ATR/FT-IR spectrum of silicone rubber sample treated by 7 shots of argon plasma at position 3

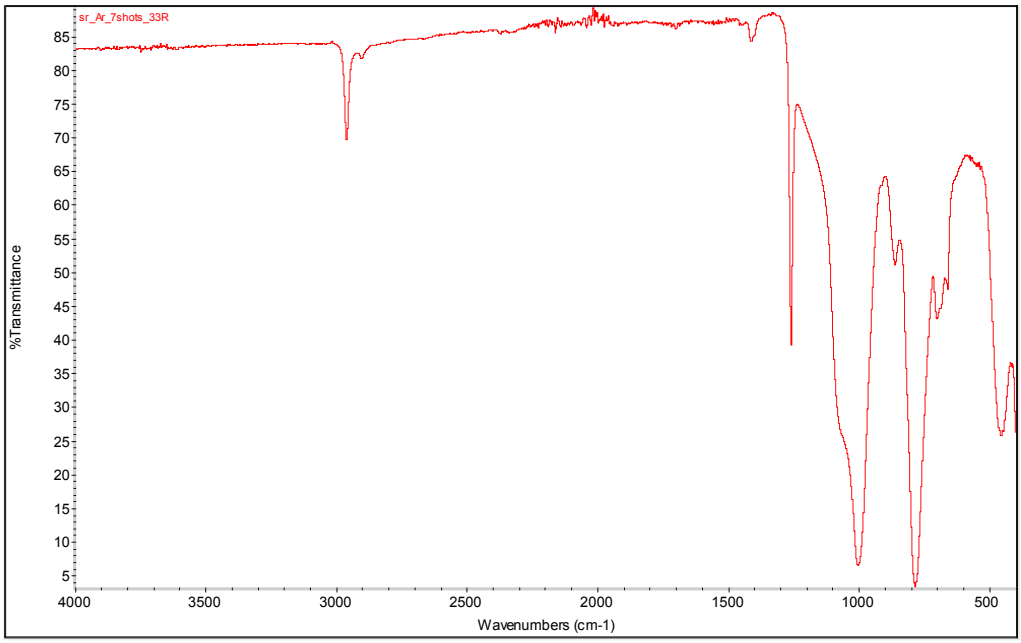

ATR/FT-IR spectrum of silicone rubber sample treated by 10 shots of argon plasma at position 1

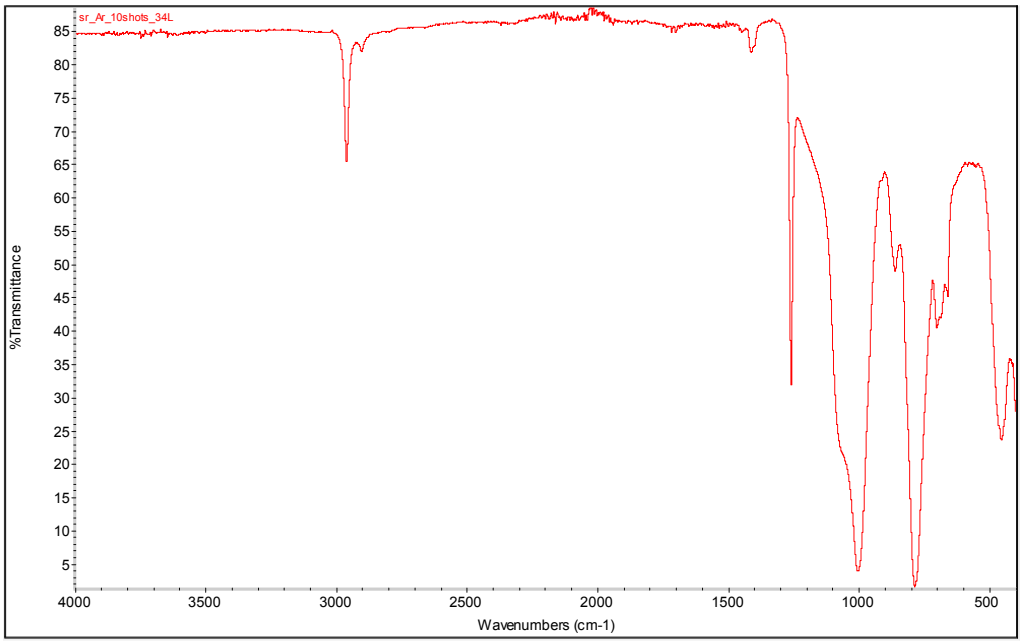

ATR/FT-IR spectrum of silicone rubber sample treated by 10 shots of argon plasma at position 2

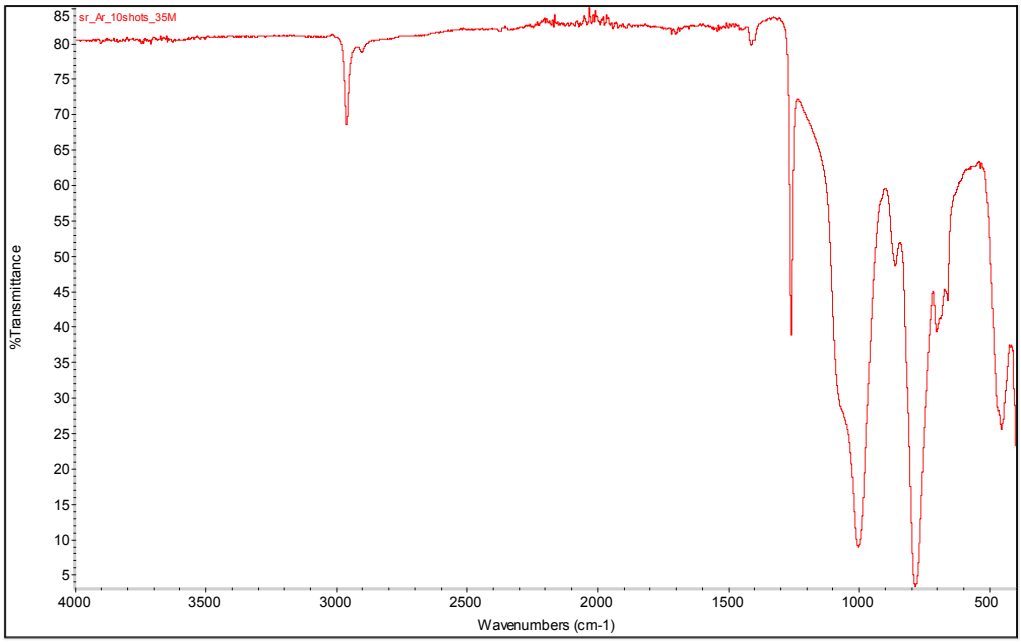

ATR/FT-IR spectrum of silicone rubber sample treated by 10 shots of argon plasma at position 3

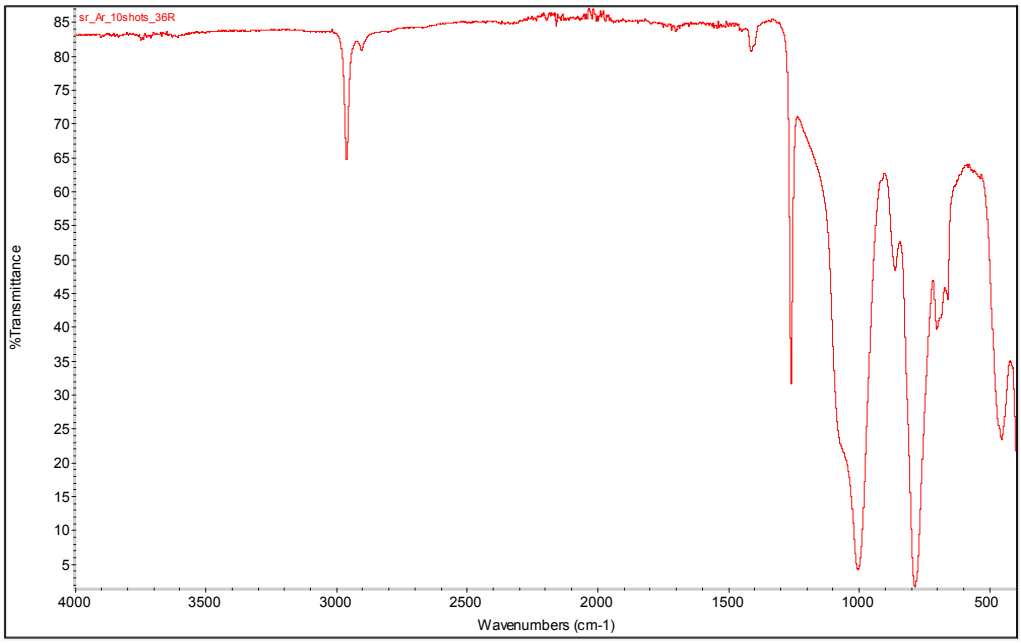

BIOGRAPHY

Mr. Werawat Sriprapai was born in Bangkok, Thailand on February 13, 1986. He received the Degree of the Bachelor of Science in Materials Science Major from Faculty of Science, Chulalongkorn University in 2008. Then, he continued his post graduate study in Applied Polymer Science and Textile Technology Major at the Department of Materials Science, Faculty of Science, Chulalongkorn University and ultimately completed the Degree of the Master of Science in Applied Polymer Science and Textile Technology in May 2010.